ISSN: 2152-7385 Volume 10, Number 9, September 2019

Scientific Research Publishing

Applied Mathematics

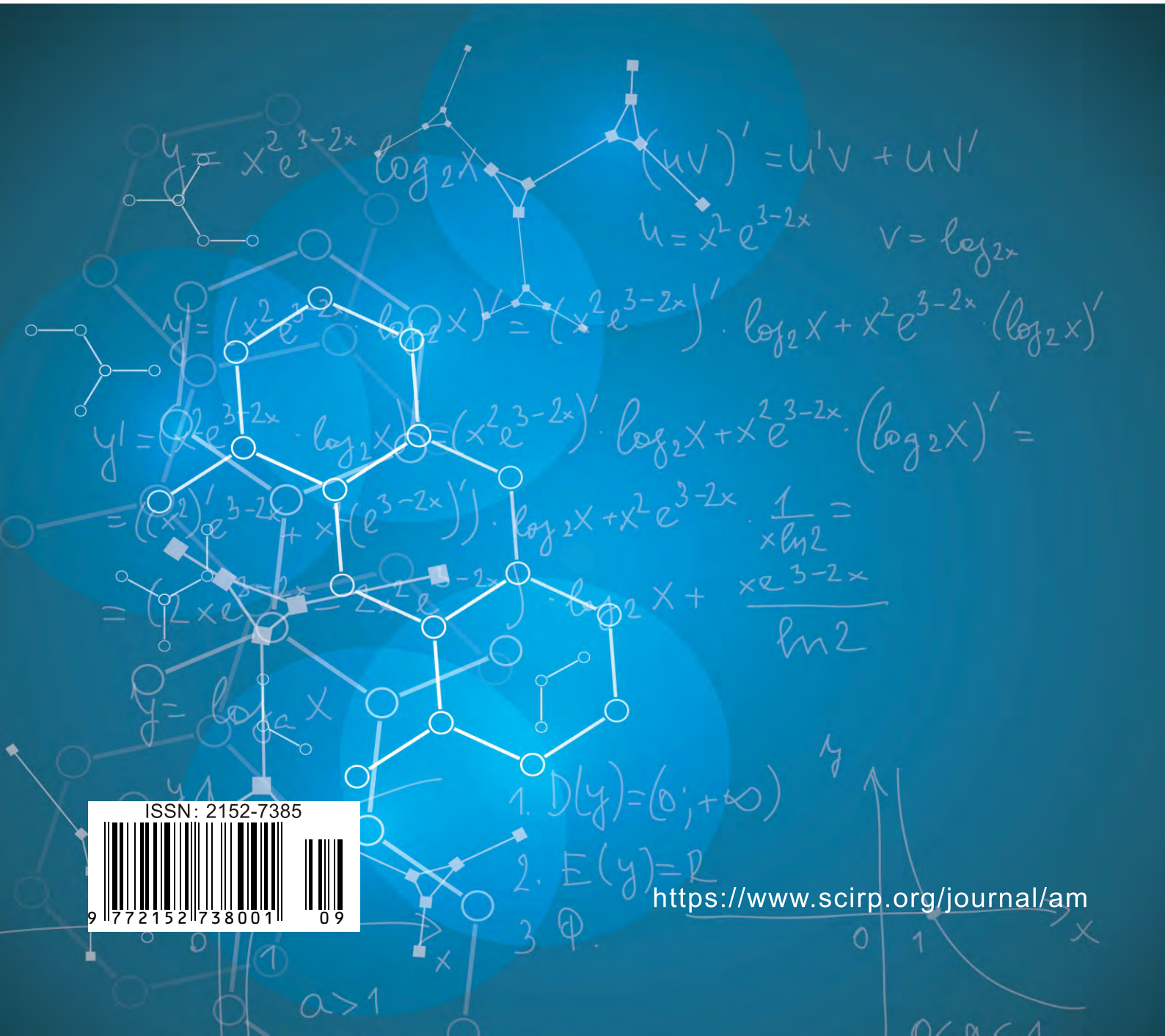

ISSN: 2152-7385

https://www.scirp.org/journal/am

Journal Editorial Board

ISSN Print: 2152-7385 ISSN Online: 2152-7393

https://www.scirp.org/journal/am

Editorial Board

Applied Mathematics, 2019, 10, 719-803
https://www.scirp.org/journal/am
ISSN Online: 2152-7393
ISSN Print: 2152-7385

Table of Contents

Volume 10 Number 9 September 2019

Applied Mathematics (AM)
Journal Information

SUBSCRIPTIONS

The *Applied Mathematics* (Online at Scientific Research Publishing, https://www.scirp.org/) is published monthly by Scientific Research Publishing, Inc., USA.

Subscription rates:
Print: $89 per copy.
To subscribe, please contact Journals Subscriptions Department, E-mail: sub@scirp.org

SERVICES

Advertisements
Advertisement Sales Department, E-mail: service@scirp.org

Reprints (minimum quantity 100 copies)
Reprints Co-ordinator, Scientific Research Publishing, Inc., USA.
E-mail: sub@scirp.org

COPYRIGHT

PRODUCTION INFORMATION

For manuscripts that have been accepted for publication, please contact:
E-mail: am@scirp.org

Applied Mathematics, 2019, 10, 719-727
https://www.scirp.org/journal/am
ISSN Online: 2152-7393
ISSN Print: 2152-7385

On Transient Simulation of Field Equations

Peter Chen

School of Mechanical and Manufacturing Engineering, University of New South Wales, Sydney, Australia
Email: peterypchen@yahoo.com.au

How to cite this paper: Chen, P. (2019) On Transient Simulation of Field Equations. *Applied Mathematics*, **10**, 719-727.
https://doi.org/10.4236/am.2019.109051

Received: August 19, 2019
Accepted: September 6, 2019
Published: September 9, 2019

Abstract

We investigate under what conditions transient simulation could be used to integrate backward in time so that the initial field could be recovered from later histories. In this paper we use realistic examples and find that, in long histories, traces of the initial field would be present only in the exact analytical solutions. We conclude that the recovery of initial field is possible only if the equations could be solved analytically or only short time periods are involved. In practice, it is not possible to detect those traces by measurements or observations. If numerical procedures are used, truncation and discretization errors are always present. Fine-tuning of system parameters used or transforming time into another pseudo time frame may allow numerical integration to be carried out backward in time. But numerical instability is still a problem. Large spurious increases found by numerical procedures are most likely due to numerical inaccuracy and instability.

Keywords

Solution of Differential Equations, Transient Simulation, Numerical Instability, Mathematical Modelling, Backward Time Integration

1. Introduction

With the availability of modern computer power, there is a rapidly increased use of mathematical models to simulate real life or physical situations [1] [2]. Mathematical models use mathematical concepts and language to represent real problems and are used in natural sciences and engineering disciplines, as well as in the social sciences. Often, solutions of the mathematical equations used in the models may not be found easily. A proven technique is to employ a pseudo transient simulation [3] [4]. The word pseudo is used to indicate that the solution is found by a transient approach but the time used is not necessarily real. However, as far as the mathematical principles and methods are concerned there is no distinction between real and pseudo time.

With success of mathematical modelling, there is a tendency to replace laboratory testing of designs by numerical experiments [5] and operator control of a system by computer control [6]. It should be noted that the accuracy and effectiveness of computer-based approach are most dependent on the model or models used. For example, maximum transient stress found by the numerical solutions of a simulation based on the long cylinder approximation would be five folds smaller than the maximum stress which actually exists at the ends of the cylinder [7]. The interpretation of results obtained by simulations is also important. Often the averages over a computational grid cell are used for numerical reasons. This means that the actual maximum inside a cell could be much greater than the cell average found. This could happen such as in the case of weather forecasting; the computer program predicted wind speeds could only be halves of the actual maxima.

For saving computational time, simpler models are often used in simulation [8]. System parameters used in those models may not be the physical properties of the system but are those found to be most suitable for matching with observations in so called "fine tuning". In such cases, it is important that the simulation is not being used far beyond the conditions employed in the calibration. In a sense this type of simulation is similar to curve fitting except that far more complicated mathematical operators are involved.

By far the more uncertain attempt involves predictions not just for what can be seen now or what would happen in the future but for predictions on what have already occurred in the past. A notable case is that astrophysicists are predicting what the universe could be billions of years ago by what they can observe now. As far as solving the field equations is concern, it is a well-established mathematical principle that solutions are possible only for the time space from zero to infinity. However, with pseudo transient treatment, the real time space from zero to negative infinity could be converted to the pseudo time space varying from zero to infinity. This would be an useful solution if it is found permissible.

In this paper, heat conduction problems are solved to give a set of analytical solutions. They are used to show why integration forward in time is always stable. Backward integration in time is permissible only if it is done analytically as any error in numerical approximates would grow exponentially. We also show that numerical backward extrapolation cannot be used to recover the initial condition even when a pseudo time is used. In another example we show that if the temperature field in details is not needed, heat conduction need not be considered. The system could be modelled by an ordinary differential equation and solved analytically. System parameters that are generally not the same as the physical properties could be found by calibration so that the system could be used for prediction, measurement or control purposes.

2. Transient Heat Conduction Equation

For a one dimensional heat conduction problem

$$\frac{\partial T(x,t)}{\partial t} = \frac{\partial^2 T(x,t)}{\partial x^2} + Q(x) \tag{1}$$

where T is the temperature and Q heat source, and all are in dimensionless. The initial condition, $T(x,0) = T^0(x)$ is given and the boundary conditions are:

$$T'(0,t) = 0; \quad \frac{\partial T(1,t)}{\partial x} - hT(1,t) = 0 \tag{2}$$

where h is the heat transfer coefficient.

Using N terms of chopped sine Fourier expansions

$$T(t,x) = \sum_{i=1}^{N} a_i f_i(t) \sin\left(\lambda_i x + \frac{\pi}{2}\right) \tag{3}$$

$$Q(x) = \sum_{i=1}^{N} q_i \sin\left(\lambda_i x + \frac{\pi}{2}\right) \tag{4}$$

$$T^0(x) = \sum_{i=1}^{N} t_i^0 \sin\left(\lambda_i x + \frac{\pi}{2}\right) \tag{5}$$

where λ_i are given by the characteristic equation derived from the boundary condition (2)

$$-\lambda_i \cos\left(\lambda_i + \frac{\pi}{2}\right) + h \sin\left(\lambda_i + \frac{\pi}{2}\right) = 0 \tag{6}$$

Substitute (3) and (4) into (1) and equate the coefficients to give

$$a_i f_i'(t) = -\lambda_i^2 a_i f(t) + q_i \tag{7}$$

The solution of the above equation that satisfies the initial condition (5) is

$$a_i f_i(t) = \frac{q_i}{\lambda_i^2}\left[1 - \exp\left(-\lambda^2 t\right)\right] + t_i^0 \exp\left(-\lambda^2 t\right) \tag{8}$$

$$\therefore \quad T(x,t) = \sum_{i=1}^{N}\left[\frac{q_i}{\lambda_i^2}\left\{1 - \exp\left(-\lambda^2 t\right)\right\} + t_i^0 \exp\left(-\lambda^2 t\right)\right] \sin\left(\lambda_i x + \frac{\pi}{2}\right) \tag{9}$$

and at $t \gg 0$, the time independent and stationary temperature is

$$T(x,t) = \sum_{i=1}^{N} \frac{q_i}{\lambda_i^2} \sin\left(\lambda_i x + \frac{\pi}{2}\right) \tag{10}$$

Obviously the initial condition, including any errors, as well as those differences between the current and the stationary temperature would decay exponentially in time leaving only the stationary components.

With the analytical solution, Equation (9), $T(0,x)$ can be recovered exactly from $T(t_N,x)$ even when $t_N \gg 0$. Using $T(t_N,x)$ as the initial value, $T(0,x)$ can be found by integrating backward to $t = 0$. This is possible because the analytical solution contains exactly every small terms associating with the factor $\exp\left(-\lambda_i^2 t_N\right)$ that combines with the very large factor $\exp\left(\lambda_i^2 t_N\right)$ to give the exact starting value.

Use as an example $Q(x) = \sin\left(x + \frac{\pi}{2}\right)$ and $T(x,0) = t^0 \sin\left(x + \frac{\pi}{2}\right)$ to show what is needed in the analytical solution before the initial value could be recov-

ered from that at time t_N. According to Equation (9) the solution is

$$T\left(x,t_N\right)=\left[\left\{1-\exp\left(-t_N\right)\right\}+t^0\exp\left(-t_N\right)\right]\sin\left(x+\frac{\pi}{2}\right) \tag{11}$$

As $t_N \gg 0$, the term $\exp\left(-t_N\right)$ is very small; it drops out from Equation(11) to give the steady solution

$$T\left(x,t_N\right)=\sin\left(x+\frac{\pi}{2}\right) \tag{12}$$

If Equation (12) is used as the initial value, integration backward to $t=-t_N$ will give the same temperature

$$T\left(x,0\right)=\left[\left\{1-\exp\left(t_N\right)\right\}+\exp\left(t_N\right)\right]\sin\left(x+\frac{\pi}{2}\right)=\sin\left(x+\frac{\pi}{2}\right) \tag{13}$$

This should not be a surprise as starting from the steady solution there should be no change in the temperature field whether it is marching forward or backward in time. Since t^0 is absent in the steady solution, the arbitrary initial value could not be recovered from backward integration. However, no matter how small the term $\exp\left(-t_N\right)$ is if the full Equation (11) is used as the initial value, integration backward from time t_N to time zero does recover t^0 exactly.

Next, consider that the starting field is slightly different to the steady field. That is

$$T^0\left(x,0\right)=\left(1+\varepsilon\right)\sin\left(x+\frac{\pi}{2}\right) \tag{14}$$

where $\varepsilon \approx 0$. Then according to Equation (11), the backward integration from the beginning to $-t_N$ is

$$\begin{aligned} T\left(x,t_N\right)&=\left[\left\{1-\exp\left(-t_N\right)\right\}+\left(1+\varepsilon\right)\exp\left(-t_N\right)\right]\sin\left(x+\frac{\pi}{2}\right)\\ &=\left[1+\varepsilon\exp\left(t_N\right)\right]\sin\left(x+\frac{\pi}{2}\right)\end{aligned} \tag{15}$$

It could be seen from Equation (15) that any error even as small as truncation error would growth exponentially without bound as the integration is progressing further and further away in the backward time direction. This spurious solution would sooner or later swamp the real solution. It should be noted that when starting with an analytical solution, $\varepsilon = 0$ and hence stability is not a problem.

3. Pseudo Transient Approach

In a real and physical situation, it is impossible to run a system backward in time. But in mathematics, integration can be carried out forward as well as backward in time. For an initial value problem, however, it is generally accepted that solutions can be found only for the time space from zero to infinity. In order to comply with this condition, a pseudo time, $\theta = t_{end} - t$ is used, where t_{end} is a nominal positive value in the real time space. Then the pseudo time space used is from zero forward to t_{end}. It also corresponds to the real time space from t_{end} to zero. That is backward in real time space. With this pseudo time, Equation (1)

becomes

$$\frac{\partial T(x,\theta)}{\partial \theta} = -\frac{\partial^2 T(x,\theta)}{\partial x^2} - Q(x) \tag{14}$$

The solution based on chopped sine Fourier expansion in Equations (3)-(5) is

$$T(\theta,x) = \sum_{i=1}^{N}\left[\frac{q_i}{\lambda_i^2}\left\{1-\exp\left(\lambda^2\theta\right)\right\} + t_i^0 \exp\left(\lambda^2\theta\right)\right]\sin\left(\lambda_i x\right) \tag{15}$$

It is apparent that numerical integration forward in pseudo time would have a numerical stability problem as any error present at the beginning would growth exponentially and swamp the solution itself. However, integration backward in time would be stable, confirming the condition that for this type of field equation numerical integration in real time should only be carried out in the forward direction.

To investigate the situation when integration is done by finite difference, suppose that Equation (14) is to be solved with $Q(x) = q\sin\left(2x+\frac{\pi}{2}\right)$ and $T(x,0) = t^0\sin\left(2x+\frac{\pi}{2}\right)$. Then, only one term in the Fourier series needs to be considered. Let the left hand side be replaced by Crank-Nicolson finite difference.

At $t = t^i$, $T\left(x, t=t^i\right) = T^i\sin\left(2x+\frac{\pi}{2}\right)$ with superscript i denotes the time step. Then $\frac{T^{i+1}-T^i}{\Delta\theta} = 2\left(T^{i+1}+T^i\right) - q$

$$\therefore\ T^{i+1} = \frac{1+2\Delta\theta}{1-2\Delta\theta}T^i - q\Delta\theta \simeq \left(1+4\Delta\theta\right)T^i - q\Delta\theta \tag{16}$$

If an inaccurate $\tilde{T}^i = T^i + \varepsilon$ is used in Equation (16), the estimated $\tilde{T}^{i+1} = \left(1+4\Delta\theta\right)\left(T^i+\varepsilon\right) - q\Delta\theta$ and

$$\tilde{T}^{i+1} - T^{i+1} = \left(1+\Delta\theta\right)\varepsilon \tag{17}$$

It can be seen that for a numerically unstable system, any error will grow in the forward time integration even when Crank-Nicolson difference scheme has been used.

4. A Point Model Approach

Consider as an example temperature in a heat generating body. If heat conduction is not considered, the mathematical equation representing such a model may not involve any boundary condition. Then it is not an initial boundary value problem, and there could be no restriction for forward or backward integration in time. But, there are still conditions that need to be fulfilled before a solution could be used to predict future or past events.

When electric current is passing through a heating element, due to the resistance heat is generated in the element. At the beginning, some of this heat is loss to the surrounding and the remainder causes a raise in the temperature. The

heat loss can be calculated by knowing the heat transfer coefficient and the temperature difference between the heating element and the surrounding. The temperature rise can be calculated if the heat capacity of the element is known. A stationary temperature will be reached when the rate of heat generation is equal to that of heat loss. Using a point model approach, temperature is represented by a single value and could be found by the following ordinary differential equation:

$$\frac{\mathrm{d}T}{\mathrm{d}t} = \frac{1}{c}\left[Q - hT\right] = c_1 - c_2 T \tag{18}$$

where T is the temperature relative to the surrounding temperature, Q the heat generation rate, h the heat transfer coefficient, c the heat capacity and t is time. In this equation, $c_1 = \frac{Q}{c}$ and $c_2 = \frac{h}{c}$ are parameters characteristic of the system. Equation (18) can be cast in a normalized form where all the quantities involved are dimensionless. Although c_1 and c_2, are related to the physical properties such as conductivity, density, heat capacity as well as to the system dimensions and how cooling is being carried out, they could be directly determined from the system by calibration. The analytical solution for Equation (18) is:

$$T = \frac{c_1}{c_2} + \left[T_0 - \frac{c_1}{c_2}\right]\exp\left(-c_2 t\right) \tag{19}$$

where T_0 is the initial temperature at $t = 0$. The solutions for different starting temperature are shown in Figure 1.

As there is a one to one relationship between T and t, this arrangement could be used as a time-measuring device by using two temperature readings to find out the time between them. One of the essential conditions is that the temperature at the starting must be known so that the appropriate curve may be used. For example, depending on which curve is used a temperature reading of 85 will give different times since the system is turned on. Only knowing the initial temperature, the curve could be selected correctly.

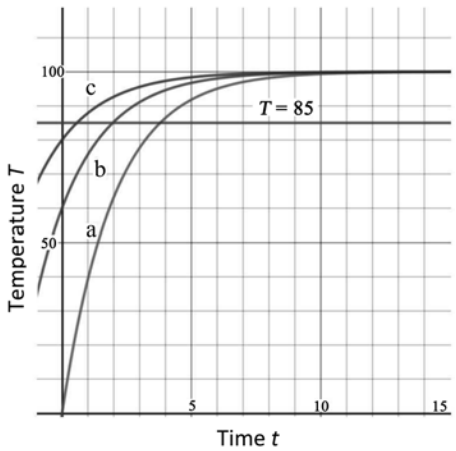

Figure 1. Temperature histories in dimensionless time for $c_1 = 0.5$, $c_2 = 50$ and $T_0 = 0$ (Curve *a*), 60 (Curve *b*) and 80 (Curve *c*).

For good measurement sensibility, the device must be designed to operate over the range $t<5$. When $t>10$ there is very little change of temperature with time and the device is no longer sensitive enough for measurement. On the other hand, as a controlling device, the chosen operating parameters should be such that $t>10$ could be reached within the design specification for the change to attain equilibrium quickly. Also needed is that the operation conditions must be close to those used in the calibration.

Perhaps one feature unique to this device as compared with other clocks is the fact that time lapse of a past event could be found. That is to measure time backward. This principle is used in radiometric dating that is described by the same Equation (19) with $c_1 = 0$. The accuracy relies on the fact that the half-life of a radioactive isotope is a constant and could be easily determined. However, to measure the time accurately the initial conditions must be known. That is only the time lapse between two known events can be found.

5. Linearization of a Non-Linear Problem

There are not many cases where non-linear problems have analytical solutions. A numerical approach would be needed to replace the problem by a linearized approximation at each forward time step. In non-linear form, Equation (18) becomes

$$\frac{\mathrm{d}T(t)}{\mathrm{d}t}=\frac{1}{c(T,t)}\left[Q(T,t)-h(T,t)T(t)\right]=c_1(T,t)-c_2(T,t)T(t) \tag{20}$$

The temperature and time dependency is replaced by the averages at the i^{th} and $(i+1)^{\text{th}}$ time step so that in linearized form

$$\frac{\mathrm{d}T(t)}{\mathrm{d}t}=\tilde{c}_1-\tilde{c}_2T(\bar{t}) \tag{21}$$

where $\tilde{c}_1=\frac{1}{2}\left[c_1\left(T^{i+1},t^{i+1}\right)+c_1\left(T^{i},t^{i}\right)\right]$, $\tilde{c}_2=\frac{1}{2}\left[c_2\left(T^{i+1},t^{i+1}\right)+c_2\left(T^{i},t^{i}\right)\right]$, and $\bar{t}=\frac{1}{2}\left(t^{i}+t^{i+1}\right)$. As T^{i+1} is yet to be determined, iteration is needed in the forward integration procedure. If a stationary solution does exist, this scheme should be stable. Solution of Equation (21) is in the same form as Equation (19) and the integration could be carried from t^i to t^{i+1} smoothly. Should there be any error such as that due to numerical truncation; the error would decay exponentially and eventually disappear from the final solution. However, if a backward integration in time is carried out, an error would grow exponentially, meaning that the backward time integration would be unstable also for a non-linear problem. Therefore, $T(t\gg 0)$ could not be used to recover $T(t=0)$ by backward integration due to two reasons: 1) due to exponential decay the contribution of the initial value has already become insignificant in $T(t\gg 0)$, and 2) the initial value so obtained could have come from very small error in the starting input.

The same approach could be applied to more complex field, for example, dynamic study of a rotor in a turbine based on a point model [9], propagation of complex electromagnetic waves in optical fibres [10] and matter-wave laser [11]. In every case, providing the system is operating within parametric stability domain, stationary solutions could be found numerically from arbitrarily chosen initial guesses. In all those cases, iterations are needed to solve the linearized equations. It is not possible to back track from the stationary solutions and recover the initial values because they are arbitrarily chosen.

6. Conclusions

Every physical problem that could be described by a well-posed transient field equation starts with an initial value. For a real and conservative system this initial value would decay and eventually disappear leaving only the stationary solution. It would be normally impossible to recover the initial value from the stationary solution by working backward in time. If it was possible to identify the very small remnant of the initial value after a long time history, the recovery relies on tracing back exactly its histories at every step. This is certainly not possible in a numerical procedure.

Forward numerical integration in a conservative transient field equation is normally stable. But backward time integration of the same system is numerically unstable.

System parameters could be fine-tuned to allow backward time integration. However, problems about the recovery of the initial value and numerical stability also apply to this fine-tuned system.

No matter how well-tuned a system could be the time interval between two events cannot be accurately measured unless the fields for the two events are known.

Observations in a conservative system in equilibrium should not change in time either forward or backward. If a numerical model predicts the field intensity, for example temperature is very much larger in the past, such a prediction can only come from numerical instability and inaccuracy in the measurements.

Conflicts of Interest

The author declares no conflicts of interest regarding the publication of this paper.

References

[1] Gershenfeld, N. (1998) The Nature of Mathematical Modeling. Cambridge University Press, Cambridge.

[2] Lin, C.C. and Segel, L.A. (1988) Mathematics Applied to Deterministic Problems in the Natural Sciences. SIAM, Philadelphia. https://doi.org/10.1137/1.9781611971347

[3] Mallinson, G.D. and de Vahl Davis, D. (1973) The Method of the False Transient for the Solution of Coupled Elliptic Equations. *Journal of Computational Physics*, **12**, 435-461. https://doi.org/10.1016/0021-9991(73)90097-1

[4] Shestakov, A.I., Milovich, J.L. and Noy, A. (2002) Solution of the Nonlinear Poisson-Boltzmann Equation Using Pseudo-Transient Continuation and the Finite Element Method. *Journal of Colloid and Interface Science*, **247**, 62-79. https://doi.org/10.1006/jcis.2001.8033

[5] Bourdin, B., Francfort, G.A. and Marigo, J.-J. (2000) Numerical Experiments in Revisited Brittle Fracture. *Journal of the Mechanics and Physics of Solids*, **48**, 797-826. https://doi.org/10.1016/S0022-5096(99)00028-9

[6] Renner, I.W., *et al.* (2015) Point Process Models for Presence-Only Analysis. *Methods in Ecology and Evolution*, **6**, 366-379. https://doi.org/10.1111/2041-210X.12352

[7] Chen, P.Y.P. (2014) Axisymmetric Thermal Stresses in an Anisotropic Finite Hollow Cylinder. In: Hetnarski, R.B., Ed., *Encyclopedia of Thermal Stresses*, Springer, Dordrecht, 295-304. https://www.springer.com/gp/book/9789400727380 https://doi.org/10.1007/978-94-007-2739-7_210

[8] Paul, R.P. (1981) Robot Manipulators. The MIT Press, Cambridge and London.

[9] Chen, P.Y.P., Feng, N., Hahn, E. and Wu, W. (2005) Recent Development in Turbomachinery Modeling Improved Balancing and Vibration Response Analysis. *Journal of Engineering for Gas Turbines and Power*, **127**, 646-653. https://doi.org/10.1115/1.1850942

[10] Chen, P.Y.P., Malomed, B.A. and Chu, P.L. (2006) Optimal Preprocessing of Pulses for Dispersion Management. *Journal of the Optical Society of America B*, **23**, 1257-1261. https://doi.org/10.1364/JOSAB.23.001257

[11] Chen, P.Y.P. and Malomed, B.A. (2006) Stable Circulation Modes in a Dual-Core Matter-Wave Soliton Laser. *Journal of Physics B*: *Atomic*, *Molecular and Optical Physics*, **39**, 2803-2813. https://doi.org/10.1088/0953-4075/39/12/014

Applied Mathematics, 2019, 10, 728-742
https://www.scirp.org/journal/am
ISSN Online: 2152-7393
ISSN Print: 2152-7385

Analysis of an Inventory System for Items with Stochastic Demand and Time Dependent Three-Parameter Weibull Deterioration Function

Nwoba Pius Ophokenshi[1], Chukwu Walford Ikechukwu Emmanuel[2], Maliki Olaniyi Sadik[3]

[1]Department of Industrial Mathematics and Applied Statistics, Ebonyi State University, Abakaliki, Nigeria
[2]Department of Statistics, University of Nigeria, Nsuka, Nigeria
[3]Department of Mathematics, Michael Okpara University of Agriculture, Umudike, Nigeria
Email: ophokenshiphd@gmail.com, walford.chukwu@unn.edu.ng, somaliki@gmail.com

How to cite this paper: Ophokenshi, N.P., Emmanuel, C.W.I. and Sadik, M.O. (2019) Analysis of an Inventory System for Items with Stochastic Demand and Time Dependent Three-Parameter Weibull Deterioration Function. *Applied Mathematics*, **10**, 728-742.
https://doi.org/10.4236/am.2019.109052

Received: June 11, 2019
Accepted: September 15, 2019
Published: September 18, 2019

Abstract

In recent times, mathematical models have been developed to describe various scenarios obtainable in the management of inventories. These models usually have as objective the minimizing of inventory costs. In this research work we propose a mathematical model of an inventory system with time-dependent three-parameter Weibull deterioration and a stochastic type demand in the form of a negative exponential distribution. Explicit expressions for the optimal values of the decision variables are obtained. Numerical examples are provided to illustrate the theoretical development.

Keywords

Inventory Model, Deteriorating Items, Weibull Distribution, Stochastic Demand, MathCAD14

1. Introduction

Inventory holding refers to producing ahead of demand and sales realizations [1]. The total investment in inventories is enormous and accounts for nearly half of the total logistics cost [2]. In view of this high cost, the management of inventory offers high potential for improvement and results in a relatively rich literature on theoretic inventory models. In inventory planning and control, the performance measures adopted should encourage the positive aspects of holding inventory such as providing flexibility, providing resources for production, providing responsive customer service. We observe that inventory arises in many

different situations. It is unlikely that the same inventory planning and control considerations will apply equally to all categories of inventory [3].

Some type of products may undergo change in value in storage. They may become partially or entirely unfit for consumption in the course of time. This change or deterioration can be defined as any process that prevents an item from being used for its intended original purpose. Following its utility, the deteriorating item can be characterized into either an item whose functionality or physical fitness deteriorates over time (e.g. fresh food or medicine) or an item whose functionality does not degrade, but where demand deteriorates over time as customers' perceived utility decreases (e.g. fashion clothes, high technology products or newspapers). Both categories pertain to the same problem but require different actions seeing that items that lose their functional characteristics and quality often cannot, or should not be kept in inventory. However, items that lose perceived utility can be kept in inventory and may be sold on a secondary market.

The main objective of inventory management for deteriorating items is to obtain optimal returns during the useful lifetime of the product [3]. This leads to three main issues: determining reasonable and appropriate methods for issuing inventory, replenishing inventory and allocating inventory. The choice of inventory valuation methods adopted in issuing inventory (*i.e.* the order in which the items are to be issued), such as methods based on time sequence including FIFO (first-in, first-out) and LIFO (last-in, first-out), depends on both the intrinsic characteristics of the inventory (e.g. lifetime, quantity, variety, issuing frequency etc.) and the influence on the company (e.g. inventory balance, cost of goods sold etc.) [4].

1.1. Mathematical Formulation

A rich literature on modelling of deteriorating inventory shows how the deterioration of products has been captured in the research problem up till now. To integrate deterioration into mathematical models, the model type (deterministic or stochastic) and the considered time horizon (infinite or finite) lead to specific methods [4].

1.2. Deterioration Process Modeling Approaches

Many researchers have analyzed inventory control of deteriorating items from different perspectives. Broadly speaking, the existing literature in this field can be divided into the following three classes from the perspective of the modeling approach. These classes are schematically illustrated in **Figure 1**.

$I(t)$: *On-hand inventory as a function of time t.*

$\theta(t)$: *Deterioration function of time t.*

$D(t)$: *Demand function of time t.*

$P(t)$: *Production rate as a function of time t.*

$H(t)$: *Holding cost of one unit in-stock for t units of time.*

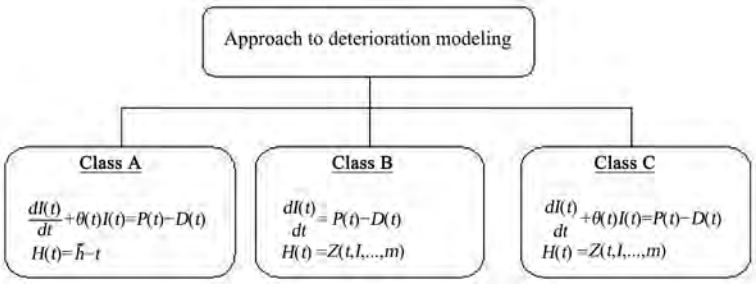

Figure 1. Categorization of deterioration modeling schemes.

$\tilde{h}$: *A positive constant.*

$Z(t,I,\cdots,m)$: *A non-linear increasing positive function of finite number of parameters such as stocking time, t, on-hand inventory, I, etc.*

1.2.1. Class A: Non-Linear Inventory Function

Most researches on deteriorating inventory consider that inventory decays with time, in different patterns. Thus, the on-hand inventory function can be determined by the differential equation:

$$\frac{\mathrm{d}I(t)}{\mathrm{d}t}+\theta(t)I(t)=P(t)-D(t) \tag{1}$$

here $I(t)$ is the inventory level at time *t*, $P(t)$ and $D(t)$ indicate the deterioration rate functions, the production rate and the demand rate as a function of time *t* respectively

In this type of research it is considered that the holding cost per unit item per unit time (holding cost rate) is constant. In other words, the holding cost is linear in terms of parameters like stocking time, *t*, and the on-hand inventory level, *I*, that can be stated as $\tilde{h}tI$, $\tilde{h}>0$ where is constant.

This kind of modeling approach is more appropriate for decaying items and was used in the earliest researches on deteriorating products. Ghare and Schrader [5] seem to have been the first to have developed an exponentially deteriorating inventory model by defining a constant decaying rate.

1.2.2. Class B: Non-Linear Holding Cost

The deterioration process directly affects the on-hand inventory function and thereby inventory holding cost modeling. In this category, the on-hand inventory function form is similar to its form of non-deteriorating products and can be obtained by the differential equation:

$$\frac{\mathrm{d}I(t)}{\mathrm{d}t}=P(t)-D(t) \tag{2}$$

Here, instead of considering the deterioration rate function, $\theta(t)$ in the on-hand inventory function, the holding cost, *H*, is considered as a non-linear increasing positive function of parameters like stocking time, *t* or on-hand inventory *I*.

Considering a non-linear time-dependent holding cost is more suitable for

deteriorating items-especially perishable ones—when the value and quality of the unsold items decrease with time, as in the case of green vegetables. For products such as electronic components, radioactive substances, volatile liquids etc., where more sophisticated tools are required for their security and safety in stock, a non-linear stock-dependent holding cost can be appropriate.

1.2.3. Class C: Non-Linear Inventory Function and Non-Linear Holding Cost

This modeling approach is more complicated than the other two. Here, both the deterioration rate function, $\theta(t)$, a feature of Class A, and the non-linear holding cost, a feature of Class B, are considered to model the inventory system of deteriorating products. In [6] the authors discussed Goh's model, considering a constant $\theta(t)$ in addition to non-linear holding cost in two time-dependent and stock-dependent cases.

1.3. The Demand Characteristics

The customer arrival rate per time period may be deterministic or stochastic, each individual demand may be deterministic or stochastic and each individual demand may also be discrete or continuous [7] [8]. Demand plays a key role in the modeling of deteriorating inventory. Aiming towards satisfying customer demand, companies employ demand forecasts as a prediction of customer behaviour. The following variations of demand labeled from the point of view of real life situations have been recognized and studied by a number of researchers such as Khanra *et al*. [9]. It is assumed that demand is known with certainty in a deterministic demand process. Stochastic demand process on the other hand basically incorporates randomness and unpredictability.

A deterministic demand distribution can be categorized into:

1) Uniform demand, *i.e*. demand is a constant, fixed number of items.

2) Time-varying demand.

3) Stock-dependent demand.

4) Price-dependent demand.

A combination of the above is also possible.

In the case of stochastic demand models, a further distinction is made between a specific type of probability distribution and an arbitrary probability distribution. Although modeling in a deterministic setting is more straightforward, a stronger focus on stochastic modeling of deteriorating inventory is suggested in order to better represent inventory control in practice since customer demand is variable in time and uncertain in terms of quantification.

1.4. Stochastic Demand Function

From a real life point of view, a stochastic demand distribution is more reasonable, because demand and supply is not always known but can be controlled by using probability distribution function. Although less than 20% of the developed models in the literature (after 2001) can be classified as stochastic demand mod-

els, Bakker *et al*. [10]. However, before 2001 researchers mostly concentrated on developing basic models under certain conditions, such as inventory models with stock dependent items. Based on Goyal and Giri [11], stochastic demand functions in the existing literature can be seen in two ways:

- Taking into consideration a specific type of probability distribution function (PDF) such as Ravichandram [12] and Weiss [13] who developed inventory models for deteriorating products assuming Poisson demand function.
- Considering an arbitrary probability distribution function (PDF) for end customer's demand such as Aggoun *et al*. [14] and Lian *et al*. [15]. According to Bakker *et al*., since 2001 only about 4% of developed researches on deteriorating inventories provide models with an arbitrary probability distribution for demand.

1.5. Proposed Deterioration Model

The Weibull distribution $W(t)=\alpha\beta(t-\gamma)^{\beta-1}\exp\left(-\alpha(t-\gamma)^{\beta}\right), t>0$, having exponential and Rayleigh as submodels, is often used for modeling lifetime data. When modeling monotone hazard rates, the Weibull distribution may be an initial choice because of its negatively and positively skewed density shape. Rinne [16] suggested that a three-parameter generalization of the Weibull distribution deals with general situations in modeling survival process with various shapes in the hazard function. Chakrabarty *et al*. [17] provided rationale for considering three-parameter Weibull deterioration rate. They discovered that many products that start deteriorating appreciably only after a certain period (e.g. after they are produced) and for which the rate of deterioration increases over time have a deterioration rate best described by a Weibull distribution (**Figure 2**).

1.6. Negative Exponential Distribution

The low flow of traffic can be modeled using the negative exponential distribution. The probability density of the negative exponential distribution is given as

$$f(t)=\lambda e^{-\lambda t},\ t\geq 0 \tag{3}$$

where λ is a parameter that determines the shape of the distribution. **Figure 3** displays the exponential distribution for some values of λ.

We observe that the probability that the random variable t is greater than or equal to zero is given by;

$$p(t\geq 0)=\int_0^{\infty} f(t)\mathrm{d}t=\int_0^{\infty}\lambda e^{-\lambda t}\mathrm{d}t=1$$

The probability that the random variable t is greater than a specific value h is

$$p(t\geq h)=1-p(t<h)=1-\int_0^{h}\lambda e^{-\lambda t}\mathrm{d}t=e^{-\lambda h}$$

Unlike many other distributions, one of the key advantages of the negative exponential distribution is the existence of a closed form solution for the probability density function.

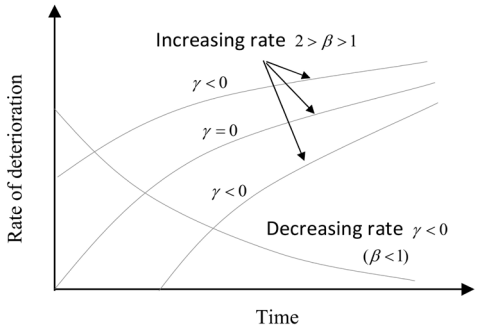

Figure 2. Rate of deterioration-time relationship for a three-parameter Weibull distribution.

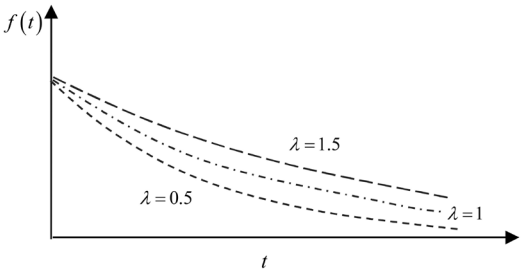

Figure 3. Graphical profile of the negative exponential distribution for various values of λ.

1.7. Notations and Assumptions of the Model

We adopt the following notations and assumptions in the derivation of our model.

Notations:

c_1: inventory holding cost per unit per unit time.

c_2: shortage cost per unit per unit time.

c_3: ordering cost per order.

c_4: unit purchasing cost.

$D(t)$: demand rate at any time, $t \geq 0$.

T: cycle time.

I_0: initial inventory size.

$\theta(t) = \alpha\beta(t-\gamma)^{\beta-1}$: instantaneous rate function for a three-parameter Weibull distribution; where α is the scale parameter, β is the shape parameter and γ is the location parameter. Also, $0 < \alpha \ll 1$.

t_1: time during which there is no shortage.

κ: a constant value between 0 and 1.

T^*: optimal value of T.

I_0^*: optimal value of I_0.

t_1^*: optimal value of t_1.

κ^*: optimal value of κ.

Assumptions

1) The inventory system under consideration deals with single item.

2) The planning horizon is infinite.

3) The demand rate is stochastic and given by the negative exponential distribution as a function of time *t*, *i.e.* $D(t)=\lambda e^{-\lambda t}$, where $\lambda>0$, is the parameter of the distribution.

4) Shortages in the inventory are allowed and completely backlogged.

5) The supply is instantaneous and the lead time is zero.

6) Deteriorated unit is not repaired or replaced during a given cycle.

7) The holding cost, ordering cost, shortage cost and unit cost remain constant over time.

8) There are no quantity discounts.

9) The distribution of the time to deterioration of the items follows the three-parameter Weibull distribution, *i.e.*
$W(t)=\alpha\beta(t-\gamma)^{\beta-1}\exp\left(-\alpha(t-\gamma)^{\beta}\right), t>0$. The instantaneous rate function is $\theta(t)=\alpha\beta(t-\gamma)^{\beta-1}$.

2. Mathematical Formulation of the Model

At the beginning of the cycle, the inventory level $I(t)$ reaches its maximum $I(0)=I_0$ units of item at time $t=0$. During the interval $[0,t_1]$, the inventory level depletes due to the combine effects of demand and deterioration. At $t=t_1$, the inventory level is zero and all the demand hereafter (*i.e.* $T-t_1$) is completely backlogged. The total number of backordered items is replaced by the next replenishment. A graphical representation of this inventory system is depicted in Figure 4. Since the depletion of the units is due to demand and deterioration, the rate of change of the inventory level at any time t is governed by the differential equations:

$$\frac{\mathrm{d}I(t)}{\mathrm{d}t}+\theta(t)I(t)=P(t)-D(t),\quad 0\le t<t_1 \tag{4}$$

with boundary conditions $I(0)=I_0$ and $I(t_1)=0$. Furthermore the production rate $P(t)$ is zero in this case, thus in the interval $0\le t<t_1$, the initial value problem to be solved is;

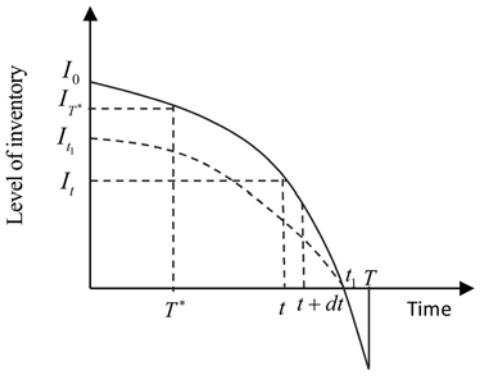

Figure 4. An Economic Order Quantity (EOQ) model with shortages and deterioration.

$$\frac{\mathrm{d}I(t)}{\mathrm{d}t}+\theta(t)I(t)=-D(t),\quad I(0)=I_0,\ I(t_1)=0 \tag{5}$$

In the interval $t_1 \le t \le T$, the initial value problem becomes;

$$\frac{\mathrm{d}I(t)}{\mathrm{d}t}=-D(t),\quad I(t_1)=0 \tag{6}$$

Employing the previously stated assumptions, we have:

$$\frac{\mathrm{d}I(t)}{\mathrm{d}t}+\alpha\beta(t-\gamma)^{\beta-1}I(t)=-\lambda\mathrm{e}^{-\lambda t},\ 0\le t<t_1 \tag{7}$$

$$\frac{\mathrm{d}I(t)}{\mathrm{d}t}=-\lambda\mathrm{e}^{-\lambda t},\quad t_1\le t\le T \tag{8}$$

2.1. Solution of the Model

Equation (7) is a first order differential equation and its integrating factor is:

$$\exp\left[\alpha\beta\int(t-\gamma)^{\beta-1}\,\mathrm{d}t\right]=\mathrm{e}^{\alpha(t-\gamma)^{\beta}} \tag{9}$$

$$\frac{\mathrm{d}}{\mathrm{d}t}\left[I(t)\mathrm{e}^{\alpha(t-\gamma)^{\beta}}\right]=-\lambda\mathrm{e}^{-\lambda t}\mathrm{e}^{\alpha(t-\gamma)^{\beta}}$$

$$\therefore\quad \left[I(t)\mathrm{e}^{\alpha(t-\gamma)^{\beta}}\right]_t^{t_1}=-\lambda\int_t^{t_1}\mathrm{e}^{-\lambda t+\alpha(t-\gamma)^{\beta}}\,\mathrm{d}t$$

Taking first order approximation of the integrand, we have

$$\mathrm{e}^{-\lambda t+\alpha(t-\gamma)^{\beta}}\approx 1+\left\{-\lambda t+\alpha(t-\gamma)^{\beta}\right\}=1-\lambda t+\alpha(t-\gamma)^{\beta}$$

$$\begin{aligned}\Rightarrow\ & I(t_1)\mathrm{e}^{\alpha(t_1-\gamma)^{\beta}}-I(t)\mathrm{e}^{\alpha(t-\gamma)^{\beta}}\\ &=-\lambda\int_t^{t_1}\left\{1-\lambda t+\alpha(t-\gamma)^{\beta}\right\}\mathrm{d}t\\ &=\frac{2\alpha\lambda\left[(t-\gamma)^{\beta+1}-(t_1-\gamma)^{\beta+1}\right]+\lambda(t-t_1)(2\beta-\lambda t-\lambda t_1+2)-\beta\lambda^2\left(t^2-t_1^2\right)}{2(\beta+1)}\end{aligned}$$

Applying the boundary condition $I(t_1)=0$, we get

$$\begin{aligned}& I(t)\mathrm{e}^{\alpha(t-\gamma)^{\beta}}\\ &=\frac{2\alpha\lambda\left[(t-\gamma)^{\beta+1}-(t_1-\gamma)^{\beta+1}\right]+\lambda(t-t_1)(2\beta-\lambda t-\lambda t_1+2)-\beta\lambda^2\left(t^2-t_1^2\right)}{2(\beta+1)}\end{aligned}$$

$$\Rightarrow I(t)=\frac{2\alpha\lambda\left[(t-\gamma)^{\beta+1}-(t_1-\gamma)^{\beta+1}\right]+\lambda(t-t_1)(2\beta-\lambda t-\lambda t_1+2)-\beta\lambda^2\left(t^2-t_1^2\right)}{2(\beta+1)}\mathrm{e}^{-\alpha(t-\gamma)^{\beta}} \tag{10}$$

Hence

$$I(0)=I_0=\frac{2\alpha\lambda\left[(-\gamma)^{\beta+1}-(t_1-\gamma)^{\beta+1}\right]-\lambda t_1(2\beta-\lambda t_1+2)+\beta\lambda^2t_1^2}{2(\beta+1)}\mathrm{e}^{-\alpha(-\gamma)^{\beta}} \tag{11}$$

From Equation (8), in the interval $t_1\le t\le T$ we obtain the solution

$$\left[I(t)\right]_{t_1}^{t} = -\lambda\int_{t_1}^{t} \mathrm{e}^{-\lambda t}\mathrm{d}t = -\lambda\left[-\frac{1}{\lambda}\mathrm{e}^{-\lambda t}\right]_{t_1}^{t} = \mathrm{e}^{-\lambda t} - \mathrm{e}^{-\lambda t_1}$$

$$\therefore\ I(t) = \mathrm{e}^{-\lambda t} - \mathrm{e}^{-\lambda t_1} \tag{12}$$

Hence, the inventory level at any time $t \in [0,T]$ is given by

$$I(t) = \begin{cases} \dfrac{2\alpha\lambda\left[(t-\gamma)^{\beta+1} - (t_1-\gamma)^{\beta+1}\right] + \lambda(t-t_1)(2\beta - \lambda t - \lambda t_1 + 2) - \beta\lambda^2\left(t^2 - t_1^2\right)}{2(\beta+1)}\mathrm{e}^{-\alpha(t-\gamma)^{\beta}} & 0 \le t < t_1 \\ \mathrm{e}^{-\lambda t} - \mathrm{e}^{-\lambda t_1} & t_1 \le t \le T \end{cases} \tag{13}$$

The total cost per unit time, $\phi(T,t_1)$, of the inventory system consist of the deterioration cost (*DC*), the shortage cost (*SC*), the holding cost (*HC*) and the ordering cost (*OC*). Put differently, the total cost per unit time is:

$$\phi(T,t_1) = \frac{1}{T}(DC + SC + HC + OC) \tag{14}$$

We derive the components of the total relevant cost as follows:

The total quantity of deteriorated items in the time interval $[0,t_1]$ is given by

$$\begin{aligned} D &= \text{Initial inventory} - \text{Total demand within } [0,t_1] \\ &= I_0 - \int_0^{t_1} \lambda\mathrm{e}^{-\lambda t}\mathrm{d}t = I_0 - \left(1 - \mathrm{e}^{-\lambda t_1}\right) \end{aligned} \tag{15}$$

Thus, the deterioration cost per unit time is

$$DC = c_1\left(I_0 - 1 + \mathrm{e}^{-\lambda t_1}\right) \tag{16}$$

The average shortage cost within $[t_1,T]$ is

$$SC = c_2\int_{t_1}^{T} \lambda\mathrm{e}^{-\lambda t}(T-t)\mathrm{d}t = \frac{c_2}{\lambda}\left[(\lambda T - \lambda t_1 - 1)\mathrm{e}^{-\lambda t_1} + \mathrm{e}^{-\lambda T}\right] \tag{17}$$

The average inventory holding cost accumulated over the period $[0,t_1]$ is:

$$HC = c_3\int_0^{t_1} I(t)\mathrm{d}t \tag{18}$$

The total inventory cost per unit time is:

$$\phi(T,t_1) = \frac{1}{T}\left\{c_1\left(I_0 - 1 + \mathrm{e}^{-\lambda t_1}\right) + \frac{c_2}{\lambda}\left[(\lambda T - \lambda t_1 - 1)\mathrm{e}^{-\lambda t_1} + \mathrm{e}^{-\lambda T}\right] + c_3\int_0^{t_1} I(t)\mathrm{d}t + c_4\right\} \tag{19}$$

Here c_1, c_2, c_3 are constants as well as c_4 the ordering cost, assumed constant.

We assume $t_1 = \kappa T$; $0 < \kappa < 1$. This assumption appears reasonable since the length of the shortage interval is a fraction of the cycle time. Substituting $t_1 = \kappa T$ in Equation (19), we get:

$$\phi(T,\kappa) = \frac{1}{T}\left\{c_1\left(I_0^{\kappa} - 1 + \mathrm{e}^{-\lambda\kappa T}\right) + \frac{c_2}{\lambda}\left[(\lambda T - \lambda\kappa T - 1)\mathrm{e}^{-\lambda\kappa T} + \mathrm{e}^{-\lambda T}\right] + c_3\int_0^{\kappa T} I(t)\mathrm{d}t + c_4\right\} \tag{20}$$

$$I_0^{\kappa} = \frac{2\alpha\lambda\left[(-\gamma)^{\beta+1} - (\kappa T - \gamma)^{\beta+1}\right] - \lambda\kappa T(2\beta - \lambda\kappa T + 2) + \beta\lambda^2\kappa^2T^2}{2(\beta+1)}\mathrm{e}^{-\alpha(-\gamma)^{\beta}} \tag{21}$$

We now proceed to determine the optimal values of T and κ. The total av-

erage cost per unit time $\phi(T,\kappa)$ is now a function of two variables T and κ, its partial derivatives with respect to T and κ are computed and the result equated to zero. We have

$$\frac{\partial}{\partial T}\phi(T,\kappa)=\frac{1}{T}\left\{c_1\left(\frac{\partial I_0^{\kappa}}{\partial T}+\frac{\partial \mathrm{e}^{-\lambda\kappa T}}{\partial T}\right)+\frac{c_2}{\lambda}\left[\frac{\partial}{\partial T}(\lambda T-\lambda\kappa T-1)\mathrm{e}^{-\lambda\kappa T}+\frac{\partial}{\partial T}\mathrm{e}^{-\lambda T}\right]+c_3\frac{\partial}{\partial T}\int_0^{\kappa T}I(t)\mathrm{d}t+c_4\right\}$$

$$\frac{\partial I_0^{\kappa}}{\partial T}=\frac{\mathrm{e}^{-\alpha(-\gamma)^{\beta}}}{2(\beta+1)}\left[\kappa\lambda(2\beta-\kappa\lambda T+2)-\kappa^2\lambda^2T-2\kappa^2\lambda^2\beta T+2\alpha\kappa\lambda(\beta+1)(\kappa T-\gamma)^{\beta}\right] \quad (22)$$

$$\frac{\partial}{\partial T}(\lambda T-\lambda\kappa T-1)\mathrm{e}^{-\lambda\kappa T}=\lambda\mathrm{e}^{-\lambda\kappa T}(1-\kappa)-\lambda\kappa\mathrm{e}^{-\lambda\kappa T}(\lambda\kappa T-\lambda T+1) \quad (23)$$

The Lebnitz rule for differentiating the integral $I(\alpha)=\int_{a(\alpha)}^{b(\alpha)}f(x,\alpha)\mathrm{d}x$ is given by

$$\frac{\mathrm{d}I(\alpha)}{\mathrm{d}\alpha}=f(b,\alpha)\frac{\mathrm{d}b}{\mathrm{d}\alpha}-f(b,\alpha)\frac{\mathrm{d}a}{\mathrm{d}\alpha}+\int_a^b\frac{\partial f(x,\alpha)}{\partial\alpha}\mathrm{d}x$$

Applying this rule to $\frac{\partial}{\partial T}\int_0^{\kappa T}I(t,T)\mathrm{d}t$, we get

$$\frac{\partial}{\partial T}\int_0^{\kappa T}I(t,T)\mathrm{d}t=\int_0^{\kappa T}\frac{\partial}{\partial T}I(t,T)\mathrm{d}t+\kappa I(\kappa,T) \quad (24)$$

Hence

$$\begin{aligned}\frac{\partial}{\partial T}\phi(T,\kappa)=\frac{1}{T}\Bigg\{&\frac{c_1\mathrm{e}^{-\alpha(-\gamma)^{\beta}}}{2(\beta+1)}\Big[\kappa\lambda(2\beta-\kappa\lambda T+2)-\kappa^2\lambda^2T-2\kappa^2\lambda^2\beta T\\&+2\alpha\kappa\lambda(\beta+1)(\kappa T-\gamma)^{\beta}\Big]-\lambda\kappa\mathrm{e}^{-\lambda\kappa T}\\&+\frac{c_2}{\lambda}\Big[\lambda\mathrm{e}^{-\lambda\kappa T}(1-\kappa)-\lambda\kappa\mathrm{e}^{-\lambda\kappa T}(\lambda\kappa T-\lambda T+1)-\lambda\mathrm{e}^{-\lambda T}\Big] \quad (25)\\&+c_3\int_0^{\kappa T}\frac{\partial}{\partial T}I(t,T)\mathrm{d}t+\kappa I(\kappa,T)\Bigg\}\\=0\end{aligned}$$

Similarly;

$$\frac{\partial}{\partial\kappa}\phi(T,\kappa)=\frac{1}{T}\left\{c_1\left(\frac{\partial I_0^{\kappa}}{\partial\kappa}+\frac{\partial \mathrm{e}^{-\lambda\kappa T}}{\partial\kappa}\right)+\frac{c_2}{\lambda}\left[\frac{\partial}{\partial\kappa}(\lambda T-\lambda\kappa T-1)\mathrm{e}^{-\lambda\kappa T}+\frac{\partial}{\partial\kappa}\mathrm{e}^{-\lambda T}\right]+c_3\frac{\partial}{\partial\kappa}\int_0^{\kappa T}I(t)\mathrm{d}t\right\}$$

$$\frac{\partial I_0^{\kappa}}{\partial\kappa}=\frac{\mathrm{e}^{-\alpha(-\gamma)^{\beta}}}{2(\beta+1)}\left[\lambda T(2\beta-\kappa\lambda T+2)-\kappa\lambda^2T^2-2\kappa\beta\lambda^2T^2+2\alpha\lambda T(\beta+1)(\kappa T-\gamma)^{\beta}\right] \quad (26)$$

$$\frac{\partial}{\partial\kappa}(\lambda T-\lambda\kappa T-1)\mathrm{e}^{-\lambda\kappa T}=-\lambda T\mathrm{e}^{-\lambda\kappa T}-\lambda T(\lambda\kappa T-\lambda T+1)\mathrm{e}^{-\lambda\kappa T} \quad (27)$$

and

$$\frac{\partial}{\partial \kappa}\int_0^{\kappa T} I(t,T)\,\mathrm{d}t = \int_0^{\kappa T}\frac{\partial}{\partial \kappa} I(t,T)\,\mathrm{d}t + TI(\kappa,T) \tag{29}$$

Hence

$$\begin{aligned}\frac{\partial}{\partial \kappa}\phi(T,\kappa) = \frac{1}{T}\Bigg\{&\frac{c_1 \mathrm{e}^{-\alpha(-\gamma)^{\beta}}}{2(\beta+1)}\Big[\lambda T(2\beta-\kappa\lambda T+2)-\kappa\lambda^2T^2-2\kappa\beta\lambda^2T^2\\&+2\alpha\lambda T(\beta+1)(\kappa T-\gamma)^{\beta}\Big]-\lambda\kappa\mathrm{e}^{-\lambda\kappa T}\\&+\frac{c_2}{\lambda}\Big[-\lambda T\mathrm{e}^{-\lambda\kappa T}-\lambda T(\lambda\kappa T-\lambda T+1)\mathrm{e}^{-\lambda\kappa T}\Big]\\&+c_3\int_0^{\kappa T}\frac{\partial}{\partial \kappa} I(t,T)\,\mathrm{d}t + TI(\kappa,T)\Bigg\}\\=0\end{aligned} \tag{30}$$

where

$$I(t,T) = \frac{2\alpha\lambda\left[(t-\gamma)^{\beta+1}-(\kappa T-\gamma)^{\beta+1}\right]+\lambda(t-\kappa T)(2\beta-\lambda t-\lambda\kappa T+2)-\beta\lambda^2\left(t^2-\kappa^2T^2\right)}{2(\beta+1)}\mathrm{e}^{-\alpha(t-\gamma)^{\beta}}$$

and

$$\begin{cases}\dfrac{\partial}{\partial T} I(t,T) = -\dfrac{\kappa\lambda^2(t-\kappa T)+\kappa\lambda(2\beta-\lambda t-\kappa\lambda T+2)-2\beta\kappa^2\lambda^2T+2\alpha\kappa\beta(\beta+1)(\kappa T-\gamma)^{\beta}}{2(\beta+1)}\mathrm{e}^{-\alpha(t-\gamma)^{\beta}}\\[2ex]\dfrac{\partial}{\partial \kappa} I(t,T) = -\dfrac{T\lambda^2(t-\kappa T)+T\lambda(2\beta-\lambda t-\kappa\lambda T+2)-2\beta\kappa\lambda^2T^2+2T\alpha\beta(\beta+1)(\kappa T-\gamma)^{\beta}}{2(\beta+1)}\mathrm{e}^{-\alpha(t-\gamma)^{\beta}}\end{cases}$$

2.2. Remark

Equations (25) and (30) provide the necessary condition for T^* and κ^* to be minimum points of $\phi(T,\kappa)$.

The sufficient condition for these values to minimize $\phi(T,\kappa)$ is that the Hesssian matrix H must be positive definite. Here

$$H = \nabla\phi^2(T,\kappa) = \begin{pmatrix}\dfrac{\partial^2\phi}{\partial T^2} & \dfrac{\partial^2\phi}{\partial T\partial\kappa}\\[2ex]\dfrac{\partial^2\phi}{\partial T\partial\kappa} & \dfrac{\partial^2\phi}{\partial\kappa^2}\end{pmatrix}$$

Thus the sufficient condition for optimality is $\dfrac{\partial^2\phi}{\partial T^2}>0, \dfrac{\partial^2\phi}{\partial\kappa^2}>0$ and $\dfrac{\partial^2\phi}{\partial T^2}\dfrac{\partial^2\phi}{\partial\kappa^2}-\left(\dfrac{\partial^2\phi}{\partial T\partial\kappa}\right)^2>0$.

Since $I(t)=\mathrm{e}^{-\lambda t}-\mathrm{e}^{-\lambda t_1}$ for $t_1\le t\le T$, the total back-order quantity for the cycle is $I^* = I_0^* + \mathrm{e}^{-\lambda T^*}-\mathrm{e}^{-\lambda t_1^*}$.

2.3. Optimal Inventory Policy for the Model

In this section, we provide the optimal inventory policy for the proposed model.

The procedure for reaching this optimum policy is also given. The optimal inventory policy for the proposed model is:

Order I^* units for every T^* time units. Use $e^{-\lambda T^*} - e^{-\lambda t_1^*}$ units to offset the backordered quantity and begin a new cycle with I_0^κ units. The total inventory cost per unit time associated with the proposed model is:

$$\phi(T,\kappa) = \frac{1}{T}\left\{c_1\left(I_0^\kappa - 1 + e^{-\lambda\kappa T}\right) + \frac{c_2}{\lambda}\left[\left(\lambda T - \lambda\kappa T - 1\right)e^{-\lambda\kappa T} + e^{-\lambda T}\right] + c_3\int_0^{\kappa T} I(t)\,dt + c_4\right\}$$

2.4. Solution Algorithm

We give the following steps for computing the optimal ordering quantity, optimal cycle time and the optimal total cost for the model:

Step 1: Solve Equations (25) and (30) simultaneously to get the optimal values T^* and κ^* for T and κ respectively.

Step 2: If at T^* and κ^* the sufficiency condition is satisfied, then go to step 3 else stop and declare the solution infeasible.

Step 3: Substitute T^* and κ^* into $t_1 = \kappa T$ to obtain t_1^*.

Step 4: Determine the optimal EOQ I_0^* by substituting the values of T^* and κ^* into Equation (11).

Step 5: Substitute the values of I_0^*, T^* and κ^* into Equation (20) to get the optimal total average cost $\phi(T,\kappa)$.

2.5. Numerical Analysis and Results

In this section we employ MathCAD 14 [18] to obtain numerical solution to the highly nonlinear system of Equations (25) and (30). This will provide us with the optimal solutions for the average cost function for some specified data. We consider the following inventory data adapted from Ghosh and Chaudhuri (2004):

$c_1 = 2.40$, $c_2 = 5$, $c_3 = 100.00$, $c_4 = 20.00$, $\alpha = 0.001$, $\beta = 8$, $\gamma = 0.1$, $\lambda = 0.1$, $\kappa = 0.85$, $T = 2$.

The format for the MathCAD 14 solve block follows;

- *Initial values for the unknown variables* (κ, T).
- *Given.*
- *Equation* 1.
- *Equation* 2.
- *Find* (κ, T).

2.6. Mathcad Solve Block Solution

$c_1 := 2.40$ $c_2 := 5$ $c_3 := 100$ $\alpha := 0.01$ $\beta := 8$ $\lambda := 1.5$ $\gamma := 0.4$

$\kappa := 0.85$ $T := 2$ Initial values of the variables

Given

$$\frac{c_1\cdot\exp\left[-\alpha\cdot(-\gamma)^{\beta}\right]}{2\cdot(\beta+1)}\cdot\left[\kappa\cdot\lambda\cdot(2\cdot\beta-\kappa\cdot\lambda\cdot T+2)-\kappa^2\cdot\lambda^2\cdot T-2\cdot\kappa^2\cdot\lambda^2\cdot\beta\cdot T+2\cdot\alpha\cdot\lambda\cdot\kappa\cdot(\beta+1)\cdot(\kappa\cdot T-\gamma)^{\beta}\right]$$

$$-\lambda\cdot\kappa\cdot\exp(-\lambda\cdot\kappa\cdot T)+\frac{c_2}{\lambda}\cdot\left[\lambda\cdot\exp(-\lambda\cdot\kappa\cdot T)\cdot(1-\kappa)-\lambda\cdot\kappa\cdot\exp(-\lambda\cdot\kappa\cdot T)\cdot(\lambda\cdot\kappa\cdot T-\lambda\cdot T+1)-\lambda\cdot\exp(-\lambda\cdot T)\right]$$

$$+\frac{(-1)\cdot c_3}{2\cdot(\beta+1)}\cdot\int_0^{\kappa\cdot T}\lambda\cdot\exp\left[-\lambda\cdot t-\alpha\cdot(t-\gamma)^{\beta}\right]$$

$$\cdot\left[\kappa\cdot\lambda^2(t-\kappa\cdot T)+\kappa\cdot\lambda(2\cdot\beta-\lambda\cdot t+\kappa\cdot\lambda\cdot t+2)-2\cdot\beta\cdot\kappa^2\cdot\lambda^2\cdot T+2\alpha\cdot\kappa\cdot\beta\cdot(\beta+1)\cdot(\kappa\cdot T-\gamma)^{\beta}\right]\mathrm{d}t$$

$$+\kappa\cdot\left[\frac{2\cdot\alpha\cdot\lambda\cdot\left[(\kappa-\gamma)^{\beta+1}-(\kappa\cdot T-\gamma)^{\beta+1}\right]+\lambda\cdot(\kappa-\kappa\cdot T)(2\cdot\beta-\lambda\cdot\kappa-\lambda\cdot\kappa\cdot T+2)-\beta\cdot\lambda^2\cdot(\kappa^2-\kappa^2\cdot T^2)}{2\cdot(\beta+1)}\right]=0$$

$$\frac{c_1\cdot\exp\left[-\alpha\cdot(-\gamma)^{\beta}\right]}{2\cdot(\beta+1)}\cdot\left[\lambda\cdot T\cdot(2\cdot\beta-\kappa\cdot\lambda\cdot T+2)-\kappa\cdot\lambda^2\cdot T^2-2\cdot\kappa\cdot\beta\cdot\lambda^2\cdot T^2+2\cdot\alpha\cdot\lambda\cdot T\cdot(\beta+1)\cdot(\kappa T-\gamma)^{\beta}\right]$$

$$-\lambda\cdot\kappa\cdot\exp(-\lambda\cdot T)+\frac{c_2}{\lambda}\cdot\left[-\lambda\cdot T\cdot\exp(-\lambda\cdot\kappa\cdot T)-\lambda\cdot T\cdot\exp(-\lambda\cdot\kappa\cdot T)\cdot(\lambda\cdot\kappa\cdot T-\lambda\cdot T+1)\right]$$

$$+\frac{(-1)\cdot c_3}{2\cdot(\beta+1)}\cdot\int_0^{\kappa\cdot T}\lambda\cdot\exp\left[-\lambda\cdot t-\alpha\cdot(t-\gamma)^{\beta}\right]$$

$$\cdot\left[T\cdot\lambda^2\cdot(t-\kappa\cdot T)+T\cdot\lambda\cdot(2\cdot\beta-\lambda\cdot t-\kappa\cdot\lambda\cdot T+2)-2\cdot\beta\cdot\kappa\cdot\lambda^2\cdot T^2+2\cdot T\cdot\alpha\cdot\beta\cdot(\beta+1)\cdot(\kappa\cdot T-\gamma)^{\beta}\right]\mathrm{d}t$$

$$+T\cdot\left[\frac{2\cdot\alpha\cdot\lambda\cdot\left[(\kappa-\gamma)^{\beta+1}-(\kappa\cdot T-\gamma)^{\beta+1}\right]+\lambda\cdot(\kappa-\kappa\cdot T)(2\cdot\beta-\lambda\cdot\kappa-\lambda\cdot\kappa\cdot T+2)-\beta\cdot\lambda^2\cdot(\kappa^2-\kappa^2\cdot T^2)}{2\cdot(\beta+1)}\right]=0$$

$$\textbf{\textit{Find}}(\kappa,T)=\begin{pmatrix}0.9460303\\2.0306513\end{pmatrix}$$

2.7. Remark

- From the solve block solution we obtain the optimal T^* and κ^* as $T^*=2.0306513$, $\kappa^*=0.9460303$.
- It is not difficult to show, using MathCAD, that for these optimal values the sufficient conditions for minimizing $\phi(T,\kappa)$ are satisfied.
- We proceed to use these values to compute the optimal t_1^* and I_0^* to be

$$t_1^*=\kappa^*T^*=1.921,$$

$$I_0^*=\frac{2\alpha\lambda\left[(-\gamma)^{\beta+1}-\left(t_1^*-\gamma\right)^{\beta+1}\right]-\lambda t_1^*\left(2\beta-\lambda t_1^*+2\right)+\beta\lambda^2 t_1^{*2}}{2(\beta+1)}\mathrm{e}^{-\alpha(-\gamma)^{\beta}}=1.197$$

- Finally, we have;

$$\phi(T,\kappa)=\frac{1}{T}\left\{c_1\left(I_0^{\kappa}-1+\mathrm{e}^{-\lambda\kappa T}\right)+\frac{c_2}{\lambda}\left[(\lambda T-\lambda\kappa T-1)\mathrm{e}^{-\lambda\kappa T}+\mathrm{e}^{-\lambda T}\right]+c_3\int_0^{\kappa T}I(t)\mathrm{d}t+c_4\right\}$$

$$=11.334$$

In summary, for the *mathematical model of an inventory system with time*

dependent three-parameter Weibull deterioration and a stochastic type demand in the form of a negative exponential distribution, we obtained the following results.

The optimum cycle time $T^* = 2.031$ *days.*

The optimum value $\kappa^* = 0.94603$.

The optimum stock-period $t_1^* = 1.921$ *days.*

The economic order quantity $I_0^* = 1.197$ *units.*

The optimum total average cost $\phi(T,\kappa)^* = \$11.334$ *per day.*

The optimum number of order, $N^* = 1/1.197 = 0.8354$ *order per day.*

2.8. Conclusions

In this work we developed an inventory model for a three-parameter Weibull deteriorating items with stochastic demand in the form of a negative exponential distribution. We derived the optimal inventory policy for the proposed model and also established the necessary and sufficient conditions for the optimal policy. In the solution of the differential equation obtained, because of the cumbersome nature of the associated integral, we were forced to make a first order approximation for the integrand involving an exponential function. This in turn enabled us to obtain a closed form solution for our model. We provided a numerical example illustrating our solution procedure. Though our solution is only approximate, we were still able to obtain very reasonable results which compared favourably with that of Ghosh and Chaudhuri [6] ($T^* = 2.145$ days, $\kappa^* = 0.8832$) for the deterministic demand case.

It is important to state that the numerical procedure for this problem relied heavily on the power of MathCAD14, which was used to solve a highly nonlinear system of equations in two unknowns, and involving a definite integral. The advantage of this numerical software is that the equations are composed as they appear in the text and need not be recast in a special format for computation.

Conflicts of Interest

The authors declare no conflicts of interest regarding the publication of this paper.

References

[1] Ritchie, E. (1980) Practical Inventory Replenishment Policies for a Linear in Demand Followed by a Period of Steady Demand. *Journal of the Operational Research Society*, **31**, 605-613. https://doi.org/10.1057/jors.1980.118

[2] Gupta, P.K. and Hira, D.S. (2002) Operations Research. S. Chand & Company Ltd., New Delhi.

[3] Rinne, H. (2009) The Weibull Distribution: A Handbook. Chapman & Hall/CRC, Boca Raton.

[4] Ritchie, E. (1985) Stock Replenishment Quantities for Unbounded Linear Increasing Demand: An Interest Consequence of the Optimal Policy. *Journal of the Operational Research Society*, **36**, 737-739. https://doi.org/10.1057/jors.1985.131

[5] Ghare, P.M. and Schrader, G.H. (1963) A Model for Exponentially Decaying Inventory System. *Journal of Industrial Engineering*, **14**, 238-243.

[6] Ghosh, S.K. and Chaudhuri, K.S. (2004) An Order-Level Inventory Model for a Deteriorating Item with Weibull Distribution Deterioration, Time-Quadratic Demand and Shortages. *Advanced Modeling and Optimization*, **6**, 21-35.

[7] Dave, U. (1986) An Order Level Inventory for Items with Variable Instantaneous Demand and Discrete Opportunities for Replenishment. *Opsearch*, **23**, 244-249.

[8] Li, R., Lan, H. and Mawhhinney, J.R. (2010) A Review on Deteriorating Inventory Study. *Journal of Service Science and Management*, **3**, 117-129. https://doi.org/10.4236/jssm.2010.31015

[9] Khanra, S., Ghosh, S.K. and Chaudhuri, K.S. (2011) An EOQ Model for a Deteriorating Item with Time Dependent Quadratic Demand under Permissible Delay in Payment. *Applied Mathematics and Computation*, **218**, 1-9. https://doi.org/10.1016/j.amc.2011.04.062

[10] Bakker, M., Riezebos, J. and Teunter, R.H. (2012) Review of Inventory Systems with Deterioration since 2001. *European Journal of Operational Research*, **221**, 275-284. https://doi.org/10.1016/j.ejor.2012.03.004

[11] Goyal, S. and Giri, B.C. (2001) Recent Trends in Modeling of Deteriorating Inventory. *European Journal of Operational Research*, **134**, 1-16. https://doi.org/10.1016/S0377-2217(00)00248-4

[12] Ravichandran, N. and Srinivasan, S.K. (1988) Multi-Item (S,S) Inventory Model with Poisson Demand, General Lead Time and Adjustable Reorder Time. IIMA Working Papers WP 1988-08-01_00838, Indian Institute of Management Ahmedabad, Research and Publication Department.

[13] Weiss, H.J. (1995) Stochastic Analysis of a Continuous Review Perishable Inventory System with Positive Lead Time and Poisson Demand. *European Journal of Operations Research*, **84**, 444-457. https://doi.org/10.1016/0377-2217(93)E0254-U

[14] Aggoun, L., Benkerouf, L. and Boumenir, A. (2001) A Stochastic Inventory Model with Stock Dependent Items. *Journal of Applied Mathematica and Stochastic Analysis*, **14**, 317-328. https://doi.org/10.1155/S1048953301000284

[15] Lian, Z., Zhao, N. and Liu, X. (2009) A Perishable Inventory Model with Markovian Renewal Demands. *International Journal of Production Economics*, **121**, 176-182. https://doi.org/10.1016/j.ijpe.2009.04.026

[16] Rinne, H. (2009) The Weibull Distribution: A Handbook. Chapman & Hall/CRC, Boca Raton. https://doi.org/10.1201/9781420087444

[17] Chakrabarty, T., Giri, B.C. and Chaudhuri, K.S. (1998) An EOQ Model for Items with Weibull Distribution Deterioration, Shortages and Trended Demand: An Extension of Philip's Model. *Computers & Operations Research*, **25**, 649-657. https://doi.org/10.1016/S0305-0548(97)00081-6

[18] Mathcad Version 14 (2007) PTC (Parametric Technology Corporation) Software Products. http://communications@ptc.com

Scientific Research Publishing

Applied Mathematics, 2019, 10, 743-752
https://www.scirp.org/journal/am
ISSN Online: 2152-7393
ISSN Print: 2152-7385

The Computational Complexity of Untrapped Choice Procedures

Mustapha Balewa Sanni[1,2]

[1]Université Nationale des Sciences, Technologies, Ingénierie et Mathématiques (UNSTIM) d'Abomey, Abomey, Benin
[2]Institut National Supérieur de Technologie Industrielle (INSTI) de Lokossa, Lokossa, Benin
Email: musanni@yahoo.fr

How to cite this paper: Sanni, M.B. (2019) The Computational Complexity of Untrapped Choice Procedures. *Applied Mathematics*, **10**, 743-752.
https://doi.org/10.4236/am.2019.109053

Received: September 15, 2018
Accepted: September 21, 2019
Published: September 24, 2019

Abstract

In this paper, we define two versions of Untrapped set (weak and strong Untrapped sets) over a finite set of alternatives. These versions, considered as choice procedures, extend the notion of Untrapped set in a more general case (*i.e.* when alternatives are not necessarily comparable). We show that they all coincide with Top cycle choice procedure for tournaments. In case of weak tournaments, the strong Untrapped set is equivalent to *Getcha* choice procedure and the Weak Untrapped set is exactly the Untrapped set studied in the litterature. We also present a polynomial-time algorithm for computing each set.

Keywords

Choice Procedure-Pseudo Tournament-Untrapped Set-Computational Complexity

1. Introduction

A common way to model a decision maker's preferences is to consider a binary relation R over a set A of alternatives (teams, projects, candidates, goods, etc. …). In many different contexts (Sports league, Social Choice Theory, Economics, Operational Research, etc …), the binary relation R is used to make a choice between alternatives of A. Very often this relation is assumed to be complete and asymmetric (we say that R is a tournament) or sometimes complete (R is said to be a weak tournament). The general case concerning incomplete binary relations has received less attention (see [1] [2] [3]). Incomplete preferences have been increasingly recognized as important [4] [5]. The origin of these preferences is twofold: a lack of information about the alternatives or a lack of information of the decision maker about her own tastes on the alternatives [6] [7].

From the binary relation defined on A, many mechanisms (procedures) are defined in order to choose the set of "best alternatives" also called choice sets. Some familiar choice procedures studied in the literature are the *Top cycle* choice procedure [8], the *Copeland* choice procedure [9], the *Uncovered* choice procedure [10], etc. … These choice procedures have been extensively analysed (in terms of mathematical characterizations) for tournaments and weak tournaments [see [11] [12]]. Sanni [13] has studied axiomatic characterizations of some pseudo tournaments *i.e.* reflexive and non necessary complete binary relations.

Recent work has addressed the computational complexity of many choice procedures (see for example: [14] [15]) and the literature is full of choice procedures that are difficult to compute [15] [16]. It is assumed that if computing a choice set is infeasible, the applicability of the corresponding solution concept is seriously undermined [17]. Most of the familiar procedures mentioned above are demonstrated to be tractable [17] *i.e.* belonging to class P of problems which can be solved by an algorithm whose running time is polynomial in the size of the problems instance. These procedures are then considered useful because if the computation of a choice set is intractable, the associated choice procedure is virtually rendered useless for large problem instances.

In this article, we consider the Untrapped choice procedure (UT) defined by Duggan [18] for (weak) tournaments. The resulting set is composed of alternatives x that are not directly beaten or that beat indirectly some other alternatives (especially alternatives that directely beat x). Duggan [18] proves that this choice procedure coincides with the *Top cycle* choice procedure in the case of tournaments and is nested between the *Getcha* and the *Gocha* choice procedures for weak tournaments. *UT* strongly depends on the asymmetric part of the binary relation considered.

We particularly focus, in this paper, on pseudo tournaments and we deduce another notion of the Untrapped (Strong Untrapped: *SUt*) choice procedure directely dependent on the pseudo tournament R studied. We also discuss the computational complexity of identifying the choice set for each of the choice procedures studied.

The rest of this article is structured as follows. Concepts that are used throughout this paper are given in Preliminaries (Section 2). Section 3 introduces the two extensions of the Untrapped choice procedures which are compared with two extensions of the Top cycle choice procedure. Computational complexity of Untrapped choice procedures is then explored in Section 4. Section 5 ends with an overview of the results.

2. Preliminaries

A represents a finite set of alternatives and R a binary relation defined on A (*i.e.* R is a subset of $A\times A$). If $(x,y)\in R$ we write xRy. If B is a non empty subset of A, R/B represents the restriction of R on B, *i.e.* $R/B=\{(x,y)\in B\times B / xRy\}$. The binary relation R is said to be reflexive if xRx, $\forall x\in A$. It is symmetric if

$xRy \Rightarrow yRx$, $\forall x, y \in A$. Relation R is asymmetric if $xRy \Rightarrow not(yRx)$, $\forall x, y \in A$ with $x \neq y$. It is antisymmetric if xRy and $yRx \Rightarrow x = y$, $\forall x, y \in A$. It is transitive if (xRy and yRz) $\Rightarrow$ xRz, $\forall x, y, z \in A$. It is complete if xRy or yRx, $\forall x, y \in A$. A tournament is a complete and antisymmetric relation[1]. A weak tournament is a complete relation. A pseudo tournament is any reflexive binary relation (the relation may be complete or not)[2].

Three other binary relations (*I*: indifference relation, *P*: strict preference relation and *J*: incomparability relation) are defined from *R* as follow: $\forall x, y \in A$, $xIy \Leftrightarrow (xIy$ and $yRx)$, $xPy \Leftrightarrow (xRy$ and $not(yRx))$ and $xJy \Leftrightarrow not(xRy)$ and $not(yRx)$. It can be noticed that *I* is reflexive and symmetric, *P* is asymmetric (*P* is also called the asymmetric part of *R*) and *J* is symmetric. xPy (resp. xIy) can be interpreted as *x* beats or is better than (resp. *x* is indifferent to) *y*.

A circuit is any subset $\{x_1, x_2, \cdots, x_k\}$ of A (with $k \geq 2$) such that $x_1 R x_2 R \cdots R x_k$ and $x_k R x_1$. The subset $\{x_1, x_2, \cdots, x_k\}$ is a *P*-circuit if $x_1 P x_2 P \cdots P x_k$ and $x_k P x_1$. *A* is acyclic (resp. *P*-acyclic) if it contains no circuit (resp. no P-circuit).

The transitive closure R^* of *R* is defined as follows: $\forall x, y \in A, xR^*y$ if and only if $\exists k \in \mathbb{N}$ with $k \geq 1$, $\exists x_1, x_2, \cdots, x_k \in A$, such that $\forall i \in \{1, 2, \cdots, k-1\}$, $x_i R x_{i+1}$, $x_1 = x$ et $x_k = y$. In other words xR^*y if and only if there exists at least a path of length *k* from *x* to *y* (we also say that *y* is reachable from *x*). The transitive closure P^* of *P* can also be defined in the same way (we then say that *y* is *P*-reachable from *x*).

The predecessor with respect to *R* (resp. with respect to *P*) of an alternative $x \in A$ is the set $Pred(x) = \{y \in A / yRx\}$ (resp. $Pred_P(x) = \{y \in A / yPx\}$). We also define the set $Cl(x)$ (resp. $Cl_P(x)$) as $Cl(x) = \{y \in A / yR^*x\}$ (resp. $Cl_P(x) = \{y \in A / yP^*x\}$). So $y \in Cl_P(x)$) if *y* is P-reachable from *x*.

A choice procedure is a function *C* that maps each pseudo tournament *R* to a nonempty subset $C(R)$ of *A* called the choice set.

If *R* is a tournament (resp. a weak tournament) the choice procedure is called a tournament solution (resp. a generalized or weak tournament solution) (see [15]).

We say that a choice procedure *C* is contained in a choice procedure C' if $C(R) \subseteq C'(R)$ for every pseudo tournament *R* defined on *A* (we write $C \subseteq C'$).

Many tournament or generalized tournament solutions have been studied in the litterature. A well known one is the *Top Cycle* choice procedure [8] [10]) defined by the concept of dominant set.

Definition 1. A non empty subset *D* of *A* is said to be a dominant set for a tournament *R* in *A* if xRy, $\forall x \in D$, $\forall y \in A \setminus D$.

[1]Tournaments are always supposed to be asymmetric. We suppose without lost of generality that tournament may be reflexive.

[2]Pseudo tournaments should not be confound with partial tournaments for which binary relations are asymmetric and not necessarily reflexive.

D is a minimal dominant set if D is dominant and if no subset of D is dominant.

The *Top Cycle* choice procedure of a tournament R on A is defined as $TC(R)=D$, where D is the unique minimal dominant set for the tournament R. It is easy to show that $TC(R)=\{x\in A / xR^{*}y, \forall y\in A\}$. It is also obvious that the asymmetric part of the transitive closure R^{*} is without circuit and because R^{*} is complete we have $TC(R)=M(R^{*})$. An attractive property of TC is that any alternative that beats another alternative in the *Top Cycle* is indirectly beaten by the latter.

The notion of (minimal) dominant set has been extended to the case of weak tournaments in two directions.

Definition 2. Let R be a weak tournament on A. A non empty subset D of A is a dominant (resp. undominated) set for R in A if $not(yRx)$ (resp. $not(yPx)$), $\forall x\in D$, $\forall y\in A\setminus D$.

D is a minimal dominant (resp. minimal undominated) set if D is dominant (resp. undominated) and if no subset of D is dominant (resp. undominated).

Contrary to the minimal undominated set, the minimal dominant set is unique. Schwartz [8] [19] then defined two choice procedures [*Getcha* and *Gocha*[3] choice procedures] as follow:

Definition 3. Let R be a weak tournament defined on A.

The *Getcha* choice procedure of R is defined as $Getcha(R)=D$, where D is the (unique) minimal dominant set for R in A.

The *Gocha* choice procedure is defined by: $Gocha(R)=\bigcup D_i$, where D_i is a minimal undominated set.

Both *Gocha* and *Getcha* choice procedures coincide with the *Top Cycle* (TC) when the binary relation R is a tournament. It is easy to show that $Gocha(R)\subseteq Getcha(R)$. Moreover we have [20], $Gocha(R)=M(P^{*})$ and $Getcha(R)=M(R^{*})$.

For pseudo tournaments, we adopt the same definition for dominant and undominated sets. It is then easy to see that the dominant set is no more unique, so we have the following definition.

Definition 4. Let R be a pseudo-tournament on A[4].

The *Gocha* choice procedure is defined as the union of all minimal undominated sets for R in A.

The *Getcha* choice procedure is defined as the union of all minimal dominant sets for R in A.

Lemma 1. Let D be a minimal dominant (resp. minimal undominated) set for R in A. For all $x, y\in D$, we have $xR^{*}y$ (resp. $xP^{*}y$).

Proof. We give the proof for the case of the minimal dominant set. The proof for minimal undominated set is similar.

Consider D a minimal dominant set for R in A. Suppose there exists $x, y\in D$,

[3] *Getcha* set (resp. *Gocha* set) is also called Smith set (resp. Schwartz set) in the litterature.

[4] Sanni (2010) has defined two extensions of the *Gocha* procedure and two extensions of the *Getcha* procedure.

such that $not\left(xR^*y\right)$. Since $y \in D$, there exists $y_1 \in D$ such that y_1Ry. We also have $not\left(xRy_1\right)$ [otherwise xR^*y, a contradiction to $not\left(xR^*y\right)$]. So there exists $y_2 \in D$ such that y_2Ry_1. We have $not\left(xRy_2\right)$. Similarly, there exist $y_3, y_4, \cdots, y_n \in D$ such that $y_{i+1}Ry_i$ and $not\left(xRy_{i+1}\right)$ for all $i \in \{1,2,\cdots,n-1\}$. Now consider the set $U = \left\{z \in D, zR^*y\right\}$. For all $z \in U$ and $z_0 \notin U$, we have $not\left(z_0Rz\right)$. So U is a dominant set for R in A. This contradicts the minimality of D because $x \in D$ but $x \notin U$.

The result of Deb [20] for pseudo tournaments is then generalized as follow.

Proposition 1. For a pseudo tournament R defined on A, we have:

1) $Getcha(R) = M\left(R^*\right)$

2) $Gocha(R) = M\left(P^*\right)$.

Proof. Consider $x \in M\left(R^*\right)$ and suppose $x \notin Getcha(R)$. There exists $y_1 \in A$ such that y_1Rx. If $y_1 \in Getcha(R)$, then $y_1Rx \Rightarrow y_1R^*x$ and since $x \in M\left(R^*\right)$, we have xR^*y (which is not possible). So $y_1 \notin Getcha(R)$. There exists $y_2 \in A$ such that y_2Ry_1.

For the same reasons $y_2 \notin WGe(R)$. Consider the set $U = \left\{z \in A, zR^*y_1\right\}$, we have $U \cap WGe(R) = \phi$. Moreover for all $z \in U$ and for all $z' \in A \setminus U$, we have $not\left(z'Rz\right)$. So the set U contains a dominant set for R in A which contains a minimal weak dominant set (which is not possible).

Now let $x \in Getcha(R)$ and suppose there exists $y \in A$ such that yR^*x. $x \in Getcha(R)$ implies that there exists a minima dominant set D such that $x \in D$. Then we have $y \in D$ [otherwise $\exists x_1, x_2, \cdots, x_n \in A$ such that $y = x_1Rx_2R\cdots Rx_n = x$ (which is not possible)]. so $x, y \in D$ and according to the previous lemma, we also have xR^*y.

Example. Let R be the pseudo tournament defined on $A = \{a,b,c,d,e,f,g\}$ by aPb, aIc, bPc, cPd, cPe, dPe, eIf, ePg and gPd. We also have xRx, $\forall x \in A$. The graph of R is represented by:

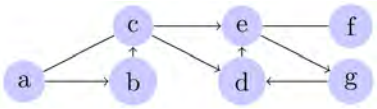

We have $Gocha(R) = \{a,f\}$, $Getcha(R) = \{a,b,c\}$, $SUt(R) = \{a,b,c,f,g\}$ and $WUt(R) = \{a,f,g\}$.

3. Untrapped Choice Procedures

We study in this section two choice procedures (strong and weak Untrapped choice procedures) for pseudo tournaments. These choice procedures generalize the concept of Untrapped choice procedure defined by Duggan [19] for weak tournaments.

Definition 5. Let R be a pseudo tournament on A. We say that x weakly (resp. strongly) traps y with respsect to R and we write xTy (resp $x\tilde{T}y$) if xPy and if $not\left(yP^*x\right)$ (resp. if xRy and if $not\left(yR^*x\right)$).

Relation T (resp $\tilde{T}$) is not necessary transitive but is P-acyclic (resp. acyclic)

[because if $x_1 T x_2 \cdots T x_n$ and $x_n T x_1$, we get $x_1 P x_2 P \cdots P x_n$ and $x_n P x_1$, which implies $x_2 P^* x_1$: this is not possible since $x_1 T x_2$]. So, we can define the set of its maximal elements. This leads to two choice procedures called weak Untrapped (resp. strong Untrapped) choice procedure, denoted by WUt (resp. SUt) and defined as follow: $WUt(R) = \{x \in A / not(yTx), \forall y \in A\}$ (resp. $SUt(R) = \{x \in A / not(y\tilde{T}x), \forall y \in A\}$).

It is easy to see that an element x of A is in $WUt(R)$[5] if and only if $not(yPx)$ or xP^*y, $\forall y \in A$.

So any alternative x which is not directly beaten or which beats indirectly some other alternatives (specially alternatives that beat directly x) is in the weak Untrapped set.

It is also easy to see that an element x of A is in SUt if and only if $not(yRx)$ or xR^*y, $\forall y \in A$.

We can say that an alternative x strongly traps another alternative y ($x\tilde{T}y$) if xPy and if $not(yR^*x)$). So $x \in SUt(R)$ if and only if $not(yPx)$ or xR^*y, $\forall y \in A$.

When relation R is a tournament (resp. weak tournament) Duggan [19], shows that $WUt(R) = SUt(R) = TC(R)$ (resp $Gocha(R) \subseteq WUt(R) \subseteq Getcha(R)$). It is obvious that for weak tournaments, we have $SUt(R) = Getcha(R)$.

The following proposition gives inclusion relations between the different choice procedures mentionned above.

Proposition 2. For a pseudo tournament R defined on A, we have the following relations (Table 1).

Legend: The symbol $\supseteq$ (resp.=, $\varnothing$) indicates that the choice set in column is always contained in (resp. is equaled to, intersects) the choice set in row.

Proof. See **Appendix**.

The previous proposition can be summarized by the following Hasse diagram.

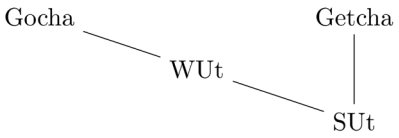

We can then notice that WUt is nested between $Gocha$ and $Getcha$ ($Gocha \subseteq WUt \subseteq Getcha$) and that $Getcha \subseteq SUt$. Missing arrows between two choice sets indicates that the two always intersect and none is included in the other.

Lemma 2.

1) $x \in SUt \Leftrightarrow Pred(x) \subseteq Cl(x)$

2) $x \in WUt \Leftrightarrow Pred_P(x) \subseteq Cl_P(x)$

[5]Duggan [19] also shows that $WUt(R)$ is the union of all maximal sets of all maximal acyclic subrelations (w.r.t. set inclusion) of R.

Table 1. Comparison of choice procedures.

	$SUt(R)$	$WUt(R)$	$Gocha(R)$	$Getcha(R)$
$SUt(R)$	=	$\supseteq$ 1.	$\supseteq$ 2.	$\supseteq$ 3.
$WUt(R)$		=	$\supseteq$ 4.	$\varnothing$ 5.
$Gocha(R)$			=	$\varnothing$ 6.
$Getcha(R)$				=

Proof.

1) ($\Rightarrow$): Let $x \in SUt(R)$.

- If $Pred(x) = \varnothing$ then $Pred(x) \subseteq Cl(x)$.
- If $Pred(x) \neq \varnothing$ then for $y \in Pred(x)$, yRx. And since $x \in SUt(R)$, we then have $xR^{*}y$; which implies that $y \in Cl(x)$.

($\Leftarrow$): Let $x \in A$ such that $Pred(x) \subseteq Cl(x)$ and suppose that $x \notin SUt(R)$; then $\exists y \in A$ such that $y\tilde{T}x$. *i.e.* $\exists y \in A$ such that yRx and $not\left(xR^{*}y\right)$. But $yRx \Rightarrow y \in Pred(x)$ $(\subseteq Cl(x))$; which means $y \in Cl(x)$, *i.e.* $xR^{*}y$: a contradiction.

2) Similar to the previous one.

4. Computational Complexity

In this section we analyze the computational complexity of the weak (resp. strong) Untrapped set. The following algorithm (based on the previous lemma) describes how to get $WUt(R)$ for a given pseudo tournament R defined on a finite set A. This algorithm can be considered for $SUt(R)$ if $Pred_{P}(x)$ (resp. $Cl_{P}(x)$)) is replaced by $Pred(x)$ (resp. $Cl(x)$)).

Let us mention that deciding whether an alternative is contained in a choice set is computationally equivalent to finding the set [18].

Algorithm 1. Untrapped set

for all x in A **do**
if $Pred_{P}(x) \subseteq Cl_{P}(x)$ **then**
$x \in WUt(R)$
end if
return $WUt(R)$
end for

It has been shown that the transitive closure of each $x \in A$ is computable in polynomial time. The same holds for the computation of predecessors of x (see [21] page 137), we can then conclude that deciding whether an alternative is contained in the weak (resp. strong) Untrapped set is in P (class of problems that can be solved in polynomial time).

5. Conclusions

Duggan [18] has defined the concept of Untrapped choice procedure for weak

tournaments (complete binary relations). This notion depends on the asymmetric part of the given binary relation. In this paper, we have introduced two versions of the Untrapped choice procedures which have been extended to pseudo tournaments (reflexive and non necessarily complete binary relations). The weak Untrapped (WUt) choice procedure also depends on the asymmetric part of the pseudo tournament while the strong Untrapped choice procedure (SUt) is directly defined by the given pseudo tournament.

We have shown that each of the new choice procedures coincides with the familiar *Top cycle* choice procedure for tournaments. In case of weak tournaments, the strong Untrapped set is equivalent to *Getcha* choice procedure and the Weak Untrapped set is exactly the Untrapped set studied by Duggan [18]. We know (see [18]) that for a weak tournament R, we have $Gocha(R) \subseteq WUt(R) \subseteq Getcha(R) (= SUt(R))$. When R is a pseudo tournament, we've seen (from proposition 2) that the three choice procedures (WUt, *Getcha* and *Gocha*) are all contained in SUt.

In terms of computational complexity, we present an algorithm to compute both the strong and the weak Untrapped choice procedure. This algorithm allows us to show that deciding whether an alternative is contained in the strong (or in the weak) Untrapped set is in P (class of problems that can be solved in polynomial time).

Conflicts of Interest

The author declares no conflicts of interest regarding the publication of this paper.

References

[1] Eliaz, K. and Ok, E.A. (2006) Indifference or Indecisiveness? Choice-Theoretic Foundations of Incomplete Preferences. *Games and Economic Behavior*, **56**, 61-86. https://doi.org/10.1016/j.geb.2005.06.007

[2] Tapk, I.G. (2007) Revealed Incomplete Preferences under Status-Quo Bias. *Mathematical Social Sciences*, **53**, 274-283. https://doi.org/10.1016/j.mathsocsci.2006.12.003

[3] Gorno, L. (2018) The Structure of Incomplete Preferences. *Economic Theory*, **66**, 159-185. https://doi.org/10.1007/s00199-017-1057-9

[4] Urena, R., Chiclana, F., Morente-Molinera, J.A. and Herrera-Viedma, E. (2015) Managing Incomplete Preference Relations in Decision Making: A Review and Future Trends. *Information Sciences*, **302**, 14-32. https://doi.org/10.1016/j.ins.2014.12.061

[5] Zhi, H. and Chao, H. (2018) Three-Way Concept Analysis for Incomplete Formal Contexts. *Mathematical Problems in Engineering*, **2018**, Article ID: 9546846. https://doi.org/10.1155/2018/9546846

[6] Hill, B. (2016) Incomplete Preferences and Confidence. *Journal of Mathematical Economics*, **65**, 83-103. https://doi.org/10.1016/j.jmateco.2016.05.007

[7] Albers, S., Bichler, M., Brandt, F., Gritzmann, P. and Kolisch, R. (2017) Algorithmic Economics und Operations Research. *Informatik-Spektrum*, **40**, 165-171.

https://doi.org/10.1007/s00287-017-1023-8

[8] Schwartz, T. (1972) Rationality and the Myth of the Maximum. *Nous*, **7**, 97-117. https://doi.org/10.2307/2216143

[9] Copeland, A. (1951) A Reasonable Social Welfare Function. *Seminar on Applications of Mathematics to Social Sciences*, University of Michigan, Ann Arbor (Mimeographed Notes).

[10] Miller, N.R. (1980) A New Solution Set for Tournaments and Majority Voting: Further Graph-Theoretical Approaches to the Theory of Voting. *American Journal of Political Science*, **24**, 68-96. https://doi.org/10.2307/2110925

[11] Laslier, J.-F. (1997) Tournament Solutions and Majority Voting. No. 7, Springer Verlag, Berlin. https://doi.org/10.1007/978-3-642-60805-6

[12] Peris, J.E. and Subiza, B. (1999) Condorcet Choice Correspondences for Weak Tournaments. *Social Choice and Welfare*, **16**, 217-231. https://doi.org/10.1007/s003550050141

[13] Sanni, M. (2010) Etude des procedures de choix fondees sur des relations binaires. PhD Thesis, Universite de Paris Dauphine, Paris.

[14] Aziz, H., Brandt, F., Elkind, E. and Skowron, P. Computational Social Choice: The First Ten Years and Beyond. In: Steffen, B. and Woeginger, G., Eds., *Computing and Software Science*, Vol. 10000 of Lecture Notes in Computer Science (LNCS), Springer, Berlin, forthcoming.

[15] Brandt, F., Brill, M. and Harrenstein, B. (2016) Tournament Solutions.

[16] Aziz, H., Brill, M., Fischer, F., Harrenstein, P., Lang, J. and Seedig, H.G. (2015) Possible and Necessary Winners of Partial Tournaments. *Journal of Artificial Intelligence Research*, **54**, 493-534. https://doi.org/10.1613/jair.4856

[17] Brandt, F., Brill, M. and Harrenstein, P. (2018) Extending Tournament Solutions. *Social Choice and Welfare*, **51**, 193-222. https://doi.org/10.1007/s00355-018-1112-x

[18] Duggan, J. (2007) A Systematic Approach to the Construction of Non-Empty Choice Sets. *Social Choice and Welfare*, **28**, 491-506. https://doi.org/10.1007/s00355-006-0176-1

[19] Brandt, F., Brill, M. and Harrenstein, P. (2014) Extending Tournament Solutions. 28*th AAAI Conference on Artificial Intelligence*, Québec City, 27-31 July 2014.

[20] Deb, R. (1977) On Schwartz's Rule. *Journal of Economic Theory*, **16**, 103-110. https://doi.org/10.1016/0022-0531(77)90125-9

[21] Lacomme, P., Prins, C. and Sevaux, M. (2003) Algorithmes de graphes. Vol. 28, Eyrolles, Paris.

Appendix

Proof of Proposition 2

1) $WUt(R) \subseteq SUt(R)$.

Let R be a pseudo tournament defined on A. $x \in WUt(R) \Rightarrow \forall y \in A$, $not(yPx)$ or $xP^*y \Rightarrow \forall y \in A$, $not(yPx)$ or $xR^*y \Rightarrow x \in SUt(R)$.

2) $Gocha(R) \subseteq SUt(R)$.

According to proof 4. and 1., we have respectively $Gocha(R) \subseteq WUt(R)$ and $WUt(R) \subseteq SUt(R)$.

3) $Getcha(R) \subseteq SUt(R)$.

Let R be a pseudo tournament defined on A and let $x \in Getcha(R)$.

Suppose $x \notin SUt(R)$. Then $\exists y \in A$ such that $y\tilde{T}x$ *i.e.* yPx and $not(xR^*y)$. A contradiction since $x \in Getcha(R)$ and $Getcha(R) = M(R^*)$.

4) $Gocha(R) \subseteq WUt(R)$.

Let R be a pseudo tournament defined on A and let $x \in Gocha(R)$.

Suppose $x \notin WUt(R)$. Then $\exists y \in A$ such that yTx. *i.e.* yPx and $not(xP^*y)$: which is not possible since $x \in Gocha(R)$ and $Gocha(R) = M(P^*)$.

5) $WUt(R) \varnothing Getcha(R)$.

Let's show that any minimal weak dominant set intersects the weaak Untrapped set.

Consider a minimal weak dominant set D' and suppose that $WUt(R) \cap D' = \varnothing$. Then for $x \in D'$ we have $x \notin WUt(R)$. So $\exists y \in WUt(R)$ such that yPx. Which is not possible because $y \notin D'$ and $x \in D'$.

The above example shows that none of *Getcha* and *WUt* choice procedure is included in the other.

6) $Gocha(R) \varnothing Getcha(R)$.

Note that every weak dominant set is a weak undominated set. So every minimal weak dominant set contains at least one minimal weak undominated set. We then have $Gocha(R) \cap Getcha(R) \neq \varnothing$.

The above example shows that none of *Getcha* and *Gocha* choice procedure is included in the other.

Applied Mathematics, 2019, 10, 753-768
https://www.scirp.org/journal/am
ISSN Online: 2152-7393
ISSN Print: 2152-7385

Analytical Algorithm for Systems of Neutral Delay Differential Equations

Aminu Barde[1,2], Normah Maan[1*]

[1]Department of Mathematical Sciences, University Technology Malaysia, Skudai, Malaysia
[2]Department of Mathematical Sciences, Abubakar Tafawa Balewa University, Bauchi, Nigeria
Email: bardealamin@yahoo.com, *normahmaan@utm.my

How to cite this paper: Barde, A. and Maan, N. (2019) Analytical Algorithm for Systems of Neutral Delay Differential Equations. *Applied Mathematics*, **10**, 753-768.
https://doi.org/10.4236/am.2019.109054

Received: August 27, 2019
Accepted: September 22, 2019
Published: September 25, 2019

Abstract

Delay differential equations (DDEs), as well as neutral delay differential equations (NDDEs), are often used as a fundamental tool to model problems arising from various areas of sciences and engineering. However, NDDEs particularly the systems of these equations are special transcendental in nature; it has therefore, become a challenging task or times almost impossible to obtain a convergent approximate analytical solution of such equation. Therefore, this study introduced an analytical method to obtain solution of linear and nonlinear systems of NDDEs. The proposed technique is a combination of Homotopy analysis method (HAM) and natural transform method, and the He's polynomial is modified to compute the series of nonlinear terms. The presented technique gives solution in a series form which converges to the exact solution or approximate solution. The convergence analysis and the maximum estimated error of the approach are also given. Some illustrative examples are given, and comparison for the accuracy of the results obtained is made with the existing ones as well as the exact solutions. The results reveal the reliability and efficiency of the method in solving systems of NDDEs and can also be used in various types of linear and nonlinear problems.

Keywords

Homotopy Analysis Method, Natural Transform, He's Polynomial and Neutral Delay Differential Equations

1. Introduction

Ordinary differential equations (ODEs) are usually used as a fundamental tool in modelling the problems of the real world. However, in most cases, the mathematical formulation of real-life problems needs to consider both the present and past states of the system behaviour. Different from (ODEs), DDE is a type of

differential equation in which the derivative of the unknown function at a certain time is given in terms of the values of the function at previous time [1]. Hence, more reliable models of real problems arising from various field of studies such as; biology, population dynamics, chemistry, and physics, control theory to mention but few are now model using DDEs as well as NDDEs [2] [3] [4] [5] [6]. Recently series of methods have been developed to find an approximate analytical solution to different types of DDEs [7]-[12]. However, most of these methods have experienced a series of challenges in finding a convergent approximate analytical solution of NDDEs in particular system of such equations. So, scientist and engineers adopt the use of numerical methods as the best approach to approximate the solutions. Therefore, more analytical approaches are highly needed for solving these equations.

This work aims to develop an analytical technique for solving linear and nonlinear systems of NDDEs from the combination of HAM and Natural transform. The proposed technique improved on the work of Rebenda and Smarda [12] by introducing the concept of NDDE into Natural transform. In addition, the various derivatives for both proportional and constants delay of NDDEs were successfully generated using the Natural transform. This work is also an extension of Efficient Analytical Approach for Nonlinear System of Retarded Delay Differential equations. This approach was developed by Barde and Maan [13] and solutions to different types of nonlinear systems of retarded DDEs were obtained in a series form which converges to exact or approximate solution.

Thus, based on the results of this pervious works, this research focuses to develop a new analytical technique that modifies Efficient Analytical Approach for Nonlinear System of Retarded Delay Differential Equations with aims to obtain approximate analytical solution for both linear and nonlinear system of NDDEs with proportional and constant delays. Using the introduced technique, the He's polynomial is adjusted in order to ease the computational difficulties of nonlinear terms of such equations. Furthermore, the convergence analysis and the maximum estimated error of the technique are also investigated.

Therefore, in this work we were able to develop a new generating function in Equation (29) that provides a convergent analytical solution to various types of linear and nonlinear system of NDDEs in a series form using few numbers of computational terms and minimal error as compared with the previous techniques. Thus, different from some of the existing methods the presented technique provides solution to different form of linear and nonlinear NDDEs without any linearization, perturbation or unnecessary assumptions. In Section 4, some illustrative examples are presented in order to show the reliability and efficiency of our algorithms over the reference methods.

2. Methods

The idea of this work is come up with analytical approach from the combination of natural transform and HAM for solving systems of linear and nonlinear NDDEs. The He's polynomial is modified to compute the series of nonlinear

terms of both proportional and constants delays.

HAM is a powerful technique introduced by Lio [14] for solving different types of linear and nonlinear problems. Details on theory and application of HAM can be found in [1] [15] [16] [17] [18].

In recent years natural transform is considered as an active topic in research due to its vast application in solving different type of differential and integral equations [19] [20] [21] [22]. This transform was derived from the renowned Fourier integral which converged to either Laplace or Sumudu transforms depending on the values of the transform variables. The basic concepts of natural transform for further use in this research are rendered below.

Definition 2.1 [23] *Let* $t \in (-\infty, \infty)$, *then the natural transform of the function* $v(t)$ *is defined by*:

$$\mathbf{N}^+\left[v(t)\right] = V(s,u) = \int_{-\infty}^{\infty} \mathrm{e}^{-st} v(ut)\,\mathrm{d}t; \quad s,u \in (0,\infty]. \tag{1}$$

where $\mathbf{N}^+$ denotes as natural transform and s,u are transforming variables.

Equation (1) can be simplified as [23]

$$\begin{aligned}
\mathbf{N}^+\left[v(t)\right] &= V(s,u) = \int_{-\infty}^{\infty} \mathrm{e}^{-st} v(ut)\,\mathrm{d}t; \quad s,u \in (0,\infty] \\
&= \int_{-\infty}^{0} \mathrm{e}^{-st} v(ut)\,\mathrm{d}t; s,u \in (-\infty,0) + \int_{0}^{\infty} \mathrm{e}^{-st} v(ut)\,\mathrm{d}t; s,u \in (0,\infty) \\
&= \mathbf{N}^-\left[v(t)\right] + \mathbf{N}^+\left[v(t)\right] \\
&= \mathbf{N}\left[v(t)H(-t)\right] + \mathbf{N}\left[v(t)H(t)\right] \\
&= V^-(s,u) + V^+(s,u)
\end{aligned} \tag{2}$$

where, $H(.)$ is the Heaviside function. Assume the function $v(t)H(t)$ is defined on $\mathbf{R}^+$ and for $t \in \mathbf{R}$ then its natural transform can be define over the set

$$A = \left\{ v(t) : \exists M, \tau_1, \tau_2 > 0, \left|v(t)\right| < M\mathrm{e}^{\frac{|t|}{\tau_j}}, t \in (-1)^j \times [0,\infty), j \in \mathbf{Z}^+ \right\}$$

as in the given integral:

$$\mathbf{N}^+\left[v(t)\right] = V^+(s,u) = \int_{0}^{\infty} \mathrm{e}^{-st} v(ut)\,\mathrm{d}t; \quad s,u \in (0,\infty]. \tag{3}$$

Theorem 2.1 [24] *The generalised natural transform of the function* $v(t)$ *is given as*

$$\mathbf{N}^+\left[v(t)\right] = V^+(s,u) = \sum_{n=0}^{\infty} \frac{n! a_n u^n}{s^{n+1}}. \tag{4}$$

Property 2.1 [23] *Let a be a non-zero constant and* $v(at) \in A$ *then*,

$$\mathbf{N}^+\left[v(at)\right] = \frac{1}{a} V\left(\frac{s}{a}, u\right). \tag{5}$$

Theorem 2.2 [20] *If* H_τ *is the Heaviside function and for any real number* $\tau \geq 0$ *we defined*

$$H_\tau(t)=\begin{cases}1, & \text{for } t\geq\tau\\ 0 & \text{for } t<\tau\end{cases}$$

Then the natural transform of the shifted function $v(t-\tau)=v(t-\tau)H_\tau(t)$ is given by

$$\mathbf{N}^+\left[v(t-\tau)H_\tau(t)\right]=\mathrm{e}^{\frac{-s\tau}{u}}\mathbf{N}^+\left[v(t)\right]. \tag{6}$$

Theorem 2.3 [24] *Let* $v^{(n)}(t)$ *be the nth derivatives of the function* $v(t)$ *then its natural transform is given by*

$$\mathbf{N}^+\left[v^n(t)\right]=V_n^+(s,u)=\frac{s^n}{u^n}V(s,u)-\sum_{k=1}^{n}\frac{s^{n-k}}{u^{(n-k)+1}}v^{k-1}(0). \tag{7}$$

Corollary 2.1

Let $v_i^{(n)}(at)$ be the *nth* derivatives of the functions $v_i(at)$ with respect to *t*, $(i=1,2,\cdots,N)$ and suppose that $\mathbf{N}^+\left[v_i(at)\right]=V_i^+(as,u)$ then we define the following

$$\mathbf{N}^+\left[v_i^n(at)\right]=V_{n,i}^+(as,u)=\frac{s^n}{(au)^n}V_i^+(as,u)-\sum_{k=1}^{n}\frac{s^{n-k}}{au^{(n-k)+1}}v_i^{(k-1)}(0) \tag{8}$$

Proof

Using an induction method, for $n=1$ and $n=2$ we respectively obtained the natural transform of first and second derivatives of $v_i(at)$ that is

$$\begin{aligned}\mathbf{N}^+\left[v_i'(at)\right]&=V_{1,i}^+(as,u)=\frac{s}{au}V_i^+(as,u)-\frac{v_i(0)}{au}\\ \mathbf{N}^+\left[v_i''(at)\right]&=V_{2,i}^+(as,u)=\frac{s^2V_i^+(as,u)-sv_i(0)}{(au)^2}-\frac{v_i'(0)}{au}\end{aligned} \tag{9}$$

Now suppose the result holds for *n*, then we have to show its also true for $n+1$. Now from Equation (9) we have

$$\begin{aligned}\mathbf{N}^+\left[v_i^{(n+1)}(at)\right]&=\mathbf{N}^+\left[\left(v_i^{(n)}(at)\right)'\right]=V_{n+1,i}^+(as,u)=\frac{s}{au}V_{n,i}^+(as,u)-\frac{v_i^{(n)}(0)}{au}\\ &=\frac{s}{au}\left[\frac{s^n}{(au)^n}V_i^+(as,u)-\sum_{k=1}^{n}\frac{s^{n-k}}{(au)^{(n-k)+1}}v_i^{(k-1)}(0)\right]-\frac{v_i^{(n)}(0)}{au}\\ &=\frac{s^{n+1}}{(au)^{n+1}}V_i^+(as,u)-\sum_{k=1}^{n+1}\frac{s^{(n-k)+1}}{(au)^{(n-k)+2}}v_i^{(k-1)}(0)\end{aligned} \tag{10}$$

which is true for $n+1$ and hence the result.

Corollary 2.2

Suppose $v_i^{(n)}(t-\tau)$ are the *nth* derivatives of the shifted functions $v_i(t-\tau)$ with respect to *t*, then their natural Transforms can be define as

$$\begin{aligned}\mathbf{N}^+\left[v_i^n(t-\tau)\right]&=\mathrm{e}^{\left(-\frac{s\tau}{u}\right)}V_{n,i}^+(s,u)\\ &=\frac{s^n}{u^n}\mathrm{e}^{\left(-\frac{s\tau}{u}\right)}V_i^+(s,u)-\sum_{k=1}^{n}\frac{s^{n-k}}{(u)^{(n-k)+1}}\left[\lim_{t\to0}v_i^{(k-1)}(t-\tau)\right]\end{aligned} \tag{11}$$

Proof

Also by induction, for $n=1$ and $n=2$ we respectively have the natural transform of first and second derivatives of $v_i(t-\tau)$, that is

$$\begin{aligned}\mathbf{N}^+\left[v_i'(t-\tau)\right] &= \frac{s}{u}\mathrm{e}^{\frac{-s\tau}{u}}V_i^+(s,u)-\frac{1}{u}\lim_{t\to 0}v_i(t-\tau)\\ \mathbf{N}^+\left[v_i''(t-\tau)\right] &= \frac{s^2\mathrm{e}^{\frac{-s\tau}{u}}V_i^+(s,u)-s\lim_{t\to 0}v_i(t-\tau)}{u^2}-\frac{\lim_{t\to 0}v_i'(t-\tau)}{u}\end{aligned} \tag{12}$$

Now assume Equation (11) is true for n and we have to show for $n+1$. From Equation (12) we have

$$\begin{aligned}&\mathbf{N}^+\left[v_i^{(n+1)}(t-\tau)\right]=\mathbf{N}^+\left[\left(v_i^n(t-\tau)\right)'\right]=\frac{s}{u}\mathbf{N}^+\left[v_i^{(n)}(t-\tau)\right]-\frac{\lim_{t\to 0}v_i^n(t-\tau)}{u}\\ &=\frac{s}{u}\left[\frac{s^n}{u^n}\mathrm{e}^{\frac{-s\tau}{u}}V_i^+(s,u)-\sum_{k=1}^{n}\frac{s^{n-k}}{u^{(n-k)+1}}\left[\lim_{t\to 0}v_i^{(k-1)}(t-\tau)\right]\right]-\frac{\lim_{t\to 0}v_i^{(n)}(t-\tau)}{u}\\ &=\frac{s^n}{u^n}\mathrm{e}^{\frac{-s\tau}{u}}V_i^+(s,u)-\sum_{k=1}^{n+1}\frac{s^{n-k+1}}{u^{(n-k)+2}}\left[\lim_{t\to 0}v_i^{(k-1)}(t-\tau)\right]\end{aligned} \tag{13}$$

which is true for $n+1$ and hence the proof.

Another important point to note is that, in both the concept of HAM and natural transform there is no direct approach for the computation of nonlinear terms of the system of NDDEs for both Proportional and constant delays. Therefore, in this research the He's polynomial will be adjusted for the series calculation of these nonlinear terms.

3. Analysis of the Result

Consider the following n-order system of NDDEs

$$\begin{aligned}&\left[v_i(t)+v_i(\alpha(t))\right]^{(n)}\\ &=F_i\left[t,v_\gamma^{(p)}(t),v_\gamma^{(p)}\left(\alpha_{i,j}(t)\right)\right],t\in[0,d],i=1,\cdots,N,J=1,\cdots,M\end{aligned} \tag{14}$$

where

$$\begin{aligned}&v_\gamma^{(p)}(t)=\left(v_1^{(p)},v_2^{(p)},\cdots,v_N^{(p)}\right),\\ &v_\gamma^{p}\left(\alpha_{i,j}(t)\right)=\left(v_1^{(p)}\left(\alpha_{i,j}(t)\right),v_2^{(k)}\left(\alpha_{i,j}(t)\right),\cdots,v_N^{(p)}\left(\alpha_{i,j}(t)\right)\right)\end{aligned}$$

for $p=0,1,2,\cdots,n-1$ and $\alpha_{i,j}(t)$ are the functions of delay terms such that $\alpha(t)=\max\left[\alpha_{i,j}(t)\right]$
with the given initial conditions

$$v_i^{(p)}(0)=v_{i,0}^{(p)},\quad v_i(t)=\psi_i(t),\quad t<0 \tag{15}$$

Now for simplicity we rewrite Equation (14) in the following form

$$L_i\left(v_i+v_i(\alpha)\right)+R_i\left(v_\gamma\right)+F\left(v_\gamma\right)=g_i(t) \tag{16}$$

Subject to a given initial conditions. The v_γ is defined as N-dimentional vector of the form $v_\gamma=\left[v_1(t),v_2(t),\cdots,v_N(t)\right]$. The linear terms are decom-

posed into bounded linear operators $L_i + R_i$ (That is there are some positive numbers $\alpha_{i,1}, \alpha_{i,2}$ such that $\{\|L_i(v_\gamma)\| \le \alpha_{i,1}\|v_\gamma\|,\ \|R_i(v_\gamma)\| \le \alpha_{i,2}\|v_\gamma\|\}$ with L_i as the highest order and R_i as remaining of the linear operators, and F_i are continuous functions satisfy the Lipschitz condition with Lipschitz constants $\mu_i \in [0,d]$ ($|f_i(v) - f_i(u)| \le \mu_i |v-u|, \forall t \in [0,d]$}) represent the non-linear terms.

Take the natural transform of both sides of Equation (16) to obtain:

$$\mathbf{N}^+\left[L_i\left(v_i + v_i(\alpha_i)\right)\right] + \mathbf{N}^+\left[R_i\left(v_\gamma\right)\right] + \mathbf{N}^+\left[F_i\left(v_\gamma\right)\right] = \mathbf{N}^+\left[g_i(t)\right] \tag{17}$$

Note: This research considered two forms of delay functions $\alpha_{i,j}(t)$ as follows:

Case I: $\alpha_{i,j}(t) = a_{i,j}t$, where $a_{i,j} \in (0,1)$ (proportional delay).

Case II: $\alpha_{i,j}(t) = t - \tau_{i,j}$, where $\tau_{i,j} > 0$ are real constants (constant delay) Therefore, by substituting the given initial condition into Equation (17), and simplify using the differential properties of natural transform we respectivily obtained the following for the two types of delay as defined in Case I and Case II.

$$\begin{aligned}
&\mathbf{N}^+\left[v_i(t) + \frac{1}{a_i^{(n+1)}}v(a_i t)\right] - \sum_{k=1}^{n}\left(1 + \frac{1}{a_i^{(n+1-k)}}\right)\frac{u^{n-k}}{s^k}v_i^{k-1}(0) \\
&+\frac{u^n}{s^n}\mathbf{N}^+\left[R_i\left(v_\gamma\right) + F_i\left(v_\gamma\right) - g_i(t)\right] = 0 \\
&\mathbf{N}^+\left[v_i(t) + \mathrm{e}^{\frac{-s\tau_i}{u}}v_i(t)\right] - \sum_{k=1}^{n}\frac{u^{n-k}}{s^k}\left[v_i^{k-1}(0) + \lim_{t\to 0}v_i^{k-1}(t-\tau_i)\right] \\
&+\frac{u^n}{s^n}\mathbf{N}^+\left[R_i\left(v_\gamma\right) + F_i\left(v_\gamma\right) - g_i(t)\right] = 0
\end{aligned} \tag{18}$$

where $a_i = \max\left[a_{i,j}\right]$ and $\tau_i = \max\left[\tau_{i,j}\right]$

Now from Equation (18) we can define the following nonlinear operators

$$\begin{aligned}
N_i\left[\phi_i(t;q)\right] &= \mathbf{N}^+\left[\phi_i(t;q) + \frac{1}{a_i^{(n+1)}}\phi_i(a_i t;q)\right] - \sum_{k=1}^{n}\left(1 + \frac{1}{a_i^{(n+1-k)}}\right)\frac{u^{n-k}}{s^k}\phi_i^{k-1}(9) \\
&+\frac{u^n}{s^n}\mathbf{N}^+\left[R_i\left(\phi_\gamma(t;q)\right) + F_i\left(\phi_\gamma(t;q)\right) - g_i(t)\right] \\
N_i\left[\phi_i(t;q)\right] &= \mathbf{N}^+\left[\phi_i(t;q) + \mathrm{e}^{\frac{-s\tau_i}{u}}\phi_i(t;q)\right] - \sum_{k=1}^{n}\frac{u^{n-k}}{s^k}\left[\phi_i^{k-1}(0) + \lim_{t\to 0}\phi_i^{k-1}(t;q-\tau_i)\right] \\
&+\frac{u^n}{s^n}\mathbf{N}^+\left[R_i\left(\phi_\gamma(t;q)\right) + F_i\left(\phi_\gamma(t;q)\right) - g_i(t)\right]
\end{aligned} \tag{19}$$

where $q \in [0,1]$ is an embedding parameter, $\phi_i(t;q)$ are functions of variables t and q.

So, by means of HAM we can construct the following Homotopy Equations as

$$(1-q)\mathbf{N}^+\left[\phi_i(t;q) - v_{i,0}(t)\right] = h_i q H_i(t) N_i\left[\phi_\gamma(t;q)\right] \tag{20}$$

where $\mathbf{N}^+$ denotes as natural transform, $v_{i,0}(t)$ are initial approximations of $v_i(t)$ and $h_i, H(t)$ are non-zero auxiliary parameters and auxiliary fuctions respectively.

Now, from Equation (20) as $q=0$ and $q=1$ we respectively obtained the following equation.

$$\begin{aligned}\phi_i(t,0) &= v_{i,0}(t)\\ \phi_i(t,1) &= v_i(t)\end{aligned} \tag{21}$$

Thus, as q increases from 0 to 1, the solutions $\phi_i(t,q)$ vary from the initial approximations $v_{i,0}(t)$ to the exact solutions $v_i(t)$. In topology, this type of variation is called deformation and Equation (20) is called zero-order deformation equation.

Therefore, the Taylor series expansion of $\phi_i(t,q)$ with respect to q can be obtained as

$$\phi_i(t,q) = \phi_i(t,0) + \sum_{m=1}^{\infty} v_{i,m}(t) q^m \tag{22}$$

where

$$v_{im}(t) = \frac{1}{m!}\frac{\partial^m \phi_i(t;q)}{\partial q^m}\bigg|_{q=0}$$

Suppose that the initial approximations $v_{i,0}(t)$, auxiliary parameters h_i and the auxiliary function $H_i(t)$ are properly chosen so that the series in Equation (22) converges at $q=1$, that is

$$\phi_i(t,1) = v_{i,0}(t) + \sum_{m=1}^{\infty} v_{i,m}(t) \tag{23}$$

Define vectors

$$\boldsymbol{v}_{i,n}(t) = \left[v_{i,0}(t), v_{i,1}(t), \cdots, v_{i,n}(t)\right] \tag{24}$$

By differentiate Equation (20) m times with respect to q and setting $q=0$ and finally divided by $m!$ we obtain the so called *mth*-order deformation equation as

$$\mathbf{N}^{+}\left[v_{i,m}(t) - \chi_m v_{i,m-1}(t)\right] = h_i H_i(t) R_{y_i m}\left[\boldsymbol{v}_{i,m-1}(t)\right] \tag{25}$$

where

$$R_{y_i,m}\left[\boldsymbol{v}_{i,m-1}(t)\right] = \frac{1}{(m-1)!}\frac{\partial^{m-1} N_i\left[\phi_i(t,q)\right]}{\partial q^{m-1}}\bigg|_{q=0} \tag{26}$$

and

$$\chi_m = \begin{cases} 0, & m \le 1 \\ 1, & m > 1 \end{cases}$$

By taking the inverse natural transform on both sides of Equation (25) we obtained

$$v_{i,m}(t) = \chi_m v_{i,m-1}(t) + h_i \mathbf{N}^{-}\left[H_i(t) R_{y_i m}\left[\boldsymbol{v}_{i,m-1}(t)\right]\right] \tag{27}$$

Therefore, $v_{i,m}(t)$ for $m \ge 1$ can be easily obtained from Equation (27), at Mth order we have

$$v_i(t)=\sum_{m=0}^{M}v_{i,m}(t) \tag{28}$$

Hence, as $M\to\infty$ the following recursive relations of Equations (14) and (15) for the two type of delay as defined respectively in Case I and Case II are obtained

$$\begin{aligned}v_{i,m}(t)&=(\chi_m+h_i)v_{i,m-1}(t)+h_i\frac{1}{a_i^n}v_{i,m-1}(a_it)\\&\quad-h_i(1-\chi_m)\mathbf{N}^-\sum_{k=1}^{n}\left(1+\frac{1}{a_i^{n-k+1}}\right)\frac{u^{k-1}}{s^k}v_i^{k-1}(0)\\&\quad+h_i\mathbf{N}^-\left\{\frac{u^n}{s^n}\mathbf{N}^+\left[R_i\left(v_{\gamma,m-1}(t)\right)+H_{i,m-1}\left(v_{\gamma_1},v_{\gamma_2},\cdots,v_{\gamma_N}\right)-g_i(t)\right]\right\},\ m\geq1\\v_{i,m}(t)&=(\chi_m+h_i)v_{i,m-1}(t)+h_iv_{i,m-1}(t-\tau_i)\\&\quad-h_i(1-\chi_m)\mathbf{N}^-\sum_{k=1}^{n}\frac{u^{k-1}}{s^k}\left[v_i^{k-1}(0)+\lim_{t\to0}v_i^{k-1}(t-\tau_i)\right]\\&\quad+h_i\mathbf{N}^-\left\{\frac{u^n}{s^n}\mathbf{N}^+\left[R_i\left(v_{\gamma,m-1}(t)\right)+H_{i,m-1}\left(v_{\gamma_1},\cdots,v_{\gamma_N}\right)-g_i(t)\right]\right\},\ m\geq1\end{aligned} \tag{29}$$

Now, the nonlinear operators $F_i(v_\gamma)$ are expanded as series of modified He's polynomials $H_{i,m-1}\left(v_{\gamma1},v_{\gamma2},\cdots,v_{\gamma n}\right)$ define as

$$H_{i,m}\left(v_{\gamma1},v_{\gamma2},\cdots,v_{\gamma N}\right)=\frac{1}{m!}\frac{\partial^m}{\partial q^m}F_i\left(\sum_{p=0}^{m}q^pv_{\gamma,p}\right)\Bigg|_{q=0} \tag{30}$$

where $v_{\gamma,i}=\left(v_{i,1},v_{i,2},\cdots,v_{i,N}\right)$ and $v_{\gamma,p}=\left(v_{1,p},v_{2,p},\cdots,v_{N,p}\right)$.

The proof for Case II (constant delay) is of the same process with that of Case I.

Theorem 3.1 *Assume* $\left(C[D],\|.\|\right)$ *is a Banach Space and let* $v_{i,m}(t)$ *be defined in* $\left(C[D],\|.\|\right)$, *where* $\|v_{i,m}\|$ *are define in form of an operators, that is* $v_{i,m}(t)=A_i\left(v_{i,m-1}(t)\right)$ *such that* $A_i(v)=-\mathbf{N}^-R_{y_i,m}\left[\vec{v}_{i,m-1}(t)\right]$ *and*

$$\left\|A_i(v)-A_i(u)\right\|\leq\delta_i\|u-v\|,\quad\forall v,u\in C[D] \tag{31}$$

where $\delta_i=(\alpha_{i,1}+\alpha_{i,2}+\mu_i)d$ for some $\delta_i\in(0,1)$. Then A_i have unique fixed points in $C[D]$. Furthermore, the Homotopy series in Equation (23) converged uniquelly to the solutions $v_i(t)$ (their respective fixed points in $C[D]$) of Equations (14) and (15).

Proof

Let $\left[C(D),\|.\|\right]$ be the Banach space of all continuous functions on $C(D)$, and from definitions of L_i,R_i and F_i in Equation (16) then we have to show that the $\{v_{i,m}\}$ are Cauchy sequences in $\left[C(D),\|.\|\right]$. Now from Equation (19) we have

$$\begin{aligned}\left\|v_{i,m}-v_{i,p}\right\|&=\left\|-\mathbf{N}^-\left[R_{y_i,m}\left[\mathbf{v}_{i,m-1}(t)\right]-R_{y_i,p}\left[\mathbf{v}_{i,p-1}(t)\right]\right]\right\|\\&=\left\|\mathbf{N}^-\left[\mathbf{N}^+\left[2\left(\phi_i(t;q)+\frac{1}{a_i^{(n+1)}}\phi_i(a_it;q)\right)\right]\right.\right.\\&\quad\left.\left.-\sum_{k=1}^{n}\left(1+\frac{1}{a_i^{(n+1-k)}}\right)\frac{u^{n-k}}{s^k}\left(\phi_{i,m}^{k-1}(0)-\phi_{i,p}^{k-1}(0)\right)\right.\right.\end{aligned}$$

$$
\begin{aligned}
&+\frac{u^n}{s^n}\mathbf{N}^+\Big[R_i\left(\phi_{i,m-1}(t;q)-\phi_{i,p-1}(t;q)\right)\\
&+F_i\left(\phi_{i,m-1}(t;q)-\phi_{i,p-1}(t;q)\right)-g_i(t)\Big]\Big\|\\
&\le\left\|\mathbf{N}^-\left\{\mathbf{N}^+\Big[L_i\left(v_{i,m-1}-v_{i,p-1}\right)+R_i\left(v_{i,m-1}-v_{i,p-1}\right)+F_i\left(v_{i,m-1}-v_{i,p-1}\right)\Big]\right\}\right\|\\
&\le\left(\alpha_{i,1}+\alpha_{i,2}+\mu_i\right)\left\|v_{i,m-1}-v_{i,p-1}\right\|\le\delta_i\left\|v_{i,m-1}-v_{i,p-1}\right\|
\end{aligned}
\tag{32}
$$

For $m=p+1$, we have

$$
\left\|v_{i,p+1}-v_{i,p}\right\|\le\delta_i\left\|v_{i,p}-v_{i,p-1}\right\|\le\delta_i^2\left\|v_{i,p-1}-v_{i,p-2}\right\|\le\cdots\le\delta_i^q\left\|v_{i,1}-v_{i,0}\right\| \tag{33}
$$

Hence, for all $m,p\in N$ with $m\ge p$, by means of Equation (33) and using triangle inequality we seccessively obtained the following

$$
\begin{aligned}
\left\|v_{i,m}-v_{i,p}\right\|&\le\left\|v_{i,m}-v_{i,m-1}\right\|+\left\|v_{i,m-1}-v_{i,m-2}\right\|+\cdots+\left\|v_{i,p+1}-v_{i,p}\right\|\\
&\le\delta_i^{m-1}\left\|v_{i,1}-v_{i,0}\right\|+\delta_i^{m-2}\left\|v_{i,1}-v_{i,0}\right\|+\cdots+\delta_i^p\left\|v_{i,1}-v_{i,0}\right\|\\
&=\delta_i^p\left\|v_{i1}-v_{i,0}\right\|\sum_{k=0}^{m-n-1}\delta_i^k\le\delta_i^p\left\|v_{i,1}-v_{i,0}\right\|\sum_{k=0}^{\infty}\delta_i^k\\
&=\delta_i^p\left\|v_{i1}-v_{i,0}\right\|\left(\frac{1}{1-\delta_i}\right).
\end{aligned}
\tag{34}
$$

Since $\delta_i<1$ then for arbitrary ε_i we can find some large $\eta_i\in N$ such that

$$
\delta_i^{\eta_i}<\frac{\varepsilon_i\left(1-\delta_i\right)}{\left\|v_{i,1}-v_{i,0}\right\|}
$$

Therefore, choosing $p,m>N$ then we obtain the following

$$
\left\|v_{i,m}-v_{i,p}\right\|\le\delta_i^p\left\|v_{i,1}-v_{i,0}\right\|\left(\frac{1}{1-\delta_i}\right)<\frac{\varepsilon_i\left(1-\delta_i\right)}{\left\|v_{i,1}-v_{i,0}\right\|}\left\|v_{i,1}-v_{i,0}\right\|\left(\frac{1}{1-\delta_i}\right)=\varepsilon_i \tag{35}
$$

This shows that $\left\{v_{i,m}\right\}$ are Cauchy sequences in $C[D]$, and hence the sequences converged. And the Proof is now completed. The proof for Case II (constant delay) is of the same process with that of Case I.

To establish the proof for the uniqueness of these solutions, let $v_i(t)$ and $u_i(t)$ be two distinct solutions of Equations (14) and (15). According to Equation (16) we have

$$
v_i(t)+v_i(\alpha)=L_i^{-1}\left[g_i(t)-R_i\left(v_\gamma\right)-F_i\left(v_\gamma\right)\right] \tag{36}
$$

where L_i^{-1} are the inverse operators defined by $\int_0^t(.)\mathrm{d}t$. Since $v_i(t)$ and $u_i(t)$ are distinct solutions of Equations (14) and (15), so from Equation (36) we obtain the following equation

$$
\begin{aligned}
&\left\|\left(v_i-u_i\right)+\left(v_{i,\alpha}-u_{i,\alpha}\right)\right\|\\
&\le\left\|\left(v_i-u_i\right)\right\|=\left\|-\int_0^t\left[R_i\left(v_i-u_i\right)+F_i\left(v_i-u_i\right)\right]\mathrm{d}t\right\|\\
&\le\int_0^t\left[\left\|R_i\left(v_i-u_i\right)\right\|+\left\|F_i\left(v_i\right)-F_i\left(u_i\right)\right\|\right]\mathrm{d}t\\
&\le\left(\alpha_{2,1}\left\|v_i-u_i\right\|+\mu_i\left\|v_i-u_i\right\|\right)d\le\delta_i\left\|v_i-u_i\right\|
\end{aligned}
\tag{37}
$$

According to Equation (37) we have $(1-\delta_i)\|v_i-u_i\| \le 0$ and since $\delta_i \in (0,1)$ then $\|v_i-u_i\| \le 0$ implies that $v_i = u_i$ and hence the proof.

Theorem 3.2 *Suppose the Homotopy series in Equation* (23) *converges to the solutions* $v_i(t)$ *of Equations* (14) *and* (15) *and let the approximations of* $v_i(t)$ *are given by the truncuted series* $\sum_{m=0}^{M} v_{i,m}(t)$. *Then the maximum absolute error is estimated to be*

$$\left\| v_i(t) - \sum_{m=0}^{M} v_{i,m}(t) \right\| \le \frac{\delta_i^n}{1-\delta_i} \left\| v_{i,0} \right\| \tag{38}$$

Proof

According to Theorem 3.1 and Equation (34) we have

$$\left\| v_{i,m} - v_{i,p} \right\| \le \frac{\delta_i^n}{1-\delta_i} \left\| v_{i,0}(t) \right\|$$

As $m \to \infty$ then $v_{i,m} \to v_i(t)$, so we have

$$\left\| v_i(t) - v_{i,p} \right\| \le \frac{\delta_i^n}{1-\delta_i} \left\| v_{i,0}(t) \right\| \tag{39}$$

Since $\delta_i \in (0,1)$ then $1-\delta_i \le 1$ and from Equation (39) we have

$$\left\| v_i(t) - \sum_{m=0}^{M} v_{i,m}(t) \right\| \le \frac{\delta_i^n}{1-\delta_i} \left\| v_{i,0}(t) \right\| \tag{40}$$

The Proof is now complete.

4. Examples and Discussion

The application of the proposed technique will be presented in this section. This involve solving some problems of linear and nonlinear systems of NDDEs with both proportional and constant delays.

Example 4.1 [10] *First we seek for a solution of the following* 2*-dimensional linear system of NDDEs with constant delay*

$$\begin{aligned} v_1'(t) &= v_1'(t-1) + 4v_2(t), \quad 0 \le t \le 2 \\ v_2'(t) &= v_1(t) - v_1(t-1), \quad 0 \le t \le 2 \end{aligned} \tag{41}$$

$$v_1(t) = \mathrm{e}^{-2t}, \quad v_2(t) = \frac{1}{2}\left(\mathrm{e}^{-2(t-1)} - \mathrm{e}^{-2t}\right), \quad t \in [-1,0].$$

Take the natural transform to both sides of Equation (41) and simplify further using Equation (11) to get

$$\begin{aligned} \mathbf{N}^+\left[v_1(t) - \mathrm{e}^{-\frac{s}{u}} v_1(t) \right] - \frac{1}{s}\left[1-\mathrm{e}^2\right] - \frac{u}{s}\mathbf{N}^+\left[4v_2(t)\right] &= 0 \\ \mathbf{N}^+\left[v_2(t)\right] - \frac{1}{s}\left[\frac{1}{2}\left(\mathrm{e}^2-1\right)\right] + \frac{u}{s}\mathbf{N}^+\left[v_1(t-1) - v_1(t)\right] &= 0 \end{aligned} \tag{42}$$

From Equation (42) define a non-linear operator

$$\begin{aligned} N\left[\phi_1(t;q)\right] &= \mathbf{N}^+\left[\phi_1(t;q) - \mathrm{e}^{-\frac{s}{u}} \phi_1(t;q) \right] - \frac{1}{s}\left[1-\mathrm{e}^2\right] - \frac{u}{s}\mathbf{N}^+\left[4\phi_2(t;q)\right] \\ N\left[\phi_2(t;q)\right] &= \mathbf{N}^+\left[\phi_2(t;q)\right] - \frac{1}{s}\left[\frac{1}{2}\left(\mathrm{e}^2-1\right)\right] + \frac{u}{s}\mathbf{N}^+\left[\phi_1(t-1;q) - \phi_1(t;q)\right] \end{aligned} \tag{43}$$

Now using Equation (29) the recursive relation of Example 4.1 can be obtained as

$$\begin{aligned} v_{1,m}(t) &= (\chi_m + h_1) v_{1,m-1}(t) - h_1 v_1(t-1) - h_1 (1-\chi_m) \mathbf{N}^- \left[\frac{1}{s} \left(1 - \mathrm{e}^2 \right) \right] \\ &\quad - h_1 \mathbf{N}^- \left\{ \frac{u}{s} \mathbf{N}^+ \left[R_1 \left(v_{2,m-1}(t) \right) \right] \right\} \\ v_{2,m}(t) &= (\chi_m + h_2) v_{2,m-1}(t) - h_2 (1-\chi_m) \mathbf{N}^- \left[\frac{1}{2s} \left(\mathrm{e}^2 - 1 \right) \right] \\ &\quad + h_2 \mathbf{N}^- \left\{ \frac{u}{s} \mathbf{N}^+ \left[R_2 \left(v_{1,m-1} \right)(t) \right] \right\}, \quad m \geq 1 \end{aligned} \tag{44}$$

By choosing an initial approximations of $v_{1,0}(t) = 1$ and $v_{2,0}(t) = \frac{1}{2}\left(\mathrm{e}^2 - 1 \right)$ and using Equation (44) we obtained the following

$$\begin{aligned} v_{1,1}(t) &= -2h_1 \left(\mathrm{e}^2 - 1 \right) t, \quad v_{2,1}(t) = h_2 \left(\mathrm{e}^2 - 1 \right) t \\ v_{1,2}(t) &= -2h_1 h_2 \left(\mathrm{e}^2 - 1 \right) t^2 - 2h_1 \left(\mathrm{e}^2 - 1 \right) t \\ v_{2,2}(t) &= \left(h_2^2 + 2h_1 h_2 + h_2 \right) \left(\mathrm{e}^2 - 1 \right) t \\ v_{1,3}(t) &= \left(h_1 h_2^2 - 3h_1 h_2 \right) \left(\mathrm{e}^2 - 1 \right) t^2 - 2h_1 \left(\mathrm{e}^2 - 1 \right) t \\ v_{2,3}(t) &= -\frac{2}{3} h_1 h_2 \left(\mathrm{e}^2 - 1 \right)^2 t^3 - \left(2h_1 h_2^2 + h_1 h_2 \right) \left(\mathrm{e}^2 - 1 \right)^2 t^2 \\ &\quad + \left(h_2^3 + 2h_2^2 + h_2 \right) \left(\mathrm{e}^2 - 1 \right) t \end{aligned} \tag{45}$$

Following the same process remaining terms of $v_{i,m}(t)$ for $m \geq 3$ can be obtained. Putting $h_1 = \frac{1}{3\left(\mathrm{e}^2 - 1 \right)}$ and $h_2 = -1$ in Equation (45), then the fifth order approximation of Example 4.1 is given as

$$\begin{aligned} v_1(t) &= 1 - 2t + 2t^2 - \frac{4}{3} t^3 + \frac{2}{3} t^4 - \frac{4}{15} t^5 + \frac{4}{45} t^6 + \cdots \\ v_2(t) &= \frac{1}{2}\left(\mathrm{e}^2 - 1 \right) - \left(\mathrm{e}^2 - 1 \right) t + \left(\mathrm{e}^2 - 1 \right) t^2 - \frac{2}{3}\left(\mathrm{e}^2 - 1 \right) t^3 \\ &\quad + \frac{1}{3}\left(\mathrm{e}^2 - 1 \right) t^4 - \frac{2}{15}\left(\mathrm{e}^2 - 1 \right) t^5 + \frac{2}{45}\left(\mathrm{e}^2 - 1 \right) t^6 + \cdots \end{aligned} \tag{46}$$

The series solutions in Equation (46) converged to exact solutions $v_1(t) = \mathrm{e}^{-2t}, v_2(t) = \frac{1}{2}\left(\mathrm{e}^{-2(t-1)} - \mathrm{e}^{-2t} \right)$ of Equation (41).

Therefore, the fifth order approximated series of the derived algorithm in Equation (29) was successfully generates the closed form solution of Example 4.1 with minimum error as shown in **Figure 1** While in most applications only numerical approximations was obtained. For instance, in [10] the numerical approximation of this problem was computed using Implicit Block method with the maximum absolute error of 1.47320 when the tolerance was 1×10^{-10} in a total number of 25 steps.

Example 4.2 [12] *Next we consider a third-order nonlinear system of NDDEs with both proportional and constant delays*

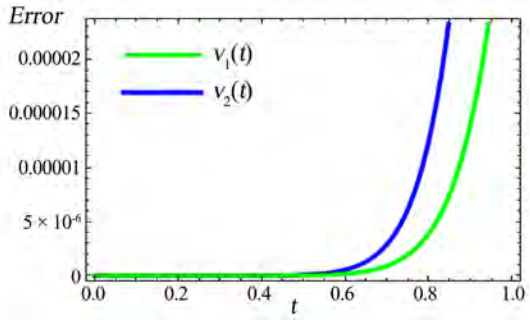

Figure 1. The behaviour of maximum absolute errors between the exact solution and fifth-order approximation of Example 4.1.

$$\begin{aligned} v_1'''(t) &= v_1'''(t-2)v_1\left(\frac{t}{3}\right)+\left(v_1(t)\right)^{\frac{2}{3}}+2t+\mathrm{e}^{-t} \\ v_2'''(t) &= \frac{1}{2}v_2'''\left(\frac{t}{2}\right)+v_2'(t-1)v_1\left(\frac{t}{3}\right), \quad t\geq 1 \end{aligned} \tag{47}$$

with initial functions

$$\phi_1(t)=\mathrm{e}^t, \quad \phi_2(t)=t^2, \quad t\in[-2,0]$$

and the given initial conditions

$$\begin{aligned} &v_1(0)=1, \quad v_1'(0)=1, \quad v_1''(0)=1 \\ &v_2(0)=0, \quad v_2'(0)=0, \quad v_2''(0)=2 \end{aligned}$$

Take the natural transform to both sides of Equation (47) and simplify further using Equation (11) to get

$$\begin{aligned} &\mathbf{N}^+\left[v_1(t)\right]-\left[\frac{1}{s}+\frac{u}{s^2}+\frac{u^2}{s^3}\right]-\frac{u^3}{s^3}\mathbf{N}^+\left[\mathrm{e}^{t-2}v_1\left(\frac{t}{2}\right)+\left(v_1(t)\right)^{\frac{2}{3}}+2t+\mathrm{e}^{-t}\right]=0 \\ &\mathbf{N}^+\left[v_2(t)-8v_2\left(\frac{t}{2}\right)\right]-\frac{u^3}{s^2}\mathbf{N}^+\left[2(1-t)v_1\left(\frac{t}{3}\right)\right]=0 \end{aligned} \tag{48}$$

From Equation (48) define a non-linear operator

$$\begin{aligned} N\left[\phi_1(t;q)\right] &= \mathbf{N}^+\left[\phi_1(t;q)\right]-\left[\frac{1}{s}+\frac{u}{s^2}+\frac{u^2}{s^3}\right] \\ &\quad -\frac{u^3}{s^3}\mathbf{N}^+\left[\mathrm{e}^{t-2}\phi_1\left(\frac{t}{2};q\right)+\left(\phi_1(t;q)\right)^{\frac{2}{3}}+2t+\mathrm{e}^{-t}\right] \\ N\left[\phi_2(t;q)\right] &= \mathbf{N}^+\left[\phi_2(t;q)-8\phi_2\left(\frac{t}{2};q\right)\right]-\frac{u^3}{s^2}\mathbf{N}^+\left[2(1-t)\phi_1\left(\frac{t}{3};q\right)\right]=0 \end{aligned} \tag{49}$$

Now using Equation (29) the recursive relation of Example 4.2 can be obtained as

$$\begin{aligned} v_{1,m}(t) &= (\chi_m+h_1)v_{1,m-1}-h_1(1-\chi_m)\mathbf{N}^-\left[\frac{1}{s}+\frac{u}{s^2}+\frac{u^2}{s^3}\right] \\ &\quad -h_1\mathbf{N}^-\left\{\frac{u^3}{s^3}\mathbf{N}^+\left[R_1\left(v_{1,m-1}(t)\right)+H_{1,m-1}\left(v_{\lambda_1},\cdots,v_{\lambda_N}\right)+g_1(t)\right]\right\} \\ v_{2,m}(t) &= (\chi_m+h_2)v_{2,m-1}(t)-4h_2v_{m-1}\left(\frac{t}{2}\right)-h_2\mathbf{N}^-\left\{\frac{u^3}{s^3}\mathbf{N}^+\left[R_2\left(v_{2,m-1}\right)(t)\right]\right\} \end{aligned} \tag{50}$$

By choosing an initial approximations of $v_{1,0}(t)=1+t+\frac{t^2}{2!}+\frac{t^3}{3!}$ and $v_{2,0}(t)=t^2$ and using Equation (50) we obtained the following

$$\begin{aligned} v_{1,1}(t) &= -\left(\frac{1+\mathrm{e}^{-2}}{6}\right)h_1t^3-\left(\frac{5+4\mathrm{e}^{-2}}{72}\right)h_1t^4-\left(\frac{16\mathrm{e}^{-2}-5}{1080}\right)h_1t^5 \\ &\quad +\left(\frac{1098\mathrm{e}^{-2}+506}{1145}\right)h_1t^6 \\ v_{2,1}(t) &= \frac{1}{3}h_2t^3-\frac{1}{27}h_2t^4-\frac{1}{108}h_2t^5+\cdots \end{aligned} \tag{51}$$

By putting $h_1=-1$ and $h_2=-2$ in the series Equation (51) we obtained the approximate solution of Example 4.2 as

$$\begin{aligned} v_1(t) &= 1+t+\frac{t^2}{2}+\left(\frac{1+\mathrm{e}^{-2}}{6}\right)t^3+\left(\frac{5+4\mathrm{e}^{-2}}{72}\right)t^4+\left(\frac{16\mathrm{e}^{-2}-5}{1080}\right)t^5 \\ &\quad -\left(\frac{1098\mathrm{e}^{-2}+506}{1145}\right)t^6 \\ v_2(t) &= t^2-\frac{2}{3}t^3+\frac{2}{27}t^4+\frac{1}{54}t^5+\cdots \end{aligned} \tag{52}$$

Using only one iteration of the derived algorithm (first order) in Equation (29) a good approximation of Example 4.2 was successfully obtained. Since this problem has no exact solution therefore, Figure 2 shows the comparison between approximate solution obtained by the proposed technique, Matlab Package DDENSD and the result obtained by Rebenda and Smarda [12] using an algorithm based on the combination of the method of steps and differential transform method (DT).

Threrefore, from Figure 2 we can observed that there is a good correspondence between the first order approximate solution of the proposed tecnique with that of Matlab Package DDENSD and DT. Hence, this shows that the presented method provides reliable results and reduces the computation size as compared with the previous techniques.

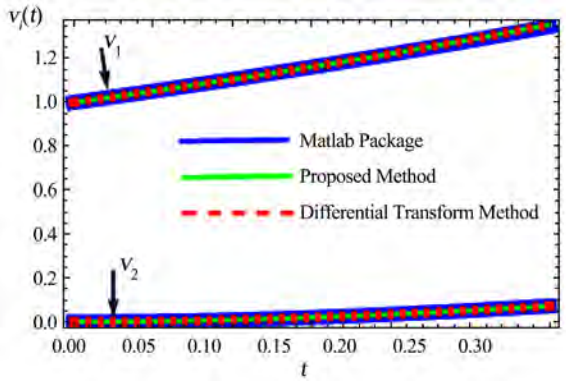

Figure 2. Comparison of solutions obtained by Matlab Package, Proposed Method and Differential Transform Method of Example 4.2.

5. Conclusion

This paper presents an efficient analytical approach suitable for solving linear and nonlinear systems of NDDEs with proportional and constant delays via HAM and natural transform. The presented algorithm adjusted the He's polynomial in order to ease the computational difficulties of both proportional and constant delays. Another advantage of this research is that a new algorithm is constructed in Equation (25) which reduces the computational work as compared to other methods, produces a much faster convergent approximate solution and handles more complicated problems (as in the case of second example) in applications than other analytical methods. Therefore, the presented approach is efficient and reliable in solving different form of linear and nonlinear systems of NDDEs which can be also applied to solve various types of linear and nonlinear problems.

Acknowledgements

The authors like express their gratitude for financial support from Transdisciplinary Research Grant Scheme (TRGS) under the research programme of Characterisation of Spatio-temporal Marine Microalgae Ecological Impact Using Multi-Sensor Over Malaysia Waters for the specific sub-project of Mathematical Modelling of Harmful Algal Blooms (HABs) in Malaysia Waters (R.J130000.7809.4L854) funded by the Ministry of Education, Malaysia. Authors also like to appreciate the Universiti Teknologi Malaysia for providing all the necessary support and facilities toward the success of this research.

Conflicts of Interest

The authors declare no conflicts of interest regarding the publication of this paper.

References

[1] Alomari, A.K., Noorani, Mohd Salmi, M.D. and Nazar, R. (2009) Solution of Delay Differential Equation by Means of Homotopy Analysis Method. *Acta Applicandae Mathematicae*, **108**, 395. https://doi.org/10.1007/s10440-008-9318-z

[2] Batzel, J. and Tran, H.T. (2000) Stability of the Human Respiratory Control System I. Analysis of a Two-Dimensional Delay State-Space Model. *Journal of Mathematical Biology*, **41**, 45-79. https://doi.org/10.1007/s002850000044

[3] Liu, L.P. and Kalmár-Nagy, T. (2010) High-Dimensional Harmonic Balance Analysis for Second-Order Delay-Differential Equations. *Journal of Vibration and Control*, **16**, 1189-1208. https://doi.org/10.1177/1077546309341134

[4] Bellen, A. and Zennaro, M. (2013) Numerical Methods for Delay Differential Equations. Oxford University Press, Oxford.

[5] Rihan, F.A., *et al.* (2014) A Time Delay Model of Tumour—Immune System Interactions: Global Dynamics, Parameter Estimation, Sensitivity Analysis. *Applied Mathematics and Computation*, **232**, 606-623. https://doi.org/10.1016/j.amc.2014.01.111

[6] Rihan, F.A., Azamov, A.A. and Al-Sakaji, J.H. (2018) An Inverse Problem for Delay

Differential Equations: Parameter Estimation, Nonlinearity, Sensitivity. *Applied Mathematics*, **12**, 63-74. https://doi.org/10.18576/amis/120106

[7] Blanco-Cocom, L., Estrella, G.A. and Avila-Vales, E. (2012) Solving Delay Differential Systems with History Functions by the Adomian Decomposition Method. *Applied Mathematics and Computation*, **37**, 5994-6011. https://doi.org/10.1016/j.amc.2011.11.082

[8] Bellour, A. and Bousselsal, M. (2014) Numerical Solution of Delay Integro-Differential Equations by Using Taylor Collocation Method. *Mathematical Methods in the Applied Sciences*, **37**, 1491-1506. https://doi.org/10.1002/mma.2910

[9] Duarte, J., Januario, C. and Martins, N. (2016) Analytical Solutions of an Economic Model by the Homotopy Analysis Method. *Applied Mathematical Sciences*, **10**, 2483-2490. https://doi.org/10.12988/ams.2016.66188

[10] Ishak, F. and Ramli, M. S.B. (2015) Implicit Block Method for Solving Neutral Delay Differential Equations. *AIP Conference Proceedings*, **1682**, Article ID: 020054. https://doi.org/10.1063/1.4932463

[11] Rebenda, J., Šmarda, Z. and Khan, Y. (2015) A Taylor Method Approach for Solving of Nonlinear Systems of Functional Differential Equations with Delay.

[12] Rebenda, J. and Šmarda, Z. (2019) Numerical Algorithm for Nonlinear Delayed Differential Systems of nth Order. *Advances in Difference Equations*, **2019**, Article No. 26. https://doi.org/10.1186/s13662-019-1961-3

[13] Barde, A. and Maan, N. (2019) Efficient Analytical Approach for Nonlinear System of Delay Differential Equations. *Computer Science*, **14**, 693-712.

[14] Liao, S.J. (1992) The Proposed Homotopy Analysis Technique for the Solution of Nonlinear Problems. Ph.D. Thesis, Shanghai Jiao Tong University, Shanghai.

[15] Liao, S.J. (2003) Beyond Perturbation: Introduction to the Homotopy Analysis Method. Chapman and Hall/CRC, New York. https://doi.org/10.1201/9780203491164

[16] Liao, S.J. and Cheung, F. (2003) Homotopy Analysis of Nonlinear Progressive Waves in Deep Water. *Journal of Engineering Mathematics*, **45**, 105-116.

[17] Liao, S.J., Su, J. and Chwang, T.A. (2006) Series Solutions for a Nonlinear Model of Combined Convective and Radiative Cooling of a Spherical Body. *International Journal of Heat and Mass Transfer*, **49**, 2437-2445. https://doi.org/10.1016/j.ijheatmasstransfer.2006.01.030

[18] Odibat, Z., Momani, S. and Xu, H. (2010) A Reliable Algorithm of Homotopy Analysis Method for Solving Nonlinear Fractional Differential Equation. *Applied Mathematical Modelling*, **34**, 593-600. https://doi.org/10.1016/j.apm.2009.06.025

[19] Khan, Z.H. and Khan, W. (2008) N-Transform-Properties and Applications. *NUST Journal of Engineering Sciences*, **1**, 127-133.

[20] Belgacem, F.B.M. and Silambarasan, R. (2012) Maxwell's Equations Solutions by Means of the Natural Transform. *International Journal of Mathematics in Engineering, Science and Aerospace*, **3**, 313-323. https://doi.org/10.1063/1.4765477

[21] Loonker, D. and Banerji, P.K. (2014) Natural Transform and Solution of Integral Equations for Distribution Spaces. *American Journal of Mathematics and Sciences*, **3**, 65-72.

[22] Al-Omari, S.K.Q. (2017) On q-Analogues of the Natural Transform of Certain q-Bessel Functions and Some Application. *Filomat*, **31**, 2587-2598. https://doi.org/10.2298/FIL1709587A

[23] Belgacem, F.B.M. and Silambarasan, R. (2012) Theory of Natural Transform. *Mathematics in Engineering, Science and Aerospace Journal*, **3**, 99-124.

https://doi.org/10.1063/1.4765477

[24] Belgacem, S.R. (2012) Advances in the Natural Transform. *AIP Conference Proceedings*, **1493**, 106. https://doi.org/10.1063/1.4765477

Applied Mathematics, 2019, 10, 769-783
https://www.scirp.org/journal/am
ISSN Online: 2152-7393
ISSN Print: 2152-7385

Mathematical Modeling on Dynamic Characteristics of the Breakdown Process in Narrow-Gap of SF_6 Based on the FCT Algorithm

Qiuping Zheng[1], Dianchun Zheng[2]

[1]Instrumentation Technology & Economy Institute, Beijing, China
[2]Harbin University of Science and Technology, Harbin, China
Email: zhengqiupingnicole@hotmail.com, zhengdianchun@126.com

How to cite this paper: Zheng, Q.P. and Zheng, D.C. (2019) Mathematical Modeling on Dynamic Characteristics of the Breakdown Process in Narrow-Gap of SF_6 Based on the FCT Algorithm. *Applied Mathematics*, **10**, 769-783.
https://doi.org/10.4236/am.2019.109055

Received: August 21, 2019
Accepted: September 23, 2019
Published: September 26, 2019

Abstract

The two-dimensional and self-consistent fluid model of the SF_6 discharge was established based on the electron and ions continuity transfer equations coupled to Poisson's equation, and also simultaneously considered the photoionization event, and then the flux corrected transport technique (FCT) was employed to numerically solve the particle flux-continuity equations, and some significant microphenomena were achieved that the dynamic behaviors of the charged particles, the spatio-temporal evolution of the discharge channel and the transformation law of the avalanche-streamer for the SF_6 narrow-gap were revealed in this paper.

Keywords

FCT, SF_6, Avalanche, Streamer, Photoionization

1. Introduction

Usually, the approaches to explore gas discharge phenomenon can be classified into experimental and theoretical methods. Experimental method can directly observe the discharge events, but the discharge mechanisms have not been clearly discovered in detail. However, the theoretical method not only gains key data for the dielectric breakdown of gases, but also some microcosmic parameters on controlling dynamic behaviors of charged particles produced in the time of the gas discharge process are founded [1] [2] [3]. Recently, the computational fluid dynamics has been widely used in the gas discharge field due to its advantages in explicit physical concept, legible image exhibition and highly calculating efficiency [4] [5] [6].

Despite the fact that the electron and ion densities can attain very steep gradients and make the shock fronts in particule fluids along the discharge channel when the gas discharge is triggered and developed in the overall process under the stimulation of electric field, the FCT technique (flux corrected transport) shows high efficiency and accuracy dealing with the intricacy situation [7] [8] [9]. By virtue of the excellent thermodynamic, dielectric and transport propeties, SF_6 is widely used in the eletrical industry, especially in the high voltage circuit breaker technology, although it might be replaced by the environment friendly insulating gases. Nevertheless, it is necessary to accurately find microcosmic mechanisms of the particle dynamical behaviors, the spatio-temporal characteristics of the electric field and the track evolution of the discharge channel along the direction of the specific discharge development for broader application domain.

This paper is organized as following: the mathematical model, the FCT algorithm and constraint conditions are carefully presented in Section 2, and the results of the mathematical simulation are analyzed in Section 3 including the following contents: 3.1, avalanche phase; 3.2, streamer formation phase; 3.3, the discharge channel evolution and the photoionization effect. Some valuable conclusions are given in Section 4.

2. The Model and FCT Algorithm

2.1. Model of the Gas Discharge

The model for the narrow-gap with parallel plate electrodes which are filled with SF_6 gas has been presented in detail [10] [11], and the spatio-temporal evolution of the SF_6 discharge overall process is mathematically modeled by a set of equations governing the transport of particles, moment and energy for ions and electrons together with the electric field equation as follows [12] [13]:

$$\frac{\partial(N_e)}{\partial t} = S_{ph} + N_e\alpha|v_e| - N_e\eta|v_e| - N_eN_p\beta - \frac{\partial(N_ev_e)}{\partial z} + \frac{\partial}{\partial z}D\frac{\partial N_e}{\partial z} \tag{1}$$

$$\frac{\partial(N_p)}{\partial t} = S_{ph} + N_e\alpha|v_e| - N_eN_p\beta - N_nN_p\beta - \frac{\partial(N_pv_p)}{\partial z} \tag{2}$$

$$\frac{\partial(N_n)}{\partial t} = N_e\eta|v_e| - N_pN_n\beta - \frac{\partial(N_nv_n)}{\partial z} \tag{3}$$

here t is the time, r and z are the radius and axis distances for the calculating subregion; N_e, N_p *and* N_n are the electron, positive and negative ion densities; v_e, v_p and v_n are respectively the electron, positive and negative ion drift velocity; the symbols α, β, η and D are ionization, adsorption, recombination coefficient and electron diffusion coefficient, respectively, their values have been taken from reference literature [14], and the S_{ph} is photoionization source term. Collision ionization process between electrons and neutral particles at atmospheric pressure radiate photons, and these photons are absorbed by molecules according to a certain probability, in this situation, once photon energy

reaches the ionization critical value, then the photoionization process occurs and produces a certain amount of the photo electron. Generally speaking, the number of photon electron is much smaller than that of the electrons generated by impact ionization. However, these photon electrons would result in the formation of the secondary avalanche, which moves towards the head of the first avalanche, composes a big avalanche and accelerates the development of the discharge process. Hence the photoionization effect plays a significant role in the gas discharge process. The term S_{ph}, being a source term due to photoionization, is represented as shown below:

$$S_{ph}(z)=\gamma_p\int_0^d \Omega(z-z')N_e(z')\alpha^*(z')\left|v_e(z')\right|\times\exp\left(-\mu\left|z-z'\right|\right)\mathrm{d}z' \tag{4}$$

here γ_p, α^* and μ are second ionization, excitation and absorption coefficients, and Ω is the solid angle subtended at z' by the disk charge at the point z. A detail solution about S_{ph} can be referred to the literature [15].

Taking into account the distortion of space charge effects on the electric field, the Poisson equation is given by:

$$\nabla^2\varphi=\frac{\partial^2\varphi}{\partial r^2}+\frac{1}{r}\frac{\partial\varphi}{\partial r}+\frac{\partial^2\varphi}{\partial z^2}=-\frac{q}{\varepsilon_0}\left(N_p-N_e-N_n\right) \tag{5}$$

where φ is the electric potential; q is the electronic charge; ε_0 is the permittivity of the free space. The current I in the external circuit due to the motion of electrons and ions between the electrodes is calculated by the Sato formula [16]:

$$I=\frac{\pi r^2 q}{d}\int_0^d\left(N_p v_p-N_n v_n-N_e v_e\right)\mathrm{d}z \tag{6}$$

here, r is the radius of the discharge channel, q is the electronic charge.

The convection term of particle's continuity Equations (1)-(3) are solved by the FCT technique and other items are used the finite difference directly to solve and the Poisson's Equation (5) is numerically resolved by the over-relaxation iteration.

2.2. FCT Algorithm

The convective terms of Equations (1), (2) and (3) are written as $\left.\frac{\partial N}{\partial t}\right|_{\text{conv}}=-\frac{\partial(Nv)}{\partial x}$, where symbol N shows the density of the particle species and v is their velocities.

Taking (rN) as the dependent variable for an axisymmetric cylindrical coordinate system, then

$$\left.\frac{\partial(rN)}{\partial t}\right|_{\text{conv}}=-\frac{\partial f}{\partial r}-\frac{\partial g}{\partial z} \tag{7}$$

where

$$f=rNv_r, g=rNv_z \tag{8}$$

The flux corrected transport algorithm is as follows [17]:

1). Compute $F^{\mathrm{L}}_{i+\frac{1}{2},j}$ and $G^{\mathrm{L}}_{i,j+\frac{1}{2}}$ by a low order monotonic scheme (donor cell).

2). Compute $F^{\mathrm{H}}_{i+\frac{1}{2},j}$ and $G^{\mathrm{H}}_{i,j+\frac{1}{2}}$ by a high order scheme.

3). Define the anti-diffusive fluxes:

$$A_{i+\frac{1}{2},j} = F^{\mathrm{H}}_{i+\frac{1}{2},j} - F^{\mathrm{L}}_{i+\frac{1}{2},j},\ A_{i,j+\frac{1}{2}} = G^{\mathrm{H}}_{i,j+\frac{1}{2}} - G^{\mathrm{L}}_{i,j+\frac{1}{2}} \tag{9}$$

4). Compute the low order time advanced solution:

$$N^{\mathrm{td}}_{i,j} = N^{\mathrm{t}}_{i,j} - \frac{1}{\Delta V_{i,j}}\left(F^{\mathrm{L}}_{i+\frac{1}{2},j} - F^{\mathrm{L}}_{i-\frac{1}{2},j} + G^{\mathrm{L}}_{i,j+\frac{1}{2}} - G^{\mathrm{L}}_{i,j-\frac{1}{2}}\right) \tag{10}$$

5). Limit the anti-diffusive fluxes:

$$A^{\mathrm{C}}_{i+\frac{1}{2},j} = A_{i+\frac{1}{2},j} C_{i+\frac{1}{2},j},\ 0 \le C_{i+\frac{1}{2},j} \le 1 \tag{11}$$

$$A^{\mathrm{C}}_{i,j+\frac{1}{2}} = A_{i,j+\frac{1}{2}} C_{i,j+\frac{1}{2}},\ 0 \le C_{i,j+\frac{1}{2}} \le 1 \tag{12}$$

6). Apply the limited anti-diffusive fluxes:

$$N^{t+\Delta t}_{i,j} = N^{\mathrm{td}}_{i,j} - \frac{1}{\Delta V_{i,j}}\left(A^{\mathrm{C}}_{i+\frac{1}{2},j} - A^{\mathrm{C}}_{i-\frac{1}{2},j} + A^{\mathrm{C}}_{i,j+\frac{1}{2}} - A^{\mathrm{C}}_{i,j-\frac{1}{2}}\right) \tag{13}$$

where $V_{i,j}$, $r_{i,j}$, $N_{i,j}$ and $C_{i,j}$ are the volume, radial distance, density and anti-diffusive coefficient of the (i,j) cell, and further details and calculation procedure on the FCT can be found in the literature [3].

2.3. Constraint Conditions

In this paper, schematic diagram and the constraint conditions for parallel-plate electrodes discharge under atmospheric pressure are set as shown in Figure 1, and the calculation model is converted to a two-dimensional structure by rotating the axis of symmetry. In the present study, the gap distance between the electrodes filled with SF_6 gas is 5 mm under the pressure 0.1 MPa and temperature

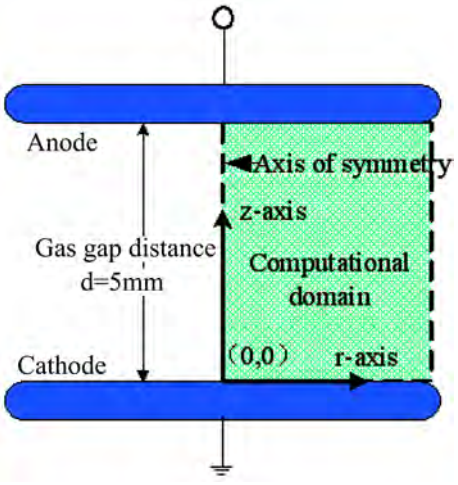

Figure 1. Schematic diagram of mathematical modeling.

300 K. The spatial mesh chosen to be uniform with 40,000 mesh points, namely, the longitudinal axis (z -axis) and the radial axis (r -axis) are all uniformly divided into 200 grids. Then $\Delta t = 0.05\times10^{-9}\,\mathrm{s}$ is taken as time step, which is significantly smaller than that required for stability of the used numerical scheme [3]. At the initial moment of time for gas discharge, the quasi–neutral plasma spot of Gaussian shape in the radial and axial directions is placed at the front of cathode:

$$n_e\big|_{t=0} = n_p\big|_{t=0} = n_0 \exp\left[-\left(\frac{r}{\delta_r}\right)^2 - \left(\frac{z-z_0}{\delta_z}\right)^2\right] \tag{14}$$

where r, z is the radial and axial coordinates respectively; the origin of coordinates ($r = z = 0$) is positioned at the center of cathode surface, the peak value density of particles (seed electrons and positive ions) is $n_0 = 10^6\,\mathrm{m}^{-3}$, the position of initial plasma $z_0 = 0.1\,\mathrm{cm}$, characteristic scales $\delta_r = 2.5\times10^{-4}\,\mathrm{m}$ and $\delta_z = 2.5\times10^{-4}\,\mathrm{m}$.

Boundary conditions for electrons and positive ions at the electrodes are as follows:

$$\left.\frac{\partial n_e}{\partial z}\right|_{z=0} = \left.\frac{\partial n_e}{\partial z}\right|_{z=d} = 0,\ \left.\frac{\partial n_p}{\partial z}\right|_{z=0} = \left.\frac{\partial n_p}{\partial z}\right|_{z=d} = 0$$

The solution of Poisson's equation is subject to the following boundary conditions:

$$V\big|_{z=0} = V_0,\ V\big|_{z=0} = 0,\ \left.\frac{\partial V}{\partial r}\right|_{r=0} = 0,\ V\big|_{r=R} = V_0\frac{z}{d}$$

where V_0 is the applied voltage, r is the radius of the computational domain.

3. Modeling Results

The space between parallel-plane electrodes 0.5 cm apart is filled SF_6 gas with standard atmospheric pressure and commercial purity, and the 46 kV DC is applied on the anode plane, then the cathode grounding. The incepting discharge of the model is trigged by the seed electrons having a Gaussian distribution near the cathode at $t = 0$ ns (located at 0.1 cm from the cathode as mentioned earlier). Under the electric field, the seed electrons obtain energy to migrate, impact the neutral molecules and produce much more charged particles, so that the current through parallel-plane electrodes is shown in **Figure 2**. The transition time of the electron for the model is about 10 ns, according to the principle of gas discharge, the whole discharge process undergoes two phases from the avalanche to the streamer phase while the discharge incepted.

3.1. Avalanche Phase

The electric field stress 92 kV/cm applied to the SF_6 gap, which slightly larger than the threshold value 89.6 kV/cm, easily renders the discharge happen smooth-

ly. With the electrons migrating to the anode and impacting with neutral molecules, an electron swarm is quickly made up as shown in Figure 3. When about 7.7 ns moment, the peak value of the electron swarm is up to the $1.01\times10^{18}\,\mathrm{cm}^{-3}$ at the point $z=0.25\,\mathrm{cm}$ apart from the cathode, and corresponding positive and negative ions densities are $3.97\times10^{18}\,\mathrm{cm}^{-3}$ and $3.22\times10^{18}\,\mathrm{cm}^{-3}$ respectively as shown in Figure 7 and Figure 8, then the distortion of the space electric field is not remarkable as shown in Figure 4 at 7.5 and 7.7 ns moments, therefore the interval from $t=0\,\mathrm{ns}$ to the $t=7.7\,\mathrm{ns}$ usually is known as the avalanche phase according to the gas discharge theory [18].

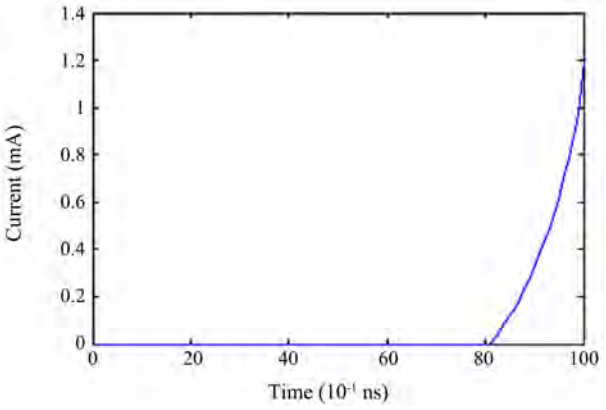

Figure 2. External circuit current.

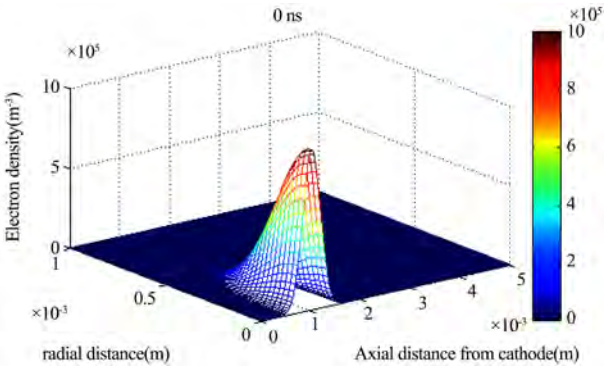

(a) Electron density at 0 ns

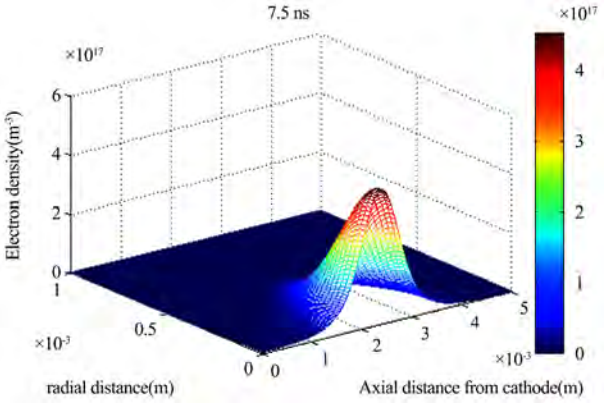

(b) Electron density at 7.5 ns

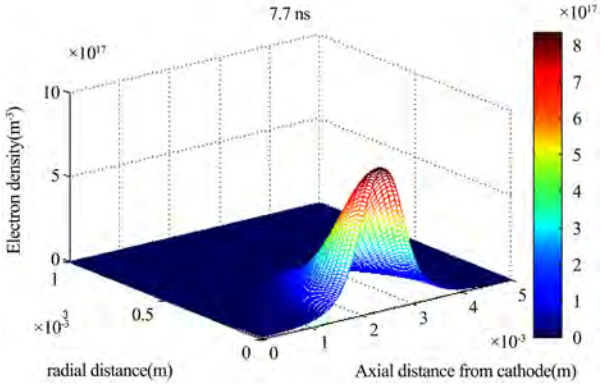

(c) Electron density at 7.7 ns

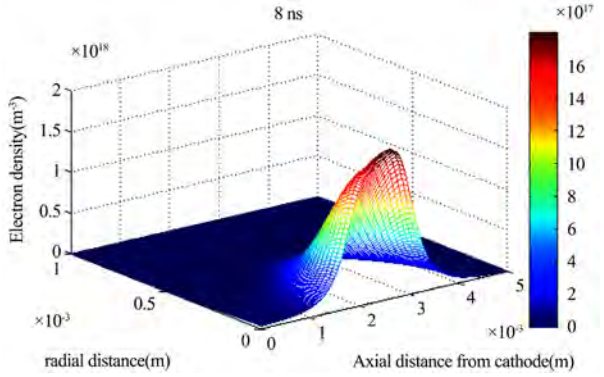

(d) Electron density at 8.0 ns

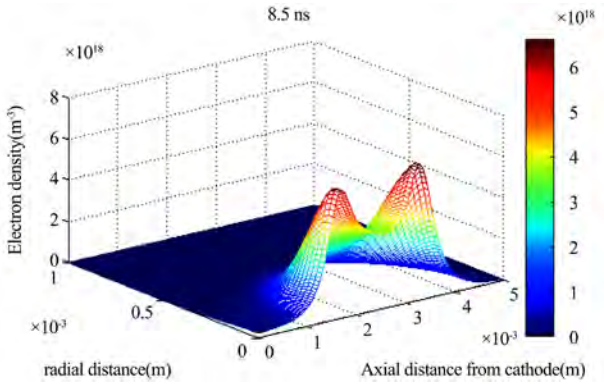

(e) Electron density at 8.5 ns

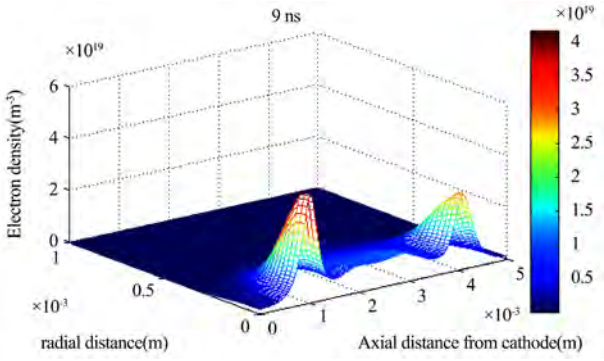

(f) Electron density at 9.0 ns

Figure 3. Electron densities at 0 ns, 7.5 ns, 7.7 ns, 8.0 ns, 8.5 ns and 9.0 ns, respectively.

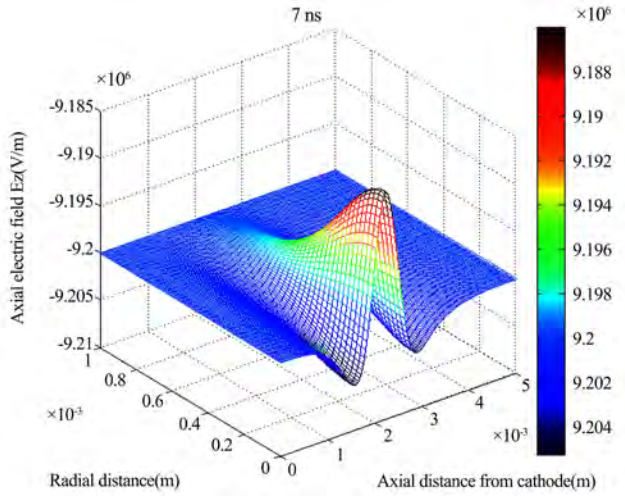

(a) Axial electric field at 7.0 ns

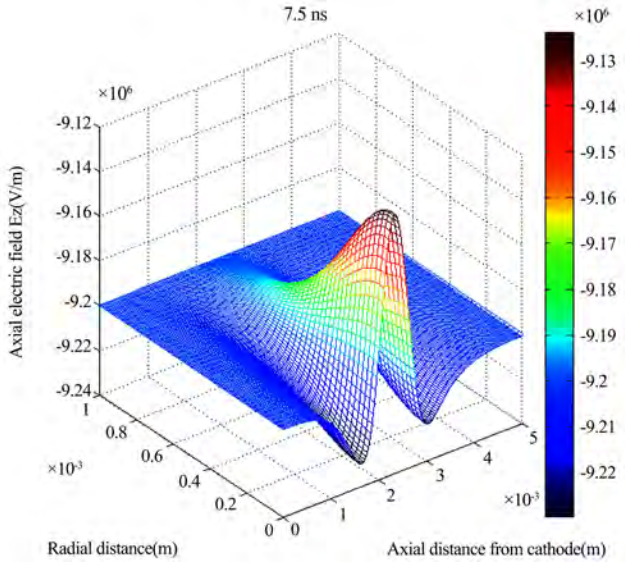

(b) Axial electric field at 7.5 ns

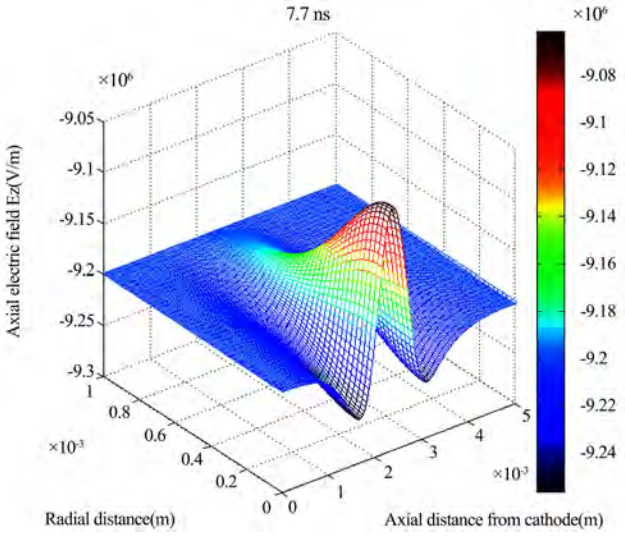

(c) Axial electric field at 7.7 ns

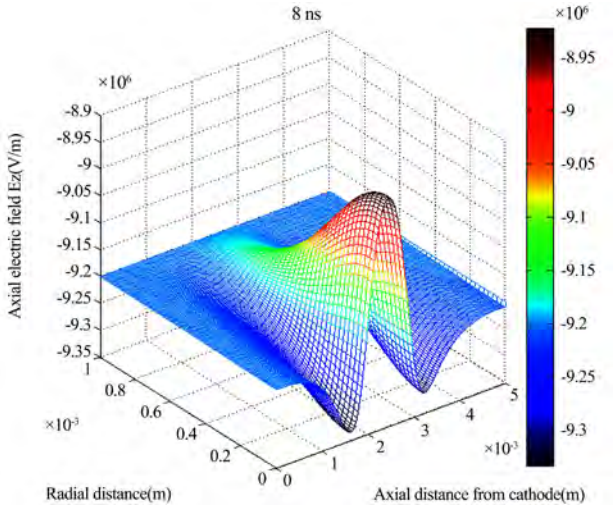

(d) Axial electric field at 8.0 ns

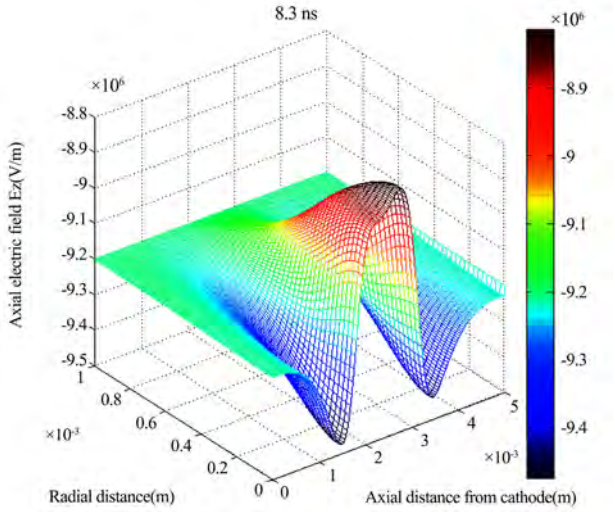

(e) Axial electric field at 8.3 ns

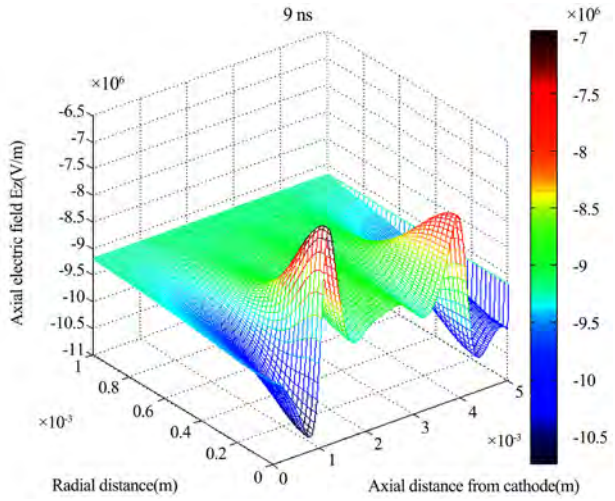

(f) Axial electric field at 9.0 ns

Figure 4. Axial electric fields for SF6 gas at 7.0 ns, 7.5 ns, 7.7 ns, 8.0 ns, 8.3 ns and 9.0 ns, respectively.

3.2. Streamer Phase

When the avalanche volume reaches to the critical value, it instantly changes the avalanche phase into the streamer phase, namely, the streamer phase formation [19] [20]. It is demonstrated in **Figure 3** and **Figure 4** that the electron densities are visibly larger than that of the avalanche phase in the interval 7.7 - 8.0 ns, although the distorting of space electric field is still slight enhancement, it is considered an initial period of the streamer phase.

From the 8.0 ns moment, the streamer discharge is rapidly development, its volume is promptly expanded and the length is also stretched quickly, and simultaneously the electric field distortion is also exacerbated as shown in **Figure 5**, then the mainly changes of the density distribution of charged particles for the electron, positive and negative ions on the axial direction are shown in **Figures 6-8**, the procedure described is rather intricacy including the dynamical behaviors of the charged particles in the electric field [21] [22].

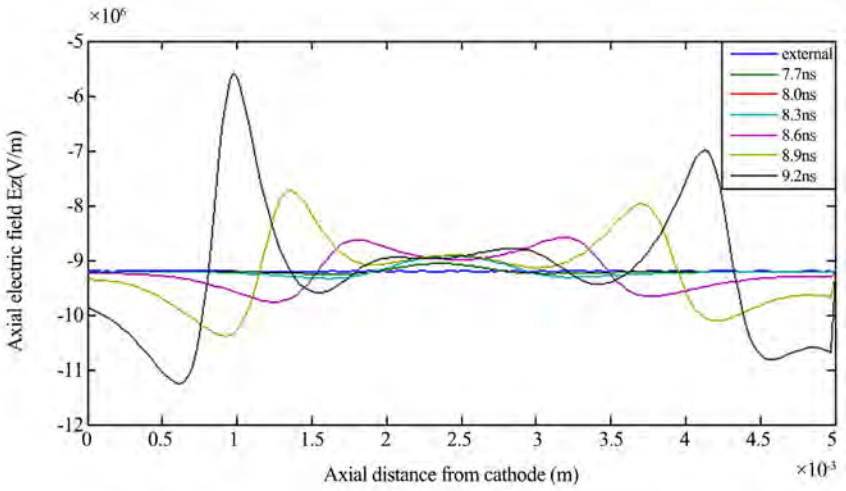

Figure 5. Axial electric field distributions at 7.7 ns, 8.0 ns, 8.3 ns, 8.6 ns, 8.9 ns and 9.2 ns, respectively.

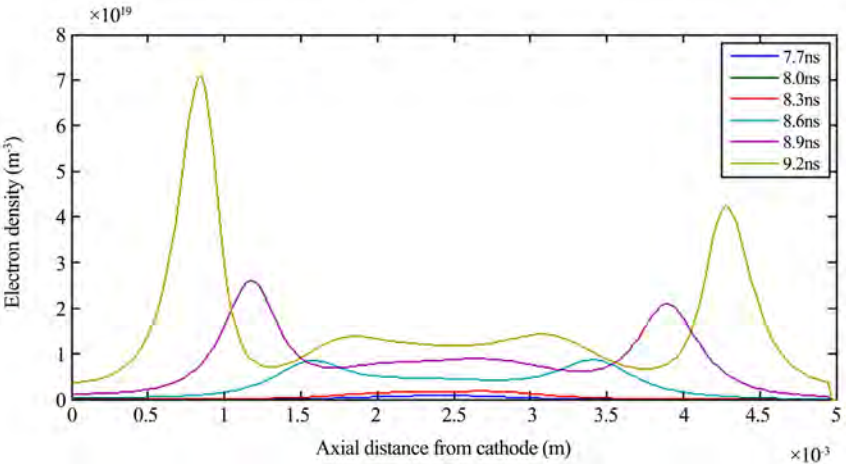

Figure 6. Axial electron distributions at 7.7 ns, 8.0 ns, 8.3 ns, 8.6 ns, 8.9 ns and 9.2 ns, respectively.

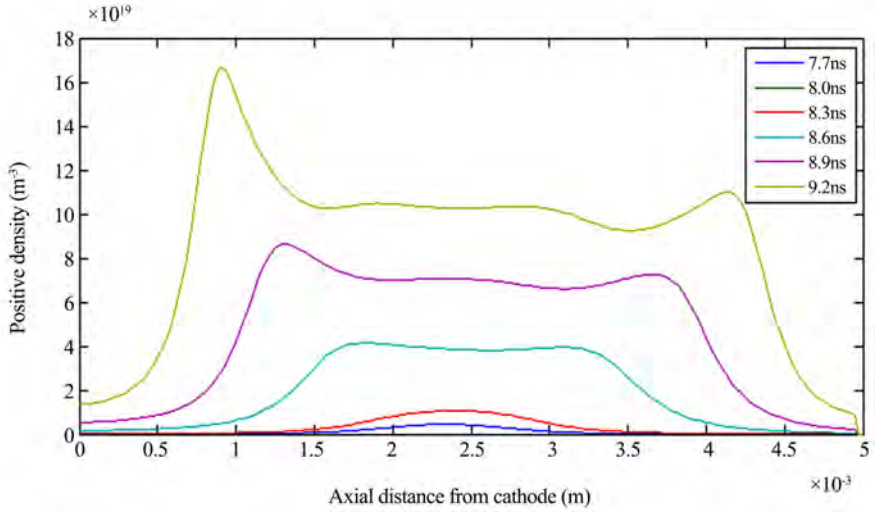

Figure 7. Axial distributions of positive ions at 7.7 ns, 8.0 ns, 8.3 ns, 8.6 ns, 8.9 ns and 9.2 ns, respectively.

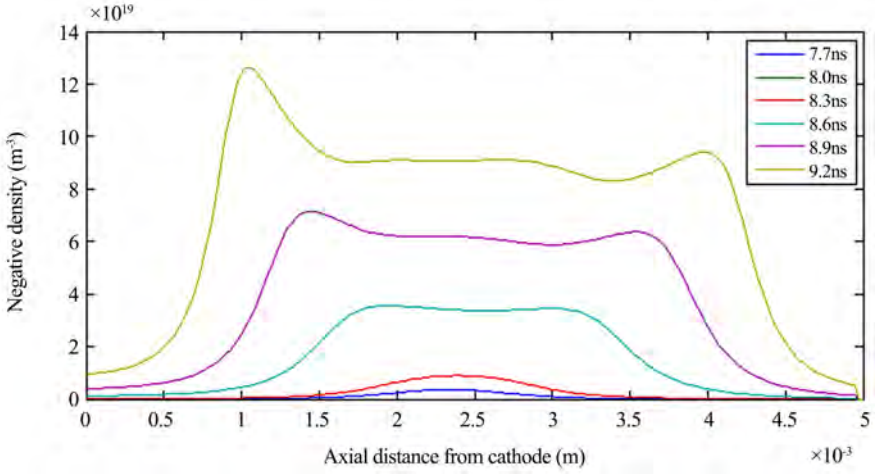

Figure 8. Axial distributions of negative ions at 7.7 ns, 8.0 ns, 8.3 ns, 8.6 ns, 8.9 ns and 9.2 ns, respectively.

1) The anode-directed streamer

When the transformation avalanche into the streamer phase, the peak value of the electron densities from location $z = 0.25$ cm at 7.7 ns to the point $z = 0.44$ cm at $t = 9.2$ ns is shown in Figure 6, and the streamer head moves to the anode at an average speed 1.33×10^{6} cm/s. The positive and negative ion densities in the anode-directed streamer head increase steadily from $4.43\times10^{18}\,\mathrm{cm}^{-3}$ to $1.09\times10^{19}\,\mathrm{cm}^{-3}$ and from $3.62\times10^{18}\,\mathrm{cm}^{-3}$ to $9.41\times10^{19}\,\mathrm{cm}^{-3}$ respectively shown in Figure 7 and Figure 8. The head of the anode-directed streamer shows the electro-negativity due to gathering most electrons and greatly enhanced field intensity of the short distance between the head with the anode plate, so that SF_6 molecule ionization in this small region is dramatically aggravated, and many more electrons are reproduced and the head radius continuously becomes bigger and bigger, the iterative process finally ends

until the head arrives at the anode plate.

2) The cathode-directed streamer

As shown in Figure 6, the curve of electron distribution at $z = 0.18$ cm and $t = 8.3$ ns presents the clearly escalating trend, that is to say, the event of the cathode-directed streamer obviously happens, then the appeared moment of the cathode-directed streamer is later than that of the anode-directed one. In contrast with anode-directed streamer, the head of the cathode-directed streamer presents the electro-positivity, because the electric field is strengthened in the short space between the cathode plate and the head, then the ionization rate of the SF_6 molecule is greatly accelerated and much stronger, the velocity of the cathode-directed streamer at 9.2 ns is 0.92×10^6 cm/s at $z = 0.088$ cm location, which is only about 70% of the velocity of the anode-directed streamer in the same moment.

3.3. Discharge Channel and Photoionization

As mentioned above, the discharge process in the narrow-gap of the SF_6 undergoes transformation from the avalanche to the streamer phase, once the streamer is triggered it soon develops respectively towards the anode and cathode plate, namely, the anode-directed streamer and the cathode-directed streamer, at the same time accompanied by the photoionization appeared, the streamer volume not only grows quickly presenting a near cylindrical shape and but also the streamer length becomes much longer till through the anode and cathode plate, then the discharge path of the both electrode is formed and known as a breakdown channel. The fact has been proved by the experiment results and theoretical demonstration, the photoionization plays an important role and not been overlook when the whole discharge process in the narrow-gap of the SF_6 undergoes transformation from the avalanche to the streamer phase. The results of the mathematical modeling in this paper shows in Figure 9, considering and ignoring photoionization could achieve different results, if you ignore the photoionization effect, you might get the false result [23].

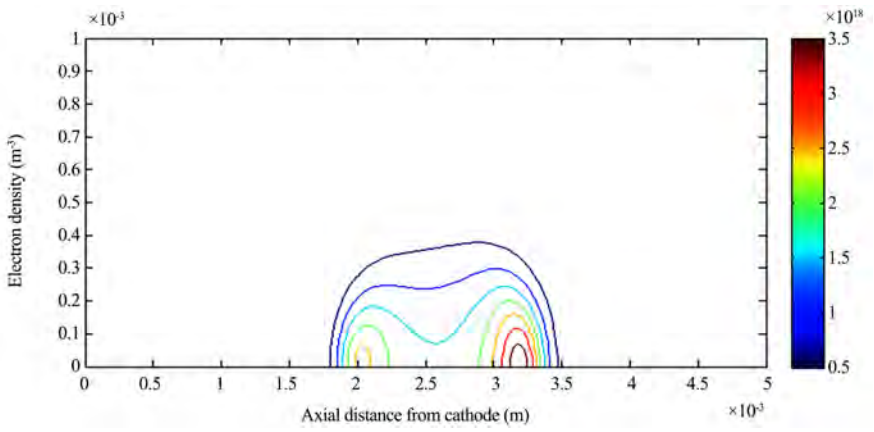

(a) ignoring photoionzation

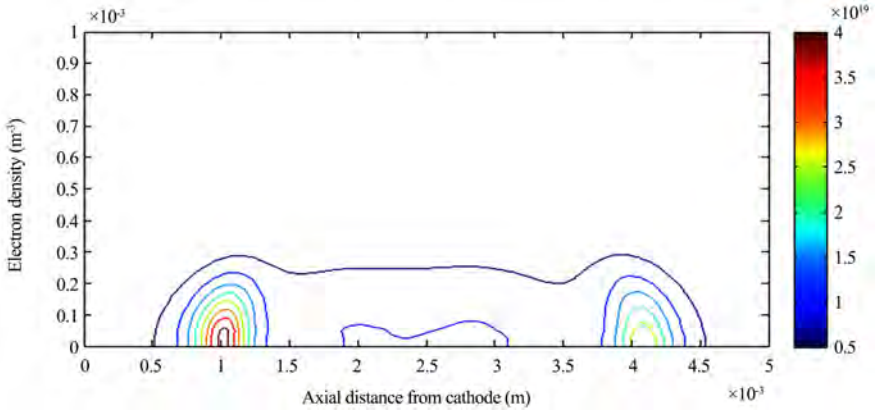

(b) considering photoionzation

Figure 9. Electron density contour in SF6 at 9 ns.

4. Conclusions

Based on the fluid model of gas discharge and the FCT algorithm, dynamic characteristics of the SF_6 breakdown process in narrow-gap has mathematically modeled and some important facts has demonstrated that the FCT algorithm is an efficient theoretical way to deal with the troublesome problems having shock fronts in the discharge channel. The results are both shown via easy visualization for the complicated course of the SF_6 discharge and revealed dynamic characteristics of the charged particles during the SF_6 discharge process in narrow-gap.

According to the mathematical model and numerical analysis results in this paper, the breakdown process in narrow-gap of SF_6 still presents two phases at the standard atmospheric pressure, and parallel-plane electrodes 0.5 cm apart and the 46 kV DC applied. Moreover, some facts are indicated that when electrons increase to a certain amount and the avalanche phase changes into the streamer phase. On the one hand, in the electron avalanche phase, the collision ionization is the key rule for producing electrons and making them grow fast until the electron swarms up to the $1.01\times10^{18}\,\mathrm{cm}^{-3}$. The microcosmic mechanisms of the particle dynamical behaviors, the spatio-temporal characteristics of the electric field and the track evolution of the discharge channel are shown in Figure 3 and Figure 4 in the interval from $t = 0$ ns to the $t = 7.7$ ns. In this interval, the collision between SF_6 molecule and seed electrons is only triggered by the external electric field. When time ranges from $t = 7.7$ ns to the 8.0 ns, a dramatic change happens in the electron number and electric field of the gas-gap; that is to say, the streamer discharge would be coming. On the other hand, in the streamer phase, from the 8.0 ns moment, the streamer discharge is rapidly developing; its volume is promptly expanded and the length is also stretched quickly, and simultaneously the electric field distortion is also exacerbated as shown in Figure 5, then the main changes of the density distribution of charged particles for the electron, and positive and negative ions on the axial direction are shown in Figures 6-8.

In a nutshell, the photoionization effect plays a pivotal role in the process of

the streamer discharge phase.

Accompanied by the photoionization, the space charges of the gas-gap are multiplicatively increased and led to extremely distorting of the electric field within the discharge channel, and then the streamer dramatically develops toward both anode and cathode plates, and a plasma region is left in the central part of the streamer; meanwhile, the distorted electric field also speeds up the streamer velocity forward to both plates till bridging the anode and cathode plate; finally, the gas-gap is absolutely broken down.

Acknowledgements

This work was supported financially by National Natural Science Foundation of China, No. 51077032.

Conflicts of Interest

The authors declare no conflicts of interest regarding the publication of this paper.

References

[1] Boris, J.P., Book, D.L. and Shasta, A. (1973) Fluid Transport Algorithm that Works. *Journal of Computational Physics*, **11**, 38-69. https://doi.org/10.1016/0021-9991(73)90147-2

[2] Zalesak, S.T. (1979) Fully Multidimensional Flux-Corrected Transport. *Journal of Computational Physics*, **31**, 335-362. https://doi.org/10.1016/0021-9991(79)90051-2

[3] Zheng, D.C. (2016) Numerical Simulation Methods for Gas Discharge. Science Press, Beijing.

[4] Morrow, R. (1986) A Survey of the Electron and Ion Transport Properties of SF_6. *IEEE Transactions on Plasma Science*, **14**, 234-239. https://doi.org/10.1109/TPS.1986.4316534

[5] Dhali, S.K. and Williams, P.F. (1987) Two-Dimensional Studies of Streamers in Gases. *Journal of Applied Physics*, **62**, 4696-4707. https://doi.org/10.1063/1.339020

[6] Kulikovsky, A.A. (1995) Two-Dimensional Simulation of the Positive Streamer in N_2 between Parallel-Plate Electrodes. *Journal of Physics D: Applied Physics*, **28**, 2483-2493. https://doi.org/10.1088/0022-3727/28/12/015

[7] Georghiou, G.E., Morrow, R. and Metaxas, A.C. (1999) The Theory of Short Gap Breakdown of Needle Point-Plane Gaps in Air Using Finite-Difference and Finite-Element Methods. *Journal of Physics D: Applied Physics*, **32**, 1370-1385. https://doi.org/10.1088/0022-3727/32/12/314

[8] Lehmann, K.K. and Callegari, C. (2002) Quantum Hydrodynamic Model for the Enhanced Moments of Inertia of Molecules in Helium Nanodroplets: Application to SF_6. *The Journal of Chemical Physics*, **117**, 1595-1603. https://doi.org/10.1063/1.1486443

[9] Pancheshnyi, S.V. and Starikovskii, A.Yu. (2003) Two-Dimensional Numerical Modelling of the Cathode-Directed Streamer Development in a Long Gap at High Voltage. *Journal of Physics D: Applied Physics*, **36**, 2683-2691. https://doi.org/10.1088/0022-3727/36/21/014

[10] Chen, X.F. (2010) The Streamer Discharge Analysis in N_2, SF_6 and Their Mixtures

under the Uniform Electric Field. Master Thesis, Harbin University of Science and Technology, Harbin.

[11] Morrow, R. (1991) Theory of Positive Corona in SF_6 Due to a Voltage Impulse. *IEEE Trans on Plasma Science*, **19**, 86-94. https://doi.org/10.1109/27.106801

[12] Morrow, R. (1987) Properties of Streamers and Streamer Channels in SF_6. *Physical Review A*, **35**, 1778. https://doi.org/10.1103/PhysRevA.35.1778

[13] Zheng, D.C. (2019) SF_6 Dielectric Behaviors and Application. Science Press, Beijing.

[14] Zhu, S.H. (2012) The Dynamic Behaviors of Discharge Process in SF_6/N_2 in Short-Gap. Master Thesis, Harbin University of Science and Technology, Harbin.

[15] Boris, J.P. and Book, D.L. (1976) Solution of Continuity Equations by the Method of Flux-Corrected Transport. *Methods in Computational Physics*, **1**, 85-129. https://doi.org/10.1016/B978-0-12-460816-0.50008-7

[16] Sato, N. (1980) Discharge Current Induced by the Motion of Charged Particles. *Journal of Physics D*: *Applied Physics*, **13**, 3-6. https://doi.org/10.1088/0022-3727/13/1/002

[17] Boris, J.P. and Book, D.L. (1973) Flux-Corrected Transport. I. SHASTA, a Fluid Transport Algorithm That Works. *Journal of Computational Physics*, **11**, 38-69. https://doi.org/10.1016/0021-9991(73)90147-2

[18] Pedersen A. (1967) Calculation of Spark Breakdown or Corona Starting Voltages in Nonuniform Fields. *IEEE Transactions on Power Apparatus and Systems*, **PAS-86**, 200-206. https://doi.org/10.1109/TPAS.1967.291836

[19] Luque, A. and Ratushnaya, V. (2008) Ute Ebert, Positive and Negative Streamers in Ambient Air: Modelling Evolution and Velocities. *Journal of Physics D*: *Applied Physics*, **41**, 1-18. https://doi.org/10.1088/0022-3727/41/23/234005

[20] Raether, H. (1964) Electron Avalanches and Breakdown in Gases. Butterworths, London, 15-22.

[21] Bonisch, S., Kalkner, W. and Pommerenke, D. (2003) Modeling of Short-Gap ESD under Consideration of Different Discharge Mechanisms. *IEEE Transactions on Plasma Science*, **31**, 736-744. https://doi.org/10.1109/TPS.2003.815823

[22] Georghiou, G.E., Papadakis, A.P., Morrow, R. and Metaxas, A.C. (2005) Numerical Modelling of at Mospheric Pressure Gas Discharges Leading to Plasma Production. *Journal of Physics D*: *Applied Physics*, **38**, 303-328. https://doi.org/10.1088/0022-3727/38/20/R01

[23] Pancheshnyi, S.V., Starikovskaia, S.M. and Starikovskii, A.Y. (2001) Role of Photoionization Processes in Propagation of Cathode-Directed Streamer. *Journal of Physics D*: *Applied Physics*, **34**, 1-11. https://doi.org/10.1088/0022-3727/34/1/317

Scientific Research Publishing

Applied Mathematics, 2019, 10, 784-803
https://www.scirp.org/journal/am
ISSN Online: 2152-7393
ISSN Print: 2152-7385

Eigenvalue Computation of Regular 4th Order Sturm-Liouville Problems*

Ahmad Alalyani

Al Baha University, Al Baha, KSA
Email: aalalyani@hotmail.com

How to cite this paper: Alalyani, A. (2019) Eigenvalue Computation of Regular 4th Order Sturm-Liouville Problems. *Applied Mathematics*, **10**, 784-803.
https://doi.org/10.4236/am.2019.109056

Received: July 21, 2019
Accepted: September 23, 2019
Published: September 26, 2019

Abstract

In this paper we present and test a numerical method for computing eigenvalues of 4th order Sturm-Liouville (SL) differential operators on finite intervals with regular boundary conditions. This method is a 4th order shooting method based on Magnus expansions (MG4) which use MG4 shooting as the integrator. This method is similar to the SLEUTH (Sturm-Liouville Eigenvalues Using Theta Matrices) method of Greenberg and Marletta which uses the 2nd order Pruess method (also known as the MG2 shooting method) for the integrator. This method often achieves near machine precision accuracies, and some comparisons of its performance against the well-known SLEUTH software package are presented.

Keywords

4th Order Sturm-Liouville Problem, Magnus Methods (MG4), Regular Boundary Conditions

1. Introduction

In this paper[1] we consider the self-adjoint differential operators which arise from the 4th order differential equation

$$L(y)=y^{(4)}(x)-\left(s(x)y'(x)\right)'+q(x)y(x)=\lambda y(x),\ a\le x\le b \tag{1}$$

when separated, self-adjoint boundary conditions are imposed at each of the two regular endpoints $x=a$ and $x=b$.

We make the assumptions:

1) $q(x)$ is continuous on $[a,b]$.

2) $s(x)$ and $s'(x)$ are continuous on $[a,b]$.

*2010 Mathematics Subject Classication 34L15; 34L16; 65L15; 70J50.

[1]The content of this paper is related to my Ph.D. dissertation [1].

3) $-\infty < a < b < \infty$.

Under these assumptions both endpoints a and b are regular endpoints. The most general separated, self-adjoint boundary conditions which can be imposed at $x = a$ and $x = b$ are

$$\begin{pmatrix} l_1(y) \\ l_2(y) \end{pmatrix} = A_1 \begin{pmatrix} y(a) \\ y''(a) \end{pmatrix} + A_2 \begin{pmatrix} -y'''(a) + s(a)y'(a) \\ -y'(a) \end{pmatrix} = \begin{pmatrix} 0 \\ 0 \end{pmatrix} \tag{2}$$

and

$$\begin{pmatrix} r_1(y) \\ r_2(y) \end{pmatrix} = B_1 \begin{pmatrix} y(b) \\ y''(b) \end{pmatrix} + B_2 \begin{pmatrix} -y'''(b) + s(b)y'(b) \\ -y'(b) \end{pmatrix} = \begin{pmatrix} 0 \\ 0 \end{pmatrix} \tag{3}$$

where A_1, A_2 and B_1, B_2 are any choice of real, 2×2 matrices satisfying the properties

$$A_1 A_2^{\mathrm{T}} - A_2 A_1^{\mathrm{T}} = 0 \tag{4}$$

$$A_1 A_1^{\mathrm{T}} + A_2 A_2^{\mathrm{T}} = I_2. \tag{5}$$

and

$$B_1 B_2^{\mathrm{T}} - B_2 B_1^{\mathrm{T}} = 0 \tag{6}$$

$$B_1 B_1^{\mathrm{T}} + B_2 B_2^{\mathrm{T}} = I_2. \tag{7}$$

The above boundary conditions can be shown to be equivalent to the general forms of boundary conditions used by Everitt [2] (in his PhD dissertation on 4th order Sturm-Liouville problems), Fulton [3] and many others.

The domain of the maximal operator L_1 associated with the Equation (1) on the closed interval $[a,b]$ is

$$D(L_1) = \left\{ f \in L_2(a,b) : f, f', f'', f''' \in AC_{loc}(a,b), Lf \in L_2(a,b) \right\}, \tag{8}$$

where AC_{loc} is the space of functions which are absolutely continuous on compact subsets of (a,b). The self-adjoint operators associated with Equation (1) are then obtained by restricting $D(L_1)$ by two boundary conditions at the left endpoint and two boundary conditions at the right endpoint as in (2) and (3), namely

$$D\left(L_{A_1,A_2,B_1,B_2}\right) = \left\{ f \in D(L_1) : l_1(f) = 0, l_2(f) = 0, r_1(f) = 0, r_2(f) = 0 \right\} \tag{9}$$

The Green's formula for the 4th order equation is

$$\int_a^b (zLy - yLz)\,\mathrm{d}x = [y,z]_{(x)}\Big|_a^b, \tag{10}$$

where the bilinear concomitant is defined as

$$[y,z]_{(x)} := \begin{vmatrix} y'''(x) & z'''(x) \\ y(x) & z(x) \end{vmatrix} - \begin{vmatrix} y''(x) & z''(x) \\ y'(x) & z'(x) \end{vmatrix} + s(x) \begin{vmatrix} y(x) & z(x) \\ y'(x) & z'(x) \end{vmatrix}. \tag{11}$$

Using this definition, and the boundary conditions (2) and (3), it can be shown that the operators L_{A_1,A_2,B_1,B_2} on $L_2(a,b)$ are symmetric; that is, for all $f, g \in D(L_1)$:

$$(f, Lg) - (Lg, f) = \int_a^b f \cdot (Lg) - g \cdot (Lf)\,\mathrm{d}x = 0. \tag{12}$$

This paper is devoted to the 4th order shooting method based on Magnus Expansions (MG4) for computation of eigenvalues of 4th order SL problems of the type (1), (2), (3) having regular endpoints.

For 2nd order SL problems, on both regular and singular intervals, there are several well developed software packages for eigenvalue and eigenfunction computations: SLEIGN [4], SLEIGN 2 [5], SLEDGE [6] [7], SLO2FM [8] [9] [10], MATSLISE [11] [12] [13]. The best source of information where their capabilities and general performance is discussed, is the book, Numerical Solution of Sturm-Liouville Problems, of John Pryce [8].

For the 4th order SL equation, the only reliable software package for eigenvalue and eigenfunction computations is ACM Algorithm 775: SUBROUTINE SLEUTH, produced by L. Greenberg and M. Marletta in 1997 [14]. This package restricts attention to problems on finite intervals with regular endpoints; at this writing there is still no readily available software for singular endpoints. The SLEUTH code handles eigenvalues and eigenfunctions only for SL problems with regular endpoints, and it is capable of handling a wide variety of possible boundary conditions. The Greenberg-Marletta algorithm is based on an integration scheme using piecewise trigonometric hyperbolic splines (the Pruess method), also known as the MG2 shooting method. This was also the underlying integration scheme in the SLEDGE package. The SLEUTH code is based on using formulas of Greenberg [14] [15] [16] for the number of eigenvalues less than λ.

Since eigenvalue/eigenfunction calculations for the 4th order equation have been tackled by many other methods we give here a brief overview of some of the existing competitive methods. The most prominent approaches to date, and those which continue to receive much attention, are as follows:

1) Extended Sampling Method (ESM) which relies on the classical Whittaker-Shannon-Kotelnikov sampling theorem [17] (also used for 2nd order SL problems).

2) Fliess Series Method [18] [19] [20] which represents the solution of an IVP for the 4th order Equation (1) in terms of iterated integrals involving the coefficient functions, $s(x)$ and $q(x)$.

3) Chebyshev Method [21]-[26] which approximates solutions of the 4th order Equation (1) by Chebyshev polynomials.

4) Boubaker Polynomials Expansion Scheme (BPES) [27] which approximates solutions of of the 4th order Equation (1) using Boubaker polynomials and utilizes a Differential Quadrature Method (DQM).

5) Spectral Parameter Power Series (SPPS) Method [28] [29] [30] which expands the solutions of the SL equation (both second and 4th order) in a convergent Taylor expansion in the eigenparameter λ. This has recently proven to have much advantages both for theoretical problems and numerical computations for SL equations.

Selection of Test Problems

To investigate the performance of the method, we make the following selection of test problems. These problems are the square of a 2nd order SL problem.

1) The square of the 2nd order Bessel equation

$$Ly = y^{(4)} - \left(s(x)y'\right)' + q(x)y = \lambda y, \quad x \in [1,5] \tag{13}$$

where

$$s(x) = \frac{-2}{4x^2}, \tag{14}$$

and

$$q(x) = \frac{1}{16x^4} + \frac{3}{2x^4}. \tag{15}$$

2) The square of the 2nd order Modified Harmonic Oscillator equation

$$Ly = y^{(4)} - \left(s(x)y'\right)' + q(x)y = \lambda y, \quad x \in [1,5] \tag{16}$$

where

$$s(x) = 2\left(x^2 + x^4\right), \tag{17}$$

and

$$q(x) = \left(x^2 + x^4\right)^2 - \left(2 + 12x^2\right). \tag{18}$$

3) The square of the 2nd order equation

$$Ly = y^{(4)} - \left(s(x)y'\right)' + q(x)y = \lambda y, \quad x \in [0,\pi] \tag{19}$$

where

$$s(x) = 2\left(\cos(x) + 2\cos(2x) + 3\cos(3x)\right), \tag{20}$$

and

$$q(x) = \left(\cos(x) + 2\cos(2x) + 3\cos(3x)\right)^2 - \left(-\cos(x) - 8\cos(2x) - 27\cos(3x)\right). \tag{21}$$

4) The square of the 2nd order Coffey-Evan equation with $\beta = 10$

$$Ly = y^{(4)} - \left(s(x)y'\right)' + q(x)y = \lambda y, \quad x \in \left[\frac{-\pi}{2}, \frac{\pi}{2}\right] \tag{22}$$

where

$$s(x) = 2\left(\beta^2 \sin^2(2x) - 2\beta\cos(2x)\right), \tag{23}$$

and

$$q(x) = \left(\beta^2 \sin^2(2x) - 2\beta\cos(2x)\right)^2 - \left(8\beta^2 \cos(4x) + 8\beta\cos(2x)\right). \tag{24}$$

5) The square of the 2nd order Legendre equation

$$Ly = y^{(4)} - \left(s(x)y'\right)' + q(x)y = \lambda y, \quad x \in \left[0, \frac{\pi}{4}\right] \tag{25}$$

where

$$s(x)=\frac{1}{2}\sec^2(x), \tag{26}$$

and

$$q(x)=\left(\frac{\sec^4(x)}{16}\right)-\left(\sec^2(x)\tan^2(x)+\frac{\sec^4(x)}{2}\right). \tag{27}$$

Problem 5, the Legendre squared equation, arises from changes of variables to the non-LNF form discussed in [31].

2. The MG4 Shooting Method Associated with the 4th Order Sturm-Liouville Equation

In this section we describe an implementation of the MG4 shooting technique for the 4th order SL Equation (1) on regular intervals with $s(x), q(x)$ continuous. The Equation (1) can be converted to the 1st order system (Atkinson [32], pp. 323-324) $Y'(x,\lambda)=A(x)\cdot Y(x,\lambda)$, where

$$Y'(x,\lambda)=\begin{pmatrix}0 & 0 & 0 & -1\\ 0 & 0 & -1 & -s(x)\\ q(x)-\lambda & 0 & 0 & 0\\ 0 & -1 & 0 & 0\end{pmatrix}Y(x,\lambda)=A(x)\cdot Y(x,\lambda), \tag{1}$$

and

$$Y(x,\lambda)=\begin{pmatrix}y(x,\lambda)\\ y''(x,\lambda)\\ -y'''(x,\lambda)+s(x)y'(x,\lambda)\\ -y'(x,\lambda)\end{pmatrix}. \tag{2}$$

Remark 2.1 Currently the most reliable software package for eigenvalues and eigenfunctions of the 4th order Sturm-Liouville equation with regular endpoints is ACM Algorithm 775: SUBROUTINE SLEUTH, produced by L. Greenberg and M. Marletta in 1997 [14], which is available from NETLIB at ORNL. The SLEUTH (Sturm-Liouville Eigenvalues Using Theta Matrices) code employs an MG2 approximation for the solution $Y(x)=\mathrm{e}^{\sigma(x)}Y_0$, (see [33], p. 283), on each mesh interval of a Hamiltonian system similar to the system (1) (the order of the derivatives in the above $Y(x,\lambda)$ vector being slightly different). The SLEUTH code is based on using formulas of Greenberg [15] [16] [34] [35] for the number of eigenvalues less than λ, so the eigenvalue algorithm is quite different than the method we are proposing here for eigenvalue computation for (1) using (1).

For the IVP, $Y'(x,\lambda)=A(x)\cdot Y(x,\lambda)$, $Y(0)=I$, where A is a constant matrix is also basic to Magnus methods for (1). We introduce the following lemma and the definitions of the Lie-group and Lie-algebra (see [36], Prop. 7.2.3 and Def. 7.2.4).

Definition 2.1 $SL(4,\mathbb{R})$ is the Lie-group and defined as:

$$SL(4,\mathbb{R}):=\{A\,|\,A \text{ is } 4\times 4 \text{ matrix with real entries and } \det(A)=1\}.$$

Definition 2.2 $sl(4,\mathbb{R})$ is the Lie-algebra and defined as:

$$sl(4,\mathbb{R}) := \{A \mid A \text{ is } 4\times 4 \text{ matrix with real entries and } \operatorname{tr}(A) = 0\}.$$

Lemma 2.1 If $X \in sl(4,\mathbb{R})$, then $\exp(X) \in SL(4,\mathbb{R})$, *i.e.*

$$\det(\exp(X)) = 1. \tag{3}$$

Remark 2.2 For any constant matrix $X \in sl(4,\mathbb{R})$, it follows from this lemma that the solution

$$Y(t,\lambda) = e^{Xt} \tag{4}$$

of the IVP,

$$Y'(t,\lambda) = X(t)\cdot Y(t,\lambda), \tag{5}$$
$$Y(0) = I,$$

lies in the Lie Group $SL(4,\mathbb{R})$.

The Magnus methods originate (see [37]) with the observation that an analytical solution of (1) with initial condition $Y(0) = Y_0$ can be written as, (see [33], p. 283),

$$Y(x) = e^{\sigma(x)}Y_0 \tag{6}$$

where

$$\begin{aligned}\sigma(x) = {} & \int_0^x A(k)\,dk + \frac{1}{2}\int_0^x \left[A(k), \int_0^k A(\xi)\,d\xi\right] dk \\ & + \frac{1}{4}\int_0^x \left[A(k), \int_0^k \left[A(\xi), \int_0^\xi A(\eta)\,d\eta\right] d\xi\right] dk \\ & + \frac{1}{12}\int_0^x \left[\left[A(k), \int_0^k A(\xi)\,d\xi\right], \int_0^k A(\eta)\,d\eta\right] dk + \cdots\end{aligned} \tag{7}$$

and where the square brackets denote the matrix commutator and are defined as:

$$[A,B] := A\cdot B - B\cdot A \tag{8}$$

The MG4 method is a well known 4th order method obtained by truncation of the above Magnus series, together with evaluation of the A matrix in (1) at two gaussian points A_1 and A_2:

For the Hamiltonian system (1), we put

$$A_1 := A\left(x_n + h\left(\frac{\sqrt{3}-1}{2\sqrt{3}}\right)\right) = A(x'), \tag{9}$$

$$A_2 := A\left(x_n + h\left(\frac{\sqrt{3}+1}{2\sqrt{3}}\right)\right) = A(x''), \tag{10}$$

(meaning that $q(x)$ and $s(x)$ in (1) are to be evaluated at $x = x'$ and $x = x''$ in the nth mesh interval $[x_n, x_{n+1}]$). Then the MG4 method of Iserles and Norsett ([38], p. 1012), and ([33], p. 288) for (1) takes the form (for a fixed step size h)

$$Y_{n+1} = \exp(h\tilde{A})\cdot Y_n, \tag{11}$$

where the transfer matrix for passing from x_n to x_{n+1} is $M := \exp(h\tilde{A})$ with

$$\begin{aligned}\tilde{A} &:= \frac{1}{2}\left(A_1 + A_2\right) + \frac{1}{4\sqrt{3}}\left[A_2, A_1\right]h \\ &= \frac{1}{2}\left(A\left(x'\right) + A\left(x''\right)\right) + \frac{1}{4\sqrt{3}}h\left(A\left(x''\right)A\left(x'\right) - A\left(x'\right)A\left(x''\right)\right) \\ &= \begin{pmatrix} 0 & 0 & 0 & -1 \\ \frac{-\sqrt{3}h\left(q_1 - q_2\right)}{12} & \frac{-\sqrt{3}h\left(s_1 - s_2\right)}{12} & -1 & \frac{-s_1 - s_2}{2} \\ \frac{q_1 + q_2}{2} - \lambda & 0 & 0 & \frac{\sqrt{3}h\left(q_1 - q_2\right)}{12} \\ 0 & -1 & 0 & \frac{\sqrt{3}h\left(s_1 - s_2\right)}{12} \end{pmatrix},\end{aligned} \tag{12}$$

where the square bracket $\left[A_2, A_1\right]$ denotes the matrix commutator and is defined as:

$$\left[A_2, A_1\right] = A_2A_1 - A_1A_2, \tag{13}$$

and

$$q_1 = q\left(x'\right), q_2 = q\left(x''\right), s_1 = s\left(x'\right), s_2 = s\left(x''\right).$$

The four eigenvalues of $\tilde{A}$ are

$$\lambda_1 = -\left[A - \frac{\sqrt{B}}{2}\right]^{\frac{1}{2}}, \tag{14}$$

$$\lambda_2 = -\left[A + \frac{\sqrt{B}}{2}\right]^{\frac{1}{2}}, \tag{15}$$

$$\lambda_3 = -\lambda_1, \tag{16}$$

$$\lambda_4 = -\lambda_2, \tag{17}$$

where

$$A = \frac{s_1 + s_2}{4} + \frac{h^2\left(s_1^2 + s_2^2\right)}{96} - \frac{h^2 s_1 s_2}{48}, \tag{18}$$

and

$$\begin{aligned}B = 4\lambda + \frac{h^4\left(s_1^4 + s_2^4\right)}{2304} - \frac{h^4\left(s_1^3 s_2 + s_1 s_2^3\right)}{576} + \frac{h^4 s_1^2 s_2^2}{384} + \frac{h^2\left(s_1^3 + s_2^3 - s_1^2 s_2 - s_1 s_2^2\right)}{48} \\ + \frac{s_1^2 + s_2^2}{4} + \frac{s_1 s_2}{2} - 2\left(q_1 + q_2\right).\end{aligned} \tag{19}$$

Eigenvalues of $\tilde{A}$ matrix:

Let us define

$$D := A - \frac{\sqrt{B}}{2}, \tag{20}$$

and

$$E := A + \frac{\sqrt{B}}{2}. \tag{21}$$

Then the following four cases of eigenvalues of $\tilde{A}$ arise, involving both

complex and real eigenvalues:

Case 1: $B>0$ and ($D>0, E>0$).

$$\lambda_1 = -|D|^{\frac{1}{2}}, \tag{22}$$

$$\lambda_2 = -|E|^{\frac{1}{2}}, \tag{23}$$

$$\lambda_3 = |D|^{\frac{1}{2}}, \tag{24}$$

$$\lambda_4 = |E|^{\frac{1}{2}}. \tag{25}$$

Case 2: $B>0$ and ($D<0, E<0$).

$$\lambda_1 = -i|D|^{\frac{1}{2}}, \tag{26}$$

$$\lambda_2 = -i|E|^{\frac{1}{2}}, \tag{27}$$

$$\lambda_3 = i|D|^{\frac{1}{2}}, \tag{28}$$

$$\lambda_4 = i|E|^{\frac{1}{2}}. \tag{29}$$

Case 3: $B>0$ and ($D<0, E>0$, where $D<E$).

$$\lambda_1 = -i|D|^{\frac{1}{2}}, \tag{30}$$

$$\lambda_2 = -|E|^{\frac{1}{2}}, \tag{31}$$

$$\lambda_3 = i|D|^{\frac{1}{2}}, \tag{32}$$

$$\lambda_4 = |E|^{\frac{1}{2}}. \tag{33}$$

Case 4: $B<0$.

$$\lambda_1 = -\left[A - \frac{i\sqrt{|B|}}{2}\right]^{\frac{1}{2}}, \tag{34}$$

$$\lambda_2 = -\left[A + \frac{i\sqrt{|B|}}{2}\right]^{\frac{1}{2}}, \tag{35}$$

$$\lambda_3 = -\lambda_1, \tag{36}$$

$$\lambda_4 = -\lambda_2. \tag{37}$$

Remark 2.3 It follows from (12) that

$$trace\left(\left(x - x_n\right)\tilde{A}\right) = 0, \tag{38}$$

so that $\left(x - x_n\right)\tilde{A} \in sl\left(4, \mathbb{R}\right)$. Also we observe that on diagonalization we have (in all the above 4 cases),

$$\begin{aligned}\det\left(\exp\left[\left(x-x_n\right)\tilde{A}\right]\right) &= \det\left(P\right)\cdot\det\left(\exp\left[\left(x-x_n\right)D\right]\right)\cdot\det\left(P^{-1}\right)\\ &= \exp\left(\left(x-x_n\right)\sum_{j=1}^{4}\lambda_j\right)=1,\end{aligned} \tag{39}$$

where $\left\{\lambda_j\right\}$, $j=1,2,3,4$, are the eigenvalues of $\tilde{A}$. Hence on each mesh interval,

$$Y\left(x,\lambda\right)=\exp\left[\left(x-x_n\right)\tilde{A}\right]\cdot Y_n\left(x,\lambda\right) \tag{40}$$

is a solution of

$$Y'\left(x,\lambda\right)=\tilde{A}\left(x\right)\cdot Y\left(x,\lambda\right) \tag{41}$$

which remains in the Lie Group, $SL\left(4,\mathbb{R}\right)$.

We consider the SL problem for Equation (1) with the following choices of Dirichlet boundary conditions at the left and right endpoints (compare (2) and (3)).

$$L\left(y\right)=y^{(4)}\left(x\right)-\left(s\left(x\right)y'\left(x\right)\right)'+q\left(x\right)y\left(x\right)=\lambda y\left(x\right),\ a\le x\le b, \tag{42}$$

$$A_1\begin{pmatrix}y\left(a\right)\\ y''\left(a\right)\end{pmatrix}+A_2\begin{pmatrix}-y'''\left(a\right)+s\left(a\right)y'\left(a\right)\\ -y'\left(a\right)\end{pmatrix}=\begin{pmatrix}y\left(a\right)\\ y''\left(a\right)\end{pmatrix}=\begin{pmatrix}l_1\left(y\right)\\ l_2\left(y\right)\end{pmatrix}=\begin{pmatrix}0\\ 0\end{pmatrix}, \tag{43}$$

$$B_1\begin{pmatrix}y\left(b\right)\\ y''\left(b\right)\end{pmatrix}+B_2\begin{pmatrix}-y'''\left(b\right)+s\left(b\right)y'\left(b\right)\\ -y'\left(b\right)\end{pmatrix}=\begin{pmatrix}y\left(b\right)\\ y''\left(b\right)\end{pmatrix}=\begin{pmatrix}r_1\left(y\right)\\ r_2\left(y\right)\end{pmatrix}=\begin{pmatrix}0\\ 0\end{pmatrix}. \tag{44}$$

where

$$A_1=\begin{pmatrix}1&0\\ 0&1\end{pmatrix}, \tag{45}$$

$$A_2=\begin{pmatrix}0&0\\ 0&0\end{pmatrix} \tag{46}$$

and

$$B_1=\begin{pmatrix}1&0\\ 0&1\end{pmatrix}, \tag{47}$$

$$B_2=\begin{pmatrix}0&0\\ 0&0\end{pmatrix}. \tag{48}$$

The left boundary conditions are implemented by fixing initial conditions for two solutions $Y_1\left(x,\lambda\right)$ and $Y_2\left(x,\lambda\right)$ of (1) at $x=a$, namely we define solutions $Y_1\left(x,\lambda\right)$ and $Y_2\left(x,\lambda\right)$ at $x=a$ by requiring

$$\begin{aligned}\left(Y_1\left(a,\lambda\right),Y_2\left(a,\lambda\right)\right) &= \begin{pmatrix}y_1\left(a,\lambda\right) & y_2\left(a,\lambda\right)\\ y_1''\left(a,\lambda\right) & y_2''\left(a,\lambda\right)\\ -y_1'''\left(a,\lambda\right)+s\left(a\right)y_1'\left(a,\lambda\right) & -y_2'''\left(a,\lambda\right)+s\left(a\right)y_2'\left(a,\lambda\right)\\ -y_1'\left(a,\lambda\right) & -y_2'\left(a,\lambda\right)\end{pmatrix}\\ &= \begin{pmatrix}0&0\\ 0&0\\ 1&0\\ 0&1\end{pmatrix}=\begin{pmatrix}0\\ I_2\end{pmatrix}.\end{aligned} \tag{49}$$

Then the corresponding solutions $\{y_1(x,\lambda), y_2(x,\lambda)\}$ of (1) automatically satisfy the boundary conditions (43) at $x=a$. Using the solutions $\{Y_1(x,\lambda), Y_2(x,\lambda)\}$ of (1) defined by (49) we define the 2×2 matrices

$$U(x,\lambda) := \begin{pmatrix} y_1(x,\lambda) & y_2(x,\lambda) \\ y_1''(x,\lambda) & y_2''(x,\lambda) \end{pmatrix}, \tag{50}$$

and

$$V(x,\lambda) := \begin{pmatrix} -y_1'''(x,\lambda)+s(x)y_1'(x,\lambda) & -y_2'''(x,\lambda)+s(x)y_2'(x,\lambda) \\ -y_1'(x,\lambda) & -y_2'(x,\lambda) \end{pmatrix}. \tag{51}$$

The two-dimensional subspace,

$$\Im = \{y(x,\lambda) : y(x,\lambda) = Ay_1(x,\lambda) + By_2(x,\lambda) \text{ for some choice of } A \text{ and } B\}, \tag{52}$$

where $y_1(x,\lambda)$ and $y_2(x,\lambda)$ are solutions of (1) corresponding to the $Y_1(x,\lambda)$ and $Y_2(x,\lambda)$ solutions of the IVP, (1) and (49), of the four-dimensional solution space of (1) satisfies the boundary conditions (43) at $x=a$.

We have the following theorem giving necessary sufficient conditions (N.S.Cs) for the eigenvalues of the SL problem for Equation (1) which has boundary conditions at $x=a$ (43) and boundary conditions at $x=b$ (44).

Theorem 2.1 1) A N.S.C. for $\lambda \in (-\infty,\infty)$ to be an eigenvalue of the SL problem for Equation (1) with boundary conditions at $x=a$ (43) and boundary conditions at $x=b$ (44), and having multiplicity one, is:

$$\begin{vmatrix} r_1(y_1) & r_1(y_2) \\ r_2(y_1) & r_2(y_2) \end{vmatrix} = \begin{vmatrix} y_1(b,\lambda) & y_2(b,\lambda) \\ y_1''(b,\lambda) & y_2''(b,\lambda) \end{vmatrix} = 0 \tag{53}$$

and

$$rank\begin{pmatrix} r_1(y_1) & r_1(y_2) \\ r_2(y_1) & r_2(y_2) \end{pmatrix} = rank\begin{pmatrix} y_1(b,\lambda) & y_2(b,\lambda) \\ y_1''(b,\lambda) & y_2''(b,\lambda) \end{pmatrix} = 1. \tag{54}$$

2) A N.S.C. for $\lambda \in (-\infty,\infty)$ to be an eigenvalue of the SL problem for Equation (1) with boundary conditions at $x=a$ (43) and boundary conditions at $x=b$ (44), and having multiplicity one, is:

$$\begin{vmatrix} r_1(y_1) & r_1(y_2) \\ r_2(y_1) & r_2(y_2) \end{vmatrix} = \begin{vmatrix} y_1(b,\lambda) & y_2(b,\lambda) \\ y_1''(b,\lambda) & y_2''(b,\lambda) \end{vmatrix} = 0 \tag{55}$$

and

$$rank\begin{pmatrix} r_1(y_1) & r_1(y_2) \\ r_2(y_1) & r_2(y_2) \end{pmatrix} = rank\begin{pmatrix} y_1(b,\lambda) & y_2(b,\lambda) \\ y_1''(b,\lambda) & y_2''(b,\lambda) \end{pmatrix} = 0. \tag{56}$$

Proof Let $\{y_1(x,\lambda), y_2(x,\lambda)\}$ be the unique solutions of the 4th order Equation (1) which are defined by the initial conditions at $x=a$ and $\{Y_1(x,\lambda), Y_2(x,\lambda)\}$ be the corresponding solutions of the Hamiltonian system (1):

$$\begin{pmatrix} y_1(a,\lambda) & y_2(a,\lambda) \\ y_1''(a,\lambda) & y_2''(a,\lambda) \\ -y_1'''(a,\lambda)+s(a)y_1'(a,\lambda) & -y_2'''(a,\lambda)+s(a)y_2'(a,\lambda) \\ -y_1'(a,\lambda) & -y_2'(a,\lambda) \end{pmatrix} = \begin{pmatrix} 0 & 0 \\ 0 & 0 \\ 1 & 0 \\ 0 & 1 \end{pmatrix} \tag{57}$$

By fixing (57) the two-dimensional space $\Im$ is fixed by the 4×2 matrix (57). The constants in the (57) matrix were chosen to ensure that the boundary conditions at $x=a$ (43) was satisfied, so we know that

$$\begin{pmatrix} l_1(y_1) \\ l_2(y_1) \end{pmatrix} = \begin{pmatrix} y_1(a,\lambda) \\ y_1''(a,\lambda) \end{pmatrix} = \begin{pmatrix} 0 \\ 0 \end{pmatrix}, \tag{58}$$

$$\begin{pmatrix} l_1(y_2) \\ l_2(y_2) \end{pmatrix} = \begin{pmatrix} y_2(a,\lambda) \\ y_2''(a,\lambda) \end{pmatrix} = \begin{pmatrix} 0 \\ 0 \end{pmatrix}, \tag{59}$$

that is, that both $y_1(x,\lambda)$ and $y_2(x,\lambda)$ satisfy the boundary conditions at $x=a$ (43). Also, of course, the space $\Im$ of solutions spanned by these two solutions $\{y_1(x,\lambda), y_2(x,\lambda)\}$ of (1) satisfies the boundary conditions at $x=a$ (43), that is

$$l_1\left(Ay_1(x,\lambda)+By_2(x,\lambda)\right)=0, \tag{60}$$

$$l_2\left(Ay_1(x,\lambda)+By_2(x,\lambda)\right)=0 \tag{61}$$

for all $A,B\in\mathbb{C}$. It remains only to apply the boundary conditions at $x=b$ (44), *i.e.* to require that

$$r_1(y)=y(b,\lambda)=0, \tag{62}$$

and

$$r_2(y)=y''(b,\lambda)=0 \tag{63}$$

for boundary conditions at $x=b$ (44). Hence, we find

$$r_1\left(Ay_1(x,\lambda)+By_2(x,\lambda)\right)=Ar_1\left(y_1(x,\lambda)\right)+Br_1\left(y_2(x,\lambda)\right)=0 \tag{64}$$

and

$$r_2\left(Ay_1(x,\lambda)+By_2(x,\lambda)\right)=Ar_2\left(y_1(x,\lambda)\right)+Br_2\left(y_2(x,\lambda)\right)=0 \tag{65}$$

as the requirement for solutions in $\Im$ to also satisfy the boundary conditions at $x=b$ (44). But the Equations (64) and (65) can have a nonzero solution for A,B if and only if

$$\begin{vmatrix} r_1(y_1) & r_1(y_2) \\ r_2(y_1) & r_2(y_2) \end{vmatrix} = \begin{vmatrix} y_1(b,\lambda) & y_2(b,\lambda) \\ y_1''(b,\lambda) & y_2''(b,\lambda) \end{vmatrix} = 0 \tag{66}$$

Hence (66) is a N.S.C. condition for λ to be an eigenvalue of the SL problem for Equation (1). The multiplicity of the eigenvalue is defined as the number of linearly independent solutions of (1) which satisfy both boundary conditions at $x=a$ and both boundary conditions at $x=b$. Since the dimension of $\Im$ is two, this can be at most two. For multiplicity one, we must have

$$rank\begin{pmatrix} r_1(y_1) & r_1(y_2) \\ r_2(y_1) & r_2(y_2) \end{pmatrix} = rank\begin{pmatrix} y_1(b,\lambda) & y_2(b,\lambda) \\ y_1''(b,\lambda) & y_2''(b,\lambda) \end{pmatrix} = 1, \tag{67}$$

and in this case the solution of the two Equations (64) and (65) will be

$$\begin{pmatrix} A \\ B \end{pmatrix} = \begin{pmatrix} \dfrac{-r_1(y_2)}{r_1(y_1)} \\ 1 \end{pmatrix}, \text{ if } r_1(y_1) \neq 0 \tag{68}$$

and

$$\begin{pmatrix} A \\ B \end{pmatrix} = \begin{pmatrix} 1 \\ 0 \end{pmatrix}, \text{ if } r_1(y_1) = 0. \tag{69}$$

In this case the eigenfunction, which is unique up to a constant multiple, is

$$y(x,\lambda) = B\left(\frac{-r_1(y_2)}{r_1(y_1)} \cdot y_1(x,\lambda) + y_2(x,\lambda)\right), \text{ if } r_1(y_1) \neq 0 \tag{70}$$

or

$$y(x,\lambda) = Ay_1(x,\lambda), \text{ if } r_1(y_1) = 0. \tag{71}$$

For multiplicity two, we need to require

$$rank\begin{pmatrix} r_1(y_1) & r_1(y_2) \\ r_2(y_1) & r_2(y_2) \end{pmatrix} = rank\begin{pmatrix} y_1(b,\lambda) & y_2(b,\lambda) \\ y_1''(b,\lambda) & y_2''(b,\lambda) \end{pmatrix} = 0, \tag{72}$$

and in this case $y_1(x,\lambda)$ and $y_2(x,\lambda)$ would be linearly independent eigenfunctions of (1). ■

More generally, the general case of boundary conditions (3) would give

$$f(\lambda) := \det\left(B_1U(b,\lambda) + B_2V(b,\lambda)\right) = 0 \tag{73}$$

as a N.S.C. for λ to be an eigenvalue of (1) with boundary conditions (44) and (3). More generally, the boundary conditions (2) could be handled by changing the initial conditions (57) appropriately.

3. Description of the MG4 Algorithm

We obtained the 4×4 transfer matrix

$$M = \exp\left(h\tilde{A}\right) \tag{1}$$

by doing the following steps:

1) Calculate the eigenvalues and the eigenvectors of $\tilde{A}$.

2) Diagonalize

$$\tilde{A} = P \cdot D \cdot P^{-1}, \tag{2}$$

where P denotes the matrix of eigenvectors of $\tilde{A}$, and D denotes the diagonal matrix of the four eigenvalues of $\tilde{A}$ (12).

3) Put

$$M = P\left(\exp(hD)\right)P^{-1}. \tag{3}$$

This gives a 4×4 transfer matrix with 4 cases of eigenvalues of $\tilde{A}$. (The matrix elements could be reduced to expressions involving sinh, cosh, sin and cos functions). Our MG4 code implements the above transfer matrix $M=\exp\left(h\tilde{A}\right)$ by doing the matrix multiplication (3) numerically. Here we describe the implementation of the MG4 method for computing the eigenvalues of the SL problem for Equation (1) with the choices of Dirichlet boundary conditions (43) and (44) at the left and right endpoints. To impose the boundary conditions (44) on $\Im$, we integrate the IVP, (1) and (49), from $x=a$ to $x=b$ using the MG4 method on the 4×2 matrix $Y(x,\lambda)$. Then when $Y(b,\lambda)$ has been computed, the boundary conditions (44),

$$y(b,\lambda)=Ay_1(b,\lambda)+By_2(b,\lambda)=0 \tag{4}$$

$$y''(b,\lambda)=Ay_1''(b,\lambda)+By_2''(b,\lambda)=0, \tag{5}$$

will be satisfied for some choices of real constants A and B, not both zero, if and only if

$$f(\lambda):=\det\left(U(b,\lambda)\right)=\begin{vmatrix} y_1(b,\lambda) & y_2(b,\lambda) \\ y_1''(b,\lambda) & y_2''(b,\lambda)\end{vmatrix}=0. \tag{6}$$

The computation is performed using an initial uniform mesh, applying bisection method with initial upper and lower bounds for a given eigenvalue λ_n, and then doubling the number of mesh points by bisecting the mesh to generate a Richardson h^4-extrapolation table over successively bisected meshes. Then the extrapolated eigenvalue is selected when the eigenvalue extrapolation error satisfies a tolerance test.

3.1. Description of h^4-Richardson's Extrapolation

If $q(x),s(x)\in C^{\infty}[a,b]$, we can assume that if MG4 method is applied we will have for each choice of h:

$$\hat{\lambda}(h)\approx\lambda_{Exact}+\tau_1h^4+\tau_2\left(h^4\right)^2+\cdots+\tau_m\left(h^4\right)^m \tag{7}$$

for some choices of real constants $\tau_1,\tau_2,\cdots,\tau_m$. For each $m=1,2,3,\cdots$

$$\hat{\lambda}(h)-\lambda_{Exact}=\tau_1h^4+\tau_2\left(h^4\right)^2+\cdots+\tau_m\left(h^4\right)^m+O\left(\left(h^4\right)^{m+1}\right)=O\left(h^4\right). \tag{8}$$

Putting

$$x_1=h_0^4 \tag{9}$$

$$x_2=h_1^4=\left(\frac{h_0}{2}\right)^4 \tag{10}$$

$$\vdots$$

$$x_i=h_{i-1}^4=\left(\frac{h_0}{2^{i-1}}\right)^4, \tag{11}$$

in Neville's algorithm ([39], 2.1.2.5b, p. 42),

$$T_{ik}(x)=T_{i,k-1}(x)+\frac{T_{i,k-1}(x)-T_{i-1,k-1}(x)}{\frac{x-x_{i-k}}{x-x_i}-1},\ 1\le k\le i,\ i=0,1,2,\cdots,n, \tag{12}$$

we find

$$T_{I-1,J-1}(0)=T_{I-1,J-2}(0)+\frac{T_{I-1,J-2}(0)-T_{I-2,J-2}(0)}{16^{J-1}-1} \tag{13}$$

where we have taken

$$k=J-1,\ i=I-1,\ x=0,\ x_i=h_{I-1}^4,\ x_{i-k}=h_{I-J}^4.$$

Applying Neville's algorithm generates the h^4-Richardson's extrapolation table for the eigenvalue computation. Defining

$$\hat{\lambda}_{IJ}:=T_{I-1,J-1}(0) \tag{14}$$

we have from (13) that

$$\hat{\lambda}_{I,J}=\hat{\lambda}_{I,J-1}+\frac{\hat{\lambda}_{I,J-1}-\hat{\lambda}_{I-1,J-1}}{16^{J-1}-1}, \tag{15}$$

where

$$\hat{\lambda}_{11}=\text{computed value for } h=h_0,$$

$$\hat{\lambda}_{21}=\text{computed value for } h=\frac{h_0}{2},$$

$$\vdots$$

$$\hat{\lambda}_{n1}=\text{computed value for } h=\frac{h_0}{2^n}.$$

here the second term in (15) is the extrapolation error. The first column of the extrapolation table, that is, the eigenvalues $\hat{\lambda}_{11},\hat{\lambda}_{21},\cdots$, are computable quantities. The columns two, three, four, five, $\cdots$, are generated from column one using (15).

3.2. Computing Large Eigenvalues by Using the Invariant-Imbedding Variables

In a manner similar to Greenberg and Marletta in their SLEUTH code (see [14], Section 3.2, pp. 461-462), we applied the change to "invariant-imbedding" variables, $VU^A, UV^A, \det U$ and $\det V$, in our code in order to provide a good stable integration scheme. We generated the "invariant-imbedding" variables by using the 2×2 matrices $U(x,\lambda)$ and $V(x,\lambda)$ which we defined in (50) and (51) for eigenvalue computation of the SL problem.

4. Numerical Results and Discussion

In this section we give some numerical outputs for each of the 5 test problems in Section 1.1, and compare with the comparable SLEUTH outputs. The 5 test problems are squares of 2nd order SL equations. For such problems the choice of Dirichlet boundary conditions for the 2nd order problem, generates, by squaring,

a 4th order SL problem whose eigenvalues are the squares of the 2nd order SL problem, Greenberg and Marletta ([14] pp. 478-481). For example, we consider in section 5 the following 2nd order SL problems

$$-y''+\left(\frac{-1}{4x^2}\right)y=\lambda y \tag{1}$$

$$y(1)=0,\ y(5)=0$$

$$-y''+\left(x^2+x^4\right)y=\lambda y \tag{2}$$

$$y(1)=0,\ y(5)=0$$

$$-y''+\left(\cos(x)+2\cos(2x)+3\cos(3x)\right)y=\lambda y \tag{3}$$

$$y(0)=0,\ y(\pi)=0$$

$$-y''+\left(\beta^2\sin^2(2x)-2\beta\cos(2x)\right)y=\lambda y \tag{4}$$

$$y\left(\frac{-\pi}{2}\right)=0,\ y\left(\frac{\pi}{2}\right)=0$$

$$-y''+\frac{1}{4}\sec^2(x)\,y=\lambda y \tag{5}$$

$$y(0)=0,\ y\left(\frac{\pi}{4}\right)=0$$

Squaring the self-adjoint operator corresponding to (1)-(5) gives the 4th order self-adjoint operator corresponding to the 4th order problems in **Tables 1-5**, respectively. Accordingly, the eigenvalues of the problems in **Tables 1-5** are the squares of the eigenvalues of the 2nd order SL problems (1)-(5), respectively. **Tables 1-5** give outputs of MG4 and SLEUTH codes on the test problems 1, 2, 3, 4 and 5 respectively, with the choices of Dirichlet boundary conditions. In these tables, we list the SLEUTH and MG4 outputs to 17 digits. The number of these digits which are correct is always a key issue in assessing the performance of a numerical algorithm. Since the exact eigenvalues of these 4th order SL problems are the squares of the exact eigenvalues of the 2nd order SL problems (1)-(5), we computed the eigenvalues of the 2nd order SL problems (1)-(5) and computed their squares to provide a benchmark against which we can compare MG4 and SLEUTH algorithm outputs. The purpose for the following tables is to make comparisons at reasonably high accuracy; so we ran the MG4 and SLEUTH codes with the tolerance parameter TOL = 10^{-12}. Outputs of the SLEDGE code (Sturm-Liouville Estimates Determined by Global Error Control) of Pruess and Fulton [6] for the problems (1)-(5) were obtained for the eigenvalue indices listed in **Tables 1-5**, and then their squares were computed to generate the second columns of **Tables 1-5**. Since SLEDGE is known to compute eigenvalues quite reliably to the user-requested accuracy, we used the squares of the SLEDGE eigenvalues as the benchmark for MG4 and SLEUTH codes in **Tables 1-5**. The error characterization E_{sledge} in columns 4 and 6 of **Tables 1-5** was computed as

$$E_{sledge} = \begin{cases} \left|\lambda_n^{(SLEDGE)} - \lambda_n\right|, & \text{if } \lambda_n < 1 \\ \left|\dfrac{\lambda_n^{(SLEDGE)} - \lambda_n}{\lambda_n^{(SLEDGE)}}\right|, & \text{if } \lambda_n \geq 1, \end{cases} \tag{6}$$

where $\lambda_n^{(SLEDGE)}$ are the SLEDGE-squared eigenvalues and λ_n are eigenvalues obtained by the SLEUTH and MG4 codes. This represents the absolute or relative eigenvalue errors of each code relative to the benchmark values obtained from SLEDGE. The obtained absolute or relative eigenvalue errors of each code are used to measure the performance of each method. In Table 1, we see that the error characterization E_{sledge} for the eigenvalues λ_0, λ_{20} and λ_{100} obtained by the SLEUTH are slightly larger than the error characterization E_{sledge} for the eigenvalues λ_0, λ_{20} and λ_{100} achieved by the MG4 method.

Table 1. Eigenvalues of Problem 1.

Eval Index	SLEDGE	SLEUTH	E_{sledge} of SLEUTH	MG4	E_{sledge} of MG4
0	0.339260710091670	0.3392607100805489	1.105e−11	0.339260710092205	5.348e−13
20	73973.71134197622	73973.711342122158	1.973e−12	73973.711342028924	7.125e−13
100	39594796.88731044	39594796.886610150	1.769e−11	39594796.887332238	5.506e−13

Table 2. Eigenvalues of Problem 2.

Eval Index	SLEDGE	SLEUTH	E_{sledge} of SLEUTH	MG4	E_{sledge} of MG4
0	236.0251207053473	236.02512061495375	3.830e−10	236.02512070536613	7.984e−14
50	3155257.7441797131	3155257.7441750434	1.480e−12	3155257.7441805508	2.655e−13
100	41735725.88393135	41735725.884191565	6.235e−12	41735725.883945607	3.415e−13

Table 3. Eigenvalues of Problem 3.

Eval Index	SLEDGE	SLEUTH	E_{sledge} of SLEUTH	MG4	E_{sledge} of MG4
0	0.2786088184066070	0.2786088184207267	1.412e−11	0.27860881843425472	2.765e−11
50	6765204.5033669453	6765204.5033744955	1.116e−12	6765204.5033704005	5.107e−13
100	104060404.5008649	104060404.50095831	8.977e−13	104060404.50091156	4.485e−13

Table 4. Eigenvalues of Problem 4.

Eval Index	SLEDGE	SLEUTH	E_{sledge} of SLEUTH	MG4	E_{sledge} of MG4
2	4871.3813098296687	4871.3813098537794	4.950e−12	4871.3813098332166	7.283e−13
50	7028539.5468045129	7028539.5468126526	1.158e−12	7028539.5467997193	6.820e−13
100	105083729.4441578	105083729.44410391	5.128e−13	105083729.44420157	4.166e−13

Table 5. Eigenvalues of Problem 5.

Eval Index	SLEDGE	SLEUTH	E_{sledge} of SLEUTH	MG4	E_{sledge} of MG4
0	265.7655513700918	265.76555137422213	1.554e−11	265.76555137021074	4.474e−13
8	1680440.528481040	1680440.5284831792	1.273e−12	1680440.5284811275	5.210e−14
30	236431164.13291141	236431164.15818894	1.069e−10	236431164.13306919	6.673e−13
100	26639566561.99389	26639566568.073307	2.282e−10	26639566561.998882	2.661e−13

In Table 2, we see that the error characterization E_{sledge} for the eigenvalues λ_0, λ_{50} and λ_{100} obtained by the SLEUTH are slightly larger than the error characterization E_{sledge} for the eigenvalues λ_0, λ_{50} and λ_{100} achieved by the MG4 method. In Table 3, we see that the error characterization E_{sledge} for the eigenvalues λ_0 and λ_{100} achieved by the MG4 method are quite comparable to the error characterization E_{sledge} for the eigenvalues λ_0 and λ_{100} obtained by the SLEUTH. But, the error characterization E_{sledge} for the eigenvalue λ_{50} obtained by the SLEUTH is slightly larger than the error characterization E_{sledge} for the eigenvalue λ_{50} achieved by the MG4 method. In Table 4, we see that the error characterization E_{sledge} for the eigenvalue λ_{100} achieved by the MG4 method is quite comparable to the error characterization E_{sledge} for the eigenvalue λ_{100} obtained by the SLEUTH. But, the error characterization E_{sledge} for the eigenvalues λ_2 and λ_{50} obtained by the SLEUTH are slightly larger than the error characterization E_{sledge} for the eigenvalues λ_2 and λ_{50} achieved by the MG4 method. In Table 5, we see that the error characterization E_{sledge} for the eigenvalues λ_0, λ_8, λ_{30} and λ_{100} obtained by the SLEUTH are slightly larger than the error characterization E_{sledge} for the eigenvalues λ_0, λ_8, λ_{30} and λ_{100} achieved by the MG4 method.

Remark 5.1 The machine precision, obtained from the FORTRAN routine EPSLON, on the desktop computer (with Pentium 4 processors) used to obtain the following outputs of the SLEUTH and SLEDGE codes was MACHEPS = 2.22D-16.

5. Conclusion

In this paper we have presented the MG4 algorithm of Iserles *et al.* [33] [40], for eigenvalue computation of regular 4th order Sturm-Liouville problems. Applying the change to "Invariant-Imbedding" variables in a manner similar to Greenberg and Marletta in their SLEUTH code [14] provides good stabilization for the MG4 algorithm, and this resulted in its capability for achieving high accuracy, very often on the order of machine precision. The MG4 algorithm appears to be competitive to the SLEUTH code.

Acknowledgements

The author would like to thank Al Baha University for their financial and moral support. The author would also like to express his sincere gratitude to the following people:

1) Professor Charles Fulton and Dr. Steven Pruess for supplying a FORTRAN 90 version of the SLEDGE code.

2) Professor M. Marletta for supplying a FORTRAN 77 version of the SLEUTH code based on use of the BLAS underlying the LAPACK software, and for suggesting a modification to it which allowed us to run SLEUTH with high accuracy requests.

Conflicts of Interest

The author declares no conflicts of interest regarding the publication of this paper.

References

[1] Alalyani, A. (2019) Numerical Methods for Eigenvalue Computation of Fourth-Order Self-Adjoint Ordinary Differential Operators. PhD Dissertation, Florida Institute of Technology, Melbourne.

[2] Everitt, W.N. (1957) The Sturm-Liouville Problem for Fourth Order Differential Equations. *The Quarterly Journal of Mathematics*, **8**, 146-160. https://doi.org/10.1093/qmath/8.1.146

[3] Fulton, C. (1989) The Bessel-Squared Equation in the Lim-2, Lim-3, Im-4 Cases. *The Quarterly Journal of Mathematics*, **40**, 423-456. https://doi.org/10.1093/qmath/40.4.423

[4] Bailey, P., Gordon, M. and Shampine, L. (1978) Automatic Solution of the Sturm-Liouville Problem. *ACM Transactions on Mathematical Software*, **4**, 193-208. https://doi.org/10.1145/355791.355792

[5] Bailey, P.B., Everitt, W.N. and Zettl, A. (2001) The SLEIGN2 Sturm-Liouville Code. *ACM Transactions on Mathematical Software*, **21**, 143-192. https://doi.org/10.1145/383738.383739

[6] Pruess, S. and Fulton, C. (1993) Mathematical Software for Sturm-Liouville Problems. *ACM Transactions on Mathematical Software*, **19**, 360-376. https://doi.org/10.1145/155743.155791

[7] Fulton, C. and Pruess, S. (1998) The Computation of Spectral Density Functions for Singular Sturm-Liouville Problems Involving Simple Continuous Spectra. *ACM Transactions on Mathematical Software*, **34**, 107-129. https://doi.org/10.1145/285861.285867

[8] Pryce, J.D. (1993) Numerical Solution of Sturm-Liouville Problems. Oxford University Press, Oxford.

[9] Pryce, J.D. and Marletta, M. (1992) Automatic Solution of Sturm-Liouville Problems Using the Pruess Method. *Journal of Computational and Applied Mathematics*, **39**, 57-78. https://doi.org/10.1016/0377-0427(92)90222-J

[10] Pryce, J. (1986) Error Control of Phase-Function Shooting Methods for Sturm-Liouville Problems. *IMA Journal of Numerical Analysis*, **6**, 103-123. https://doi.org/10.1093/imanum/6.1.103

[11] Ledoux, V., Van Daele, M. and Vanden Berghe, G. (2004) CP Methods of Higher Order for Sturm-Liouville and Schrödinger Equations. *Computer Physics Communications*, **162**, 153-165. https://doi.org/10.1016/j.cpc.2004.07.001

[12] Ledoux, V., Van Daele, M. and Vanden Berghe, G. (2005) MATSLISE: A Matlab Package for the Numerical Solution of Sturm-Liouville and Schrödinger Equations. *ACM Transactions on Mathematical Software*, **31**, 532-554. https://doi.org/10.1145/1114268.1114273

[13] Ixaru, L. (2000) CP Methods for the Schrödinger Equation. *Journal of Computational and Applied Mathematics*, **125**, 347-357. https://doi.org/10.1016/S0377-0427(00)00478-7

[14] Greenberg, L. and Marletta, M. (1997) Algorithm 775: The Code SLEUTH for Solving Fourth-Order Sturm-Liouville Problems. *ACM Transactions on Mathematical Software*, **23**, 453-493. https://doi.org/10.1145/279232.279231

[15] Greenberg, L. and Marletta, M. (1995) Oscillation Theory and Numerical Solution of Fourth-Order Sturm-Liouville Problems. *IMA Journal of Numerical Analysis*, **15**, 319-356. https://doi.org/10.1093/imanum/15.3.319

[16] Greenberg, L. (1991) An Oscillation Method for Fourth-Order, Self-Adjoint, Two-Point Boundary Value Problems with Nonlinear Eigenvalues. *SIAM Journal on Mathematical Analysis*, **22**, 1021-1042. https://doi.org/10.1137/0522067

[17] Chanane, B. (2010) Accurate Solutions of Fourth Order Sturm-Liouville Problems. *Journal of Computational and Applied Mathematics*, **234**, 3064-3071. https://doi.org/10.1016/j.cam.2010.04.023

[18] Chanane, B. (1998) Eigenvalues of Fourth Order Sturm-Liouville Problems Using Fliess Series. *Journal of Computational and Applied Mathematics*, **96**, 91-97. https://doi.org/10.1016/S0377-0427(98)00086-7

[19] Chanane, B. (2002) Fliess Series Approach to the Computation of the Eigenvalues of Fourth-Order Sturm-Liouville Problems. *Applied Mathematics Letters*, **15**, 459-563. https://doi.org/10.1016/S0893-9659(01)00159-8

[20] Chanane, B. (1998) Eigenvalues of Sturm-Liouville Problems Using Fliess Series. *Applicable Analysis*, **69**, 233-238. https://doi.org/10.1080/00036819808840659

[21] Mihaila, B. and Mihaila, I. (2002) Numerical Approximations Using Chebyshev Polynomial Expansions: El-gendi's Method Revisited. *Journal of Physics A*: *Mathematical and General*, **35**, 731-746. https://doi.org/10.1088/0305-4470/35/3/317

[22] El-Gamel, M. and Sameeh, M. (2012) An Efficient Technique for Finding the Eigenvalues of Fourth-Order Sturm-Liouville Problems. *Applied Mathematics*, **3**, 920-925. https://doi.org/10.4236/am.2012.38137

[23] El-Gamel, M. and Abd El-hady, M. (2013) Two Very Accurate and Efficient Methods for Computing Eigenvalues of Sturm-Liouville Problems. *Applied Mathematical Modeling*, **37**, 5039-5046. https://doi.org/10.1016/j.apm.2012.10.019

[24] Fox, L. (1962) Chebyshev Methods for Ordinary Differential Equations. *The Computer Journal*, **4**, 318-331. https://doi.org/10.1093/comjnl/4.4.318

[25] Saleh Taher, A.H., Malek, A. and Momeni-Masuleh, S.H. (2013) Chebyshev Differential Matrices for Efficient Computation of the Eigenvalues of Fourth-Order Sturm-Liouville Problems. *Applied Mathematical Modeling*, **37**, 4634-4642. https://doi.org/10.1016/j.apm.2012.09.062

[26] Ycel, U. (2015) Numerical Approximations of Sturm-Liouville Eigenvalues Using Chebyshev Polynomial Expansions Method. *Cogent Mathematics*, **2**, Article ID: 1045223. https://doi.org/10.1080/23311835.2015.1045223

[27] Ycel, U. and Boubaker, K. (2012) Differential Quadrature Method (DQM) and Boubaker Polynomials Expansion Scheme (BPES) for Efficient Computation of the Eigenvalues of Fourth-Order Sturm-Liouville Problems. *Applied Mathematical Modelling*, **36**, 158-167. https://doi.org/10.1016/j.apm.2011.05.030

[28] Khmelnytskaya, K., Kravchenko, V. and Baldenebro-Obeso, J. (2012) Spectral Parameter Power Series for Fourth-Order Sturm-Liouville Problems. *Applied Mathematics and Computation*, **219**, 3610-3524. https://doi.org/10.1016/j.amc.2012.09.055

[29] Kravchenko, V. and Porter, R. (2010) Spectral Parameter Power Series for Sturm-Liouville Problems. *Mathematical Methods in the Applied Sciences*, **33**, 459-468. https://doi.org/10.1002/mma.1205

[30] Kravchenko, V. and Porter, R. (2015) Eigenvalue Problems, Spectral Parameter Power Series, and Modern Applications. *Mathematical Methods in the Applied Sciences*, **38**, 1945-1969. https://doi.org/10.1002/mma.3213

[31] Fulton, C. and Krall, A. (1983) Self-Adjoint 4th Order Boundary Value Problem in the Lim-4 Case. *Proceedings of Symposium on Ordinary Differential Equations and*

Operators, Dundee, Lecture Notes in Mathematics 1032, 240-256. https://doi.org/10.1007/BFb0076800

[32] Atkinson, F. (1964) Discrete and Continuous Boundary Problems. Academic Press, New York. https://doi.org/10.1063/1.3051875

[33] Iserles, A., Marthinsen, A. and Nrsett, S.P. (1999) On the Implementation of the Method of Magnus Series for Linear Differential Equations. *BIT Numerical Mathematics*, **39**, 281-304. https://doi.org/10.1023/A:1022393913721

[34] Greenberg, L. and Marletta, M. (1997) The Validity of Richardson Extrapolation in Coefficient Approximation Methods for Fourth Order and Higher Order Self-Adjoint ODE Eigenvalue Problems. Technical Report, Department of Mathematics and Computer Science, University of Leicester, Leicester.

[35] Greenberg, L. (1991) A Prüfer Method for Calculating Eigenvalues of Self-Adjoint Systems of Ordinary Differential Equations: Parts 1 and 2. Technical Report TR91-24, University of Maryland at College Park, College Park.

[36] Gallier, J. (2005) Manifolds, Lie Groups, Lie Algebras, Riemannian Manifolds, with Applications to Computer Vision and Robotics [Lecture Notes]. Department of Computer and Information Science, University of Pennsylvania, Philadelphia.

[37] Magnus, W. (1954) On the Exponential Solution of Differential Equations for a Linear Operator. *Communications on Pure and Applied Mathematics*, **7**, 649-673. https://doi.org/10.1002/cpa.3160070404

[38] Iserles, A. and Nrsett, S.P. (1999) On the Solution of Linear Differential Equations in Lie Groups. *Philosophical Transactions of the Royal Society A*: *Mathematical, Physical and Engineering Sciences*, **357**, 983-1019. https://doi.org/10.1098/rsta.1999.0362

[39] Stoer, J. and Bulirsch, R. (1993) Introduction to Numerical Analysis. Second Edition, Springer-Verlag, New York. https://doi.org/10.1007/978-1-4757-2272-7

[40] Iserles, A., Munthe-Kaas, H.Z., Norsett, S.P. and Zanna, A. (2005) Lie-Group Methods. *Acta Numerica*, **9**, 1-148. https://doi.org/10.1017/S0962492900002154

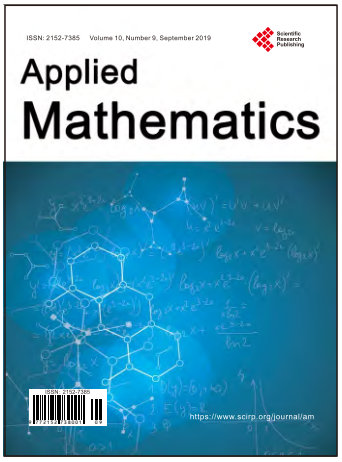

Call for Papers

Applied Mathematics (AM)

ISSN Print: 2152-7385 ISSN Online: 2152-7393
https://www.scirp.org/journal/am

Applied Mathematics **(AM)** is an international journal dedicated to the latest advancement of applied mathematics. The goal of this journal is to provide a platform for scientists and academicians all over the world to promote, share, and discuss various new issues and developments in different areas of applied mathematics.

Subject Coverage

All manuscripts must be prepared in English, and are subject to a rigorous and fair peer-review process. Accepted papers will immediately appear online followed by printed hard copy. The journal publishes original papers including but not limited to the following fields:

- Applied Probability
- Applied Statistics
- Approximation Theory
- Chaos Theory
- Combinatorics
- Complexity Theory
- Computability Theory
- Computational Methods in Mechanics and Physics
- Continuum Mechanics
- Control Theory
- Cryptography
- Discrete Geometry
- Dynamical Systems
- Elastodynamics
- Evolutionary Computation
- Financial Mathematics
- Fuzzy Logic
- Game Theory
- Graph Theory
- Information Theory
- Inverse Problems
- Linear Programming
- Mathematical Biology
- Mathematical Chemistry
- Mathematical Economics
- Mathematical Physics
- Mathematical Psychology
- Mathematical Sociology
- Matrix Computations
- Neural Networks
- Nonlinear Processes in Physics
- Numerical Analysis
- Operations Research
- Optimal Control
- Optimization
- Ordinary Differential Equations
- Partial Differential Equations
- Probability Theory
- Statistical Finance
- Stochastic Processes
- Theoretical Statistics

We are also interested in: 1) Short Reports—2-5 page papers where an author can either present an idea with theoretical background but has not yet completed the research needed for a complete paper or preliminary data; 2) Book Reviews—Comments and critiques.

Notes for Intending Authors

Submitted papers should not have been previously published nor be currently under consideration for publication elsewhere. Paper submission will be handled electronically through the website. All papers are refereed through a peer review process. For more details about the submissions, please access the website.

Website and E-mail

https://www.scirp.org/journal/am **E-mail: am@scirp.org**

What is SCIRP?

Scientific Research Publishing (SCIRP) is one of the largest Open Access journal publishers. It is currently publishing more than 200 open access, online, peer-reviewed journals covering a wide range of academic disciplines. SCIRP serves the worldwide academic communities and contributes to the progress and application of science with its publication.

What is Open Access?

All original research papers published by SCIRP are made freely and permanently accessible online immediately upon publication. To be able to provide open access journals, SCIRP defrays operation costs from authors and subscription charges only for its printed version. Open access publishing allows an immediate, worldwide, barrier-free, open access to the full text of research papers, which is in the best interests of the scientific community.

- High visibility for maximum global exposure with open access publishing model
- Rigorous peer review of research papers
- Prompt faster publication with less cost
- Guaranteed targeted, multidisciplinary audience

Scientific Research Publishing

Website: https://www.scirp.org

Subscription: sub@scirp.org

Advertisement: service@scirp.org